Synthesis of Calcium Phosphate/Designed Organic Molecule Composites

by

Nobuaki Ikawa

Submitted to Hiroshima University
In partial fulfillment of the requirements for the degree of
Philosophy of Doctor

Supervisor: Professor Dr. Tsuneji Sano

Depertment of Chemisty and Chemical Engineering,
Graduate School of Engineering,
Hiroshima University

March 2009

Referee in Chief: Professor Tsuneji Sano

Referees: Professor Shoji Yamanaka

Professor Kikuo Okuyama

Professor Takeshi Shiono

Associate Professor Shinjiro Hayakawa

Depertment of Chemisty and Chemical Engineering,
Graduate School of Engineering,
Hiroshima University

Chapter 1. Introduction

Chapter 2. Synthesis of lamellar mesostructured calcium phosphates using *n*-alkylamines as structure-directing agents in alcohol/water mixed solvent systems

Chapter 1

Introduction

1.1. Calcium phosphate

1.1.1 What is calcium phosphate?

Calcium phosphate compounds have attracted much attention for the wide variety of applications, such as biomaterials [1-3], catalysts [4-15] and adsorbents [16-21]. Since the chemical composition of calcium phosphate was clarified by J. Berzelius in the 19th century [22], different crystal structures of calcium phosphate were successfully introduced [23]. According to the definition, calcium phosphate is consisted of three kinds of major elements of calcium (oxidation state +2), phosphorus (oxidation state +5) and oxygen (oxidation state −2), and the kinds of calcium phosphate are classified into some groups by the state of phosphate.

Calcium orthophosphate is constructed by calcium and orthophosphate (PO_4^{3-}), and other kinds of phosphates such as metaphosphate (PO_3^-), pyrophosphate ($P_2O_7^{4-}$) and polyphosphate ($(PO_3)_n^{n-}$) are also components of calcium phosphates. Calcium orthophosphate is subjected to research for long years and is the most famous calcium phosphate. Therefore, calcium orthophosphate has simply been called calcium phosphate in the many books and papers (In this paper, I also describe calcium phosphate instead of calcium orthophosphate hereafter unless otherwise noted.).

There are ten non-ion-substituted calcium phosphates with different crystalline structure which is classified by the Ca/P molar ratio (0.5-2.0) and the number of crystalline water molecules (Table 1.1) [24, 25]. The basic property of calcium phosphates strongly depended on these parameters. For example, calcium phosphates with the smallest Ca/P molar ratio of 0.5 are more acidic and water-soluble than others, whether the calcium phosphate has crystalline water molecules or not [26]. There are 4 polymorphs of phosphoric acid (PO_4^{3-}, HPO_4^{2-}, $H_2PO_4^-$ and H_3PO_4), depending on the pH value in the solution (Figure 1.1) [24]. Therefore, the pH value is very important factor on the synthesis of calcium phosphates due to the ion charge matching of calcium

and phosphate ions. The reaction temperature also affects the number of the crystalline water molecules; water molecule is easily incorporated in their structure at low temperature, while at high temperature anhydrous calcium phosphates with denser structures are formed (Table 1.2) [25, 27].

Table 1. 1. Properties of the biologically relevant calcium phosphates

Ca/P molar ratio	Compound	Formula	Solubility at 25 °C, -log(K_s)	Solubility at 37 °C, -log(K_s)	pH stability range in aqueous solution 25 °C
0.5	Monocalcium phosphate monohydrate (MCPM)	$Ca(H_2PO_4)_2{\cdot}H_2O$	1.14	No data	0.0-2.0
0.5	Monocalcium phosphate anhydrrous (MCPA)	$Ca(H_2PO_4)_2$	1.14	No data	[b]
1.0	Dicalcium phosphate dihydrate (DCPD), mineral brushite	$CaHPO_4{\cdot}2H_2O$	6.59	6.63	2.0-6.0
1.0	Dicalcium phosphate anhydrate (DCPA), mineral monetite	CaH_2PO_4	6.90	7.02	[b]
1.33	Octacalcium phosphate (OCP)	$Ca_8(HPO_4)_2(PO_4)_4{\cdot}5H_2O$	96.6	95.9	5.5-7.0
1.5	α-Tricalcium phosphate (α-TCP)	α-$Ca_3(PO_4)_2$	25.5	25.5	[c]
1.5	β-Tricalcium phosphate (β-TCP)	β-$Ca_3(PO_4)_2$	28.9	29.5	[c]
1.2-2.2	Amorphous calcium phosphate (ACP)	$Ca_xH_y(PO_4)_z{\cdot}nH_2O$, n = 3-4.5	[a]	[a]	~5-12 [d]
1.5-1.67	Calcium-deficient hydroxyapatite (CDHA)	$Ca_{10}(HPO_4)_x(PO_4)_{6-x}(OH)_{2-x}$	~85.1	~85.1	6.5-9.5
1.67	Hydroxyapatite (HA)	$Ca_{10}(PO_4)_6(OH)_2$	116.8	117.2	9.5-12
1.67	Fluorapatite (FA)	$Ca_{10}(PO_4)_6F_2$	120.0	119.2	7-12
2.0	Tetracalcium phosphate (TTCP), mineral hilgenstockite	$Ca_4(PO_4)_2O$	38-44	37-42	[c]

[a] Cannot be measured precisely.
[b] Stable at temperature above 100 °C.
[c] These compounds cannot precipitated from aqueous solution
[d] Always metastable

Table 1. 2. Crystallographic data of calcium phosphates

Compound	Space group	Unit cell parameters	Z[a]	Density g cm^{-1}
MCPM	Triclinic $P\bar{1}$	a = 5.6261(5), b = 11.889(2), c = 6.4731(8) Å α= 98.633(6) °, β = 118.262(6) °, γ = 83.344(6) °	2	2.23
MCPA	Triclinic $P\bar{1}$	a = 7.5577(5), b = 8.2531(6), c = 5.5504(3) Å α= 109.87(1) °, β = 93.68(1) °, γ = 109.15(1) °	2	2.58
DCPD	Monoclinic Ia	a = 5.812(2), b = 15.180(3), c = 6.239(2) Å β = 116.42(3) °	4	2.32
DCPA	Triclinic $P\bar{1}$	a = 6.910(1), b = 6.627(2), c = 6.998(2) Å α= 96.34(2) °, β = 103.82(2) °, γ = 88.33(2) °	4	2.89
OCP	Triclinic $P\bar{1}$	a = 19.692(4), b = 9.523(2), c = 6.835(2) Å α= 90.15(2) °, β = 92.54(2) °, γ = 108.65(1) °	1	2.61
α-TCP	Monoclinic $P2_1/a$	a = 12.887(2), b = 27.280(4), c = 15.219(2) Å β = 126.20(1) °	24	2.86
β-TCP	Rhombohedral $R3Ch$	a = b = 10.4183(5), c = 37.3464(23) Å, γ = 120 °	21[b]	3.08
HA	Hexagonal $P6_3/m$	a = b = 9.4302(5), c = 6.8911(2) Å, γ = 120 °	2	3.16
FA	Hexagonal $P6_3/m$	a = b = 9.367, c = 6.884 Å, γ = 120 °	2	3.20
TTCP	Monoclinic $P2_1$	a = 7.023(1), b = 11.986(4), c = 9.473(2) Å β = 90.90(a) °	4	3.05

[a] Number of formula units per cell
[b] Per the hexagonal unit cell

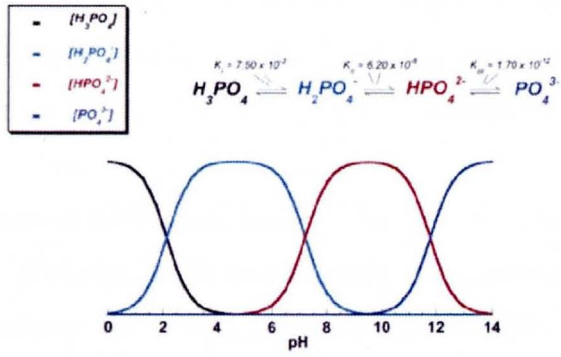

Figure 1.1. pH variation of ionic concentrations in tripotic equilibrium for phosphoric acid solution [24].

(a) MCPM and MCPA

Monocalcium phosphate monohydrate (MCPM: $Ca(H_2PO_4)_2H_2O$) and monocalcium phosphate anhydrous (MCPA: $Ca(H_2PO_4)_2$) with the Ca/P molar ratio of 0.5 are precipitated from highly acidic solutions [28]. MCPM is formed at low reaction temperature, while anhydrous MCPA can be obtained at higher temperature above 100 °C. The structure of MCPA is denser than MCPM due to absence of crystalline water molecule, leading to the difference of solubility. Although both of MCPM and MCPA are not classified into biological compounds, a small content of MCPM is included in calcium phosphate cements known as a famous artificial bone [29-33]. MCPM has also been used as fertilizers, baking powder, bakery dough, salt-curing preservers, picked and marinated foods and occasionally tooth pastes. MCPA has been used instead of MCPM, but the amount of commercial application is lower than MCPM due to its lower solubility [28, 34].

(b) DCPD and DCPA

Dicalcium phosphate dihydrate commonly called brushite (DCPD: $CaHPO_4 \cdot 2H_2O$) is easily and quickly crystallized in an aqueous solution at room temperature. While dicalcium phosphate anhydrous often called monetite (DCPA: $CaHPO_4$) can be obtained at temperature above 80 °C. DCPD is often found in biological system such as urinary stones, dental calculi and carious lesions [35]. DCPD is added to calcium phosphate cements and toothpastes for caries protection [36-38]. The other applications are a flame retardant, slow fertilizers, glass production and a calcium supplement in foods. Unlike

DCPD, DCPA is not found in pathological calcifications, and used as calcium phosphate cements, polishing agents, sources of calcium and phosphate in nutritional supplements and toothpaste components [34].

(c) OCP

Octacalcium phosphate (OCP: $Ca_8(HPO_4)_2(PO_4)_4 \cdot 5H_2O$) is only a crystalline calcium phosphate with two polymorphs of phosphates (HPO_4^{2-} and PO_4^{3-}). Therefore the range of pH value in the reaction mixture is very narrower than other calcium phosphates, because the pH value must be adjusted in which two types of phosphate units are co-existed. The structure of OCP is alternately stacked by apatitic anhydrous layer and hydrous layer (Figure 1.2) [26, 35, 39], and OCP is often found as an unstable intermediate of the thermodynamically more stable crystalline phase in aqueous systems. Biologically OCP is very important compounds, because it is stable in human dental and urinary calculi. W. E. Brown firstly proposed that OCP is the initial phase of enamel mineral formation, and bone is formed through subsequent precipitation and stepwise hydrolysis [40]. OCP have been used as artificial bones and implants [41-44].

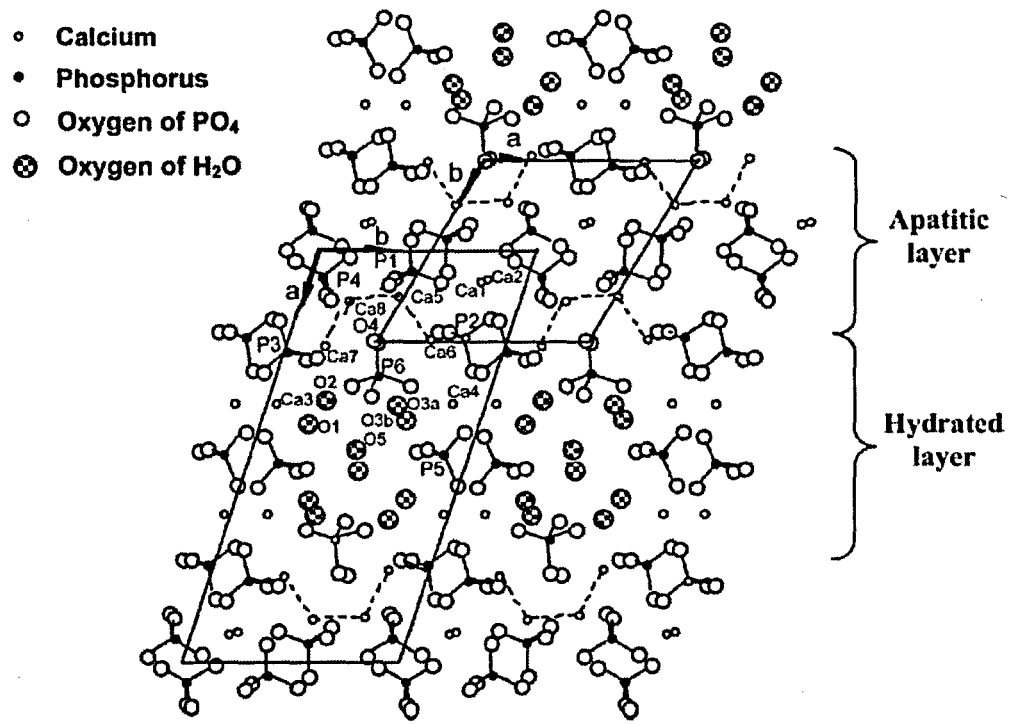

Figure 1.2. Projection of the (001) plane of octacalcium phosphate (OCP) structure [39].

(d) TCPs

β-Tricalcium phosphate (β-TCP: β-$Ca_3(PO_4)_2$) can be obtained from calcium-deficient hydroxyapatite (CDHA) at high temperature above 800 °C, but not available in aqueous solution. β-TCP is also prepared from bones after calcination, therefore β-TCP is occasionally called as "bone ash". Mg-substituted form called whitlockite is found in dental calculi, urinary stones, dentinal caries, salivary stones and arthritic cartilage. β-TCP has mainly been applied for artificial bones as not only pure form but also combinating material with hydroxyapatite (HA) called the biphasic calcium phosphate [29, 30, 45-48]. For the other applications, β-TCP is served as a bakery improver and an anti-clumping agent for dry powder foods. β-TCP can be also used as a slow releasing fertilizer for acid solids [28]. α-Tricalcium phosphate (α-TCP: α-$Ca_3(PO_4)_2$) is prepared from β-TCP at high temperature above 1125 °C. In spite of the same chemical composition of the two TCPs, the structure of α-TCP is different from β-TCP. α-TCP with lower density is transformed from β-TCP, leading to the high soluble phase. The applications of α-TCP are for biomaterials and agricultural fertilizers as well as β-TCP.

(e) HA

Hydroxyapatite (HA: $Ca_5(PO_4)_3OH$, but usually written as $Ca_{10}(PO_4)_6(OH)_2$ to denote that the crystal unit cell comprises two molecules) is the second most stable and least soluble calcium phosphate. Chemically pure HA crystallizes in the monoclinic space group $P6_3/m$ (Figure 1.3, Table 1.2), [49-51]. HA is widely used as a coating on orthopedic and dental implants, because HA is bioactive material due to the great similarity to biological apatite. HA has also been used as calcium phosphate cements, drug deliveries and toothpastes [52-59].

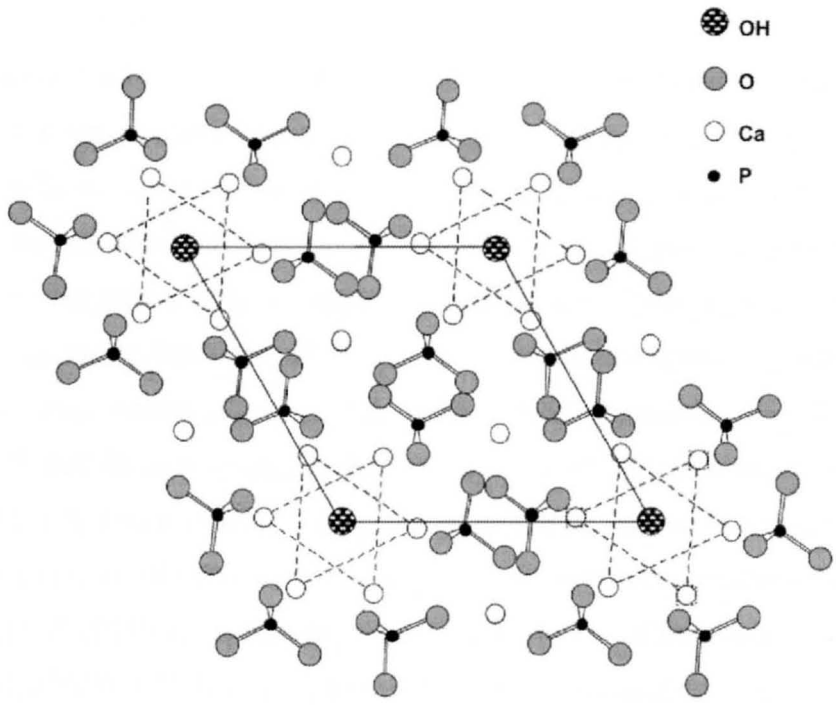

Figure 1.3. Projection of the (001) plane of hydroxyapatite (HA) structure [39].

Although pure HA cannot be formed in biological system, there are many kinds of synthetic approaches for HA. These methods can be divided into solid-state and liquid phase reactions. HA can normally be obtained in aqueous solution including exactly stoichiometric quantities of Ca and PO_4 sources at the pH value above 9 after followed steps [60]. The mixture is boiled for several days in CO_2-free atmosphere, aging, filtration, drying and usually sintering at around 1000 °C. The aging step is very important because calcium deficient hydroxyapatite is formed after the first boiling step. Usually unsintering HA is also important for avoiding of highly crystalline and often nonstoichiometric compound formations. In the case of solid reaction, HA can also be prepared from a mixture of calcium phosphates with the lower Ca/P molar ratio than HA (1.67) with Ca sources such as CaO, $Ca(OH)_2$ or $CaCO_3$ above 1200 °C [61]. A water-free synthetic method has also been performed in ethanol from $Ca(OEt)_2$ and H_3PO_4 [62, 63]. HA is also affordable from mechanochemical synthesis of a dry mixture of CaO and DCPD [64]. The crystal size of HA can be controlled by the synthetic methods and conditions. Some articles concerning to the synthesis of nano-sized HA have been reported [65].

(f) TTCP

Tetracalcium phosphate (TTCP: $Ca_4(PO_4)_2O$) is a basic crystalline calcium phosphate with the largest Ca/P molar ratio (2.0) so far. However, its solubility in water is higher than HA (Table 1.1). TTCP cannot be precipitated from aqueous solutions. It can only be prepared by a solid state reaction above 1300 °C. TTCP is comparatively unstable in aqueous solution, due to hydrolysis to HA and calcium hydroxide [49, 66]. Although TTCP cannot be found in biological system, it has been used for various self-setting calcium phosphate cements [24, 25, 33, 52, 67-71].

(g) Amorphous calcium phosphate

Amorphous calcium phosphate (ACP: $Ca_xH_y(PO_4)_z{\cdot}nH_2O$ n = 3-4.5) has often been found as a transient phase of crystalline calcium phosphates in aqueous system. ACP can be obtained from solution containing calcium and phosphate ions with very short reaction time, because calcium phosphate easily and quickly crystallizes in aqueous solution [72-77]. Therefore, ACP has been commonly synthesized by freeze-dry method due to avoiding the crystallization in even drying step [49]. The composition of ACP strongly depends on the pH value and the concentration of mixed solutions. The presence of pyrophosphate, carbonate and/or magnesium ions suppresses the crystallization of calcium phosphates in aqueous solution and stabilizes the amorphous structure, while fluoride ion enhances the crystallization [26, 78, 79]. Biologically, ACP, often containing Na, Mg, carbonate and pyrophosphate ions, is found in soft tissue pathological calcifications [26, 80-82]. In medicine, pure ACP is used in calcium phosphate cements and as a filling material in dentistry [83-86]. Bioactive composite with polymers has properties suitable for use in dentistry. Non-biomedical application of ACP is a component of mordant. In addition, ACP is used for syrup cleaning in food industry.

The structure of ACP has been uncertain so far. Infrared spectra (IR) show broad absorption band due to phosphate units. In the X-ray diffraction (XRD) measurement, a broad peak is observed, and the position of the peak is always determined by the bond distance between ion pairs of P-O (1.5 Å), O-O, Ca-O (2.3 Å), Ca-Ca, Ca-P and P-P (3-6 Å) (Figure 1.4). Morphologically, spherical particles of ACP with diameter in the range of 20-200 nm are observed in scanning electron microscopy (SEM). However, there is possibility that ACP has an apatitic structure but with a small crystal size, that is

supported by the result of X-ray absorption spectroscopic (EXAFS) analysis of biological and synthetic samples [88-90]. On the other hand, it was proposed that the basic structural unit of ACP is spherical cluster with the diameter of 9.5 Å and the composition is $Ca_9(PO_4)_6$. These clusters were found experimentally as first nuclei during the crystallization of HA, and a model was developed to research the HA crystallization [91].

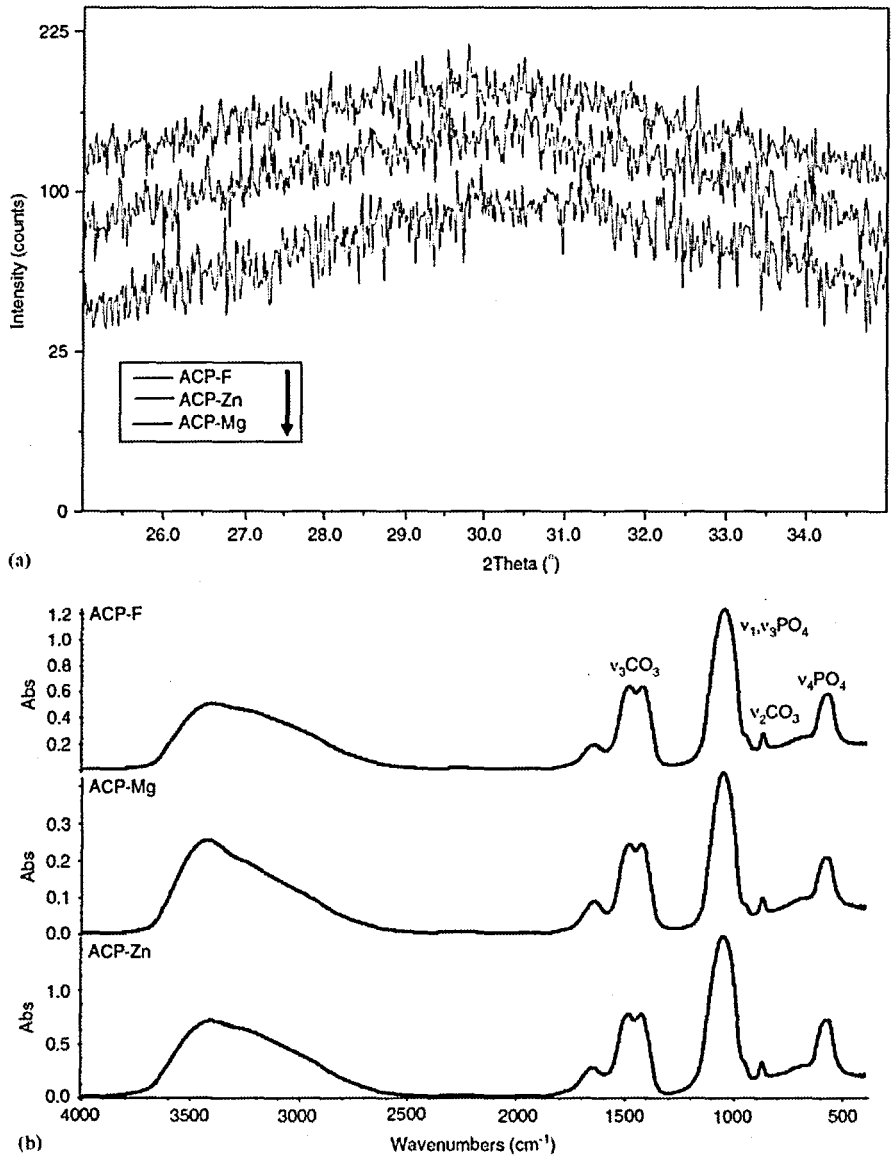

Figure 1.4. XRD patterns and FT-IR spectra of amorphous calcium phosphates doped fluorine, magnesium and zinc ions [87].

(h) Nonstoichiometric calcium phosphates

All kinds of ions in HA with the chemical composition of $Ca_{10}(PO_4)_6(OH)_2$ can partially be substituted with other ions regardless of charge number of the ions, substituents of Ca^{2+} with Mg^{2+}, Sr^{2+}, Ba^{2+}, Pb^{2+} and even monovalent K^+ and Na^+, of PO_4^{3-} with HPO_4^{2-}, CO_3^{2-}, VO_4^{3-} and AsO_4^{3-}, and of OH^- with F^-, Cl^-, Br^-, I^- and CO_3^{2-}. The substituents with different charge ions require electron-neutralization of the charge balance. Therefore, the formation of vacancies in the place of oppositely charged ions and coupling substituents of different charges are occurred, leading to the formation of nonstoichiometric apatites [92]. For example, a substituent of PO_4^{3-} with HPO_4^{2-} in HA leads to Ca^{2+} and OH^- deficient HA. The chemical composition of such calcium-deficient HA (CDHA) can be described as follow;

$$Ca_{10-x}\square_x(PO_4)_{6-x}(HPO_4)_x(OH)_{2-x}\square_x.$$

The value of x is limited within 2. While the synthesis of PO_4-deficient HA has not been reported due to the large structure of PO_4 units. In addition, there are no any reports on such substituents in other calcium phosphates so far. This would be due to that the structure of these calcium phosphates cannot be formed in the presence of other ions due to the lower density of their structure.

CDHAs with various chemical compositions can easily be prepared by the reaction between calcium and phosphate ions in aqueous solution. During this reaction, CDHAs are recrystallization and/or transformed from ACP firstly formed. Therefore, the structure, properties and applications of CDHAs are similar to those of ACP. CDHAs are poorly crystallized, and the surface area (25-100 m^2g^{-1}) is larger than other calcium phosphates. CDHA with the Ca/P molar ratio of 1.5 transforms into β-TCP upon heating above 800 °C, while CDHAs with higher Ca/P molar ratios (1.5-1.67) transform into a mixture of β-TCP and HA (called as biphasic calcium phosphate; BCP) [93-96]. Such nonstoichiometric calcium phosphates including BCP have been very important for the application of artificial bones. In addition, non-biomedical applications are similar to ACP.

CDHAs can always be found in hard tissues, because pure HA highly crystallized cannot be formed under the presence of other ions except of fluorine ions. CDHA including various ions can play an important role in regulation of ion concentrations in our body and protecting cells. Therefore, there are several types of CDHAs with

different chemical compositions to meet these requirements. For example, the chemical compositions of enamel and bone are:

Enamel: $Ca_{9.4}\square_{0.6}(PO_4)_{5.4}(HPO_4 \text{ and } CO_3)_{0.6}(OH)_{1.4}\square_{0.6}$ (x=0.6)

Bone: $Ca_{8.3}\square_{1.7}(PO_4)_{4.3}(HPO_4 \text{ and } CO_3)_{1.7}(OH \text{ and/or } CO_3)_{0.3}\square_{1.7}$ (x=1.7).

The difference of XRD and IR data between enamel and bone has been reported (Figure 1.5). CDHA in enamel is close to stoichiometric apatite, leading its lower solubility for protecting acidic attack by foods and bacterial attack. The most stable biological apatite is shark teeth partially including fluorapatite with lower solubility than stoichiometric HA. In contrast, bone mineral with many vacancies is more soluble and high ion exchange capacity for the ion regulating function.

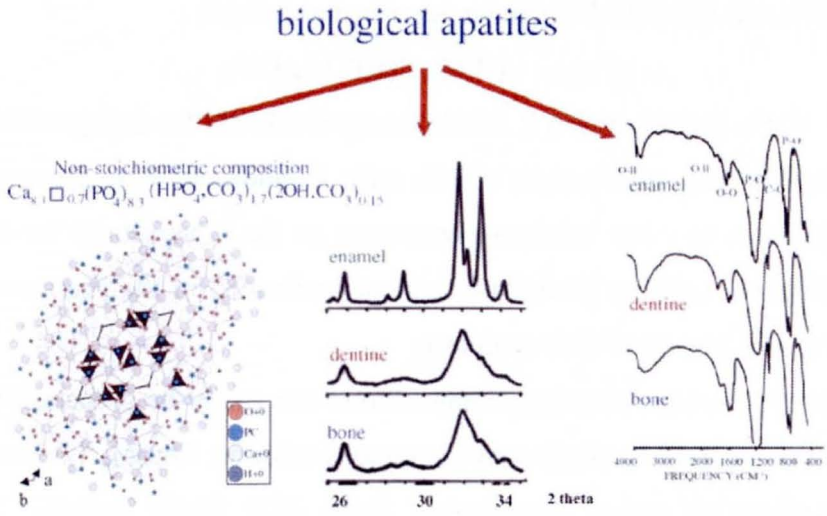

Figure 1.5. Crystal structure of biological apatite, and XRD and FT-IR of enamel, dentine and bone [97].

1.1.2. Geological calcium phosphates

Calcium phosphate has abundantly existed as phosphorites [27, 28] and apatites [27] in nature. The world deposits are guessed at exceed 150 billion tons, and the breakout is approximately phosphorites 85% and apatite 15% [27]. Almost natural calcium phosphates are accessory minerals (<5%) included in other geological minerals. The chemical composition of phosphorites, which is considered as carbonate-hydroxy-fluorapatite [27, 28], cannot easily be described. The major producing countries of phosphorites are Russia, Brazil and Zambia. While the major

producing countries of apatites, which is mainly deposited as fluorapatite with the chemical composition of $Ca_{10}(PO_4)_6F_2$, are Morocco, Russia, Kazakhstan, USA, China and Australia [27, 99-101]. Most calcium phosphate cannot be obtained as pure form but partially substituted nonstoichiometric compounds with other ions. For example, calcium ions partially replaced by Sr, Ba, Mg, Mn, K, Na and Fe ions, and phosphate and fluoride ions are also replaced by AsO_4^{3-}, CO_3^{2-} and VO_4^{3-}, and OH^-, Cl^-, Br^- and CO_3^{2-}, respectively. Thus, natural calcium phosphates are colored due to these impurities, unlike pure calcium phosphates crystal with white in color (Figure 1.6 (a),(b)). Natural calcium phosphates have mainly been used as industrial source of elementary phosphorus, phosphoric acids, various phosphorous containing chemicals and agricultural fertilizers, and the amount of these consumptions accounts for 85% of the world production [101]. The total consumption amount in the world exceeds 25 million tons per year [28].

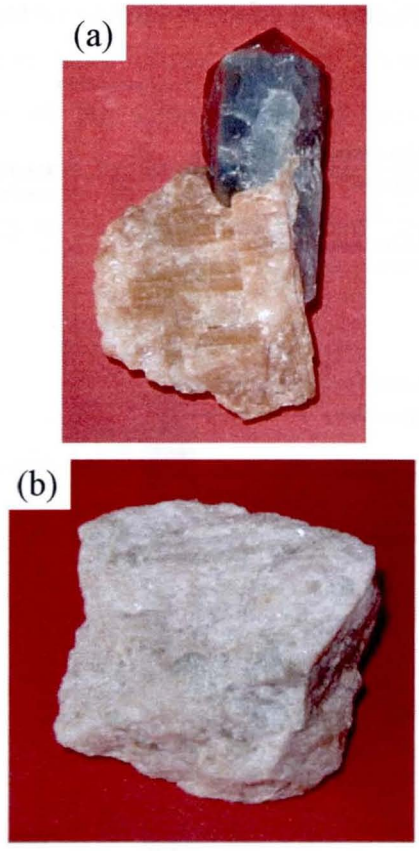

Figure 1.6. (a) Natural calcium phosphates containing impurities and (b) Pure calcium phosphate crystal with white in color [101].

1.1.3. Biological calcium phosphates

Calcium phosphates are also existed as main inorganic components of hard tissues in biological systems, such as normally bone, teeth, fish scales, deer antlers and shells, and pathologically dental pulp stones and urinary calculus [26, 80-82, 102].

All vertebrates have bones which are also called osseous tissue. Bones are composite material of inorganic species (mainly low crystallized hydroxyapatite) and biomolecules (mainly collagen), affording its proper hardness and bendability [103-107]. Usually bone means a part of a relatively dense outer layer (compact bone) which covers other cancellous (spongy and trabecular) bone (Figure 1.7). Detail information on the chemical composition of the most important human normal calcified tissues is comprised in Table 1.3 [26, 78]. Physically, bones play important roles for supporting body structures, protecting internal organs and facilitating of muscle movements. Bones also play chemically important roles, such as helping of cell formation, calcium metabolism and control of mineral ion concentration in vertebrate bodies [108].

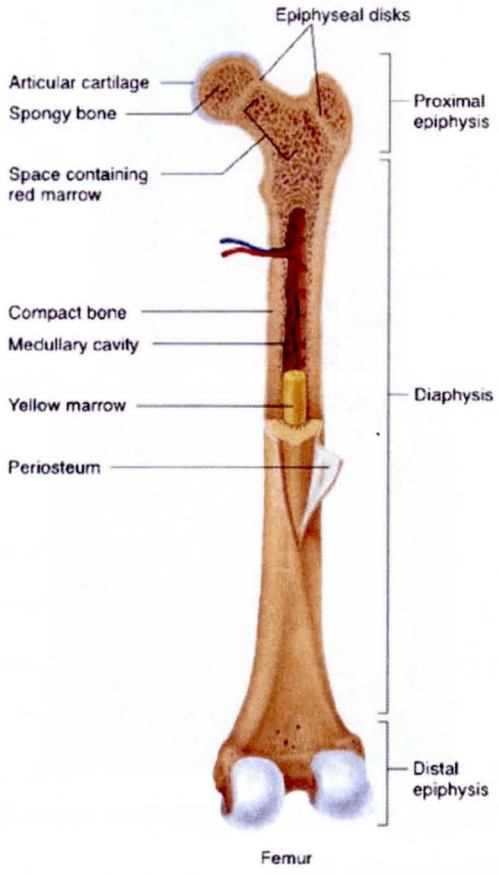

Figure 1.7. General structure of a mammalian bone [97].

Table 1. 3. Comparative composition and structural parameters of inorganic phase of adult human calcified tissue.

Composition /wt%	Enamel	Dentine	Cementum	Bone	HA
Calcium	36.5	35.1	*	34.8	39.6
Phosphrous	17.7	16.9	*	15.2	18.5
Ca/P (molar ratio)	1.63	1.61	*	1.71	1.67
Sodium	0.5	0.6	*	0.9	-
Magnesium	0.44	1.23	*	0.72	-
Pottasium	0.08	0.05	*	0.03	-
Carbonate (as CO_3^{2-})	3.5	5.6	*	7.4	-
Fluoride	0.01	0.06	*	0.03	-
Chloride	0.30	0.01	*	0.13	-
Pyrophosphate (as $P_2O_7^{4-}$)	0.022	0.10	*	0.07	-
Total inorganic	97	70	50	65	100
Total organic	1.5	20	35	25	-
Water	1.5	10	15	10	-
Typical crystal size (nm)	100 μm ×50 ×50	35 ×25 ×4	*	50 ×25 ×4	200-600
Ignition products (800 °C)	β-TCP+HA	β-TCP+HA	β-TCP+HA	HA+CaO	HA
Elastic modulus (Gpa)	80	15	*	0.34-1.38	10
Tensile strength (Mpa)	10	100	*	150	100

* Numerical values were not founf in the literature but they should similar to those of dentin

Teeth with dense structure are existed in the jaws of many vertebrates. The roles of teeth include to tear, smell and chew of food for all vertebrates and also to weapon for carnivores. Therefore, teeth have physically and chemically tough structure for compressive force (up to ~700 N), acidic foods and bacterial metabolism [109]. The structure of teeth is constructed by enamel, dentine, pulp, gum and cementum, and enamel with thickness of up to ~2 mm covers the teeth to protect other parts (Figure 1.8).

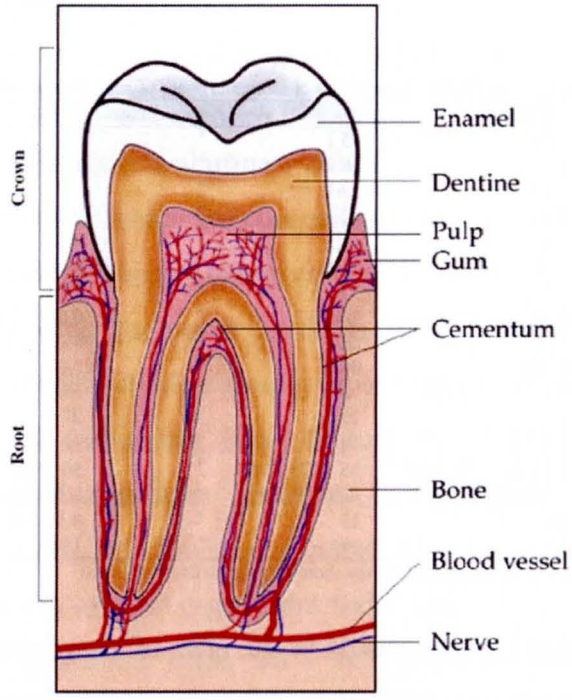

Figure 1.8. A schematic picture of a tooth. [101]

1.2. Application of calcium phosphate material

1.2.1. Calcium phosphate for biomaterial

Biomaterials are synthetic and natural materials using for replacing parts of a living system and intimately contacting between non-bioactive materials and living tissue [110], and are different from biological and biomimetic materials. Biological materials are produced by biological systems. While biomimetic materials not produced in living organisms, but these structures, compositions and properties are similar to those of biological materials. Synthetic calcium phosphates are classified into biomaterials due to these similarities to mineral bone and teeth. Application of these materials to repairing of teeth have been relative success, comparing to that shells, coral, ivory, wood, human teeth from corpses and metals had been used for covering in defected teeth reported by archaeological researchers.

In general, body might treat artificial implants as bioinert, biotolerant, bioactive or bioresourbable materials [110-112]. Calcium phosphates can be classified into bioactive and bioresorbable materials. A bioactive material tends to promote the formation of biological apatite rather than the dissolving, leading to the formation of a direct

chemical bond with bone. Such implants will provide good mechanical property in body. While, bioresorbable material will dissolve and allow a formation of new tissue. Highly crystallized HA has been proposed as a good example of bioactive materials, and porous scaffolds of BCP (α-TCP and HA or β-TCP and HA), CDHA and ACP will appear to be a example of bioresobable materials. Unfortunately, any calcium phosphate type biomaterials are not allowed to use in load-bearing area, due to their poor mechanical property. Therefore, the applications are currently limited in non-load-bearing area, such as filling of bone defects and coating of dental implants.

Biomaterials of calcium phosphates can be synthesized as various physical forms such as particles, blocks with dense or porous structure, injectable compositions, self-setting cements and coating on metal implants [113]. Especially, HA with porous structure has been paid much attention, because it can allow the formation of physical and chemical bonds with bone and to be covered with bone tissue [108]. Calcium phosphate particles with same size can be synthesized through sintering process. In this case, sintering time strongly affects the particle size, leading to the difference of surface area, pore volume and solubility. Thus, precise control of porosity, pore size and internal pore architecture are very important. General requirements for the ideal bone grafts are same size pores with the diameter of 100 μm, faster biodegradation rate than formation bone tissue and sufficient mechanical stability. Therefore, in main calcium phosphate type biomaterials, α-TCP, β-TCP and BCP are more preferable for medical use than HA, because of the higher solubility and faster resorption rate [26, 80, 114]. These calcium phosphates are also fabricated to various shapes for clinical use (Figure 1.9) [115].

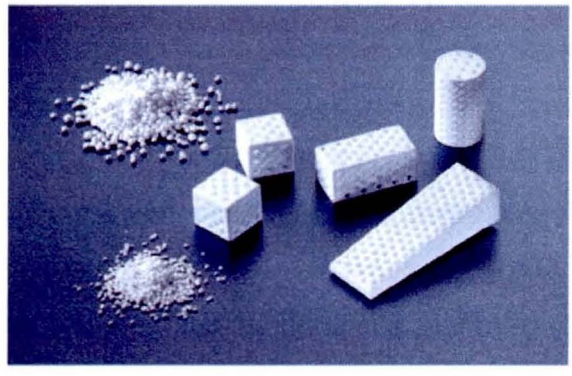

Figure 1.9. Examples of calcium phosphate based bone substitution materials.

1.2.2. Calcium phosphate cement

Calcium phosphate cement was introduced as another bone healing concept, and it can be obtained by mixing one or several reactive calcium phosphates with an aqueous solution to form a paste setting within restricted period of time [69, 116-129]. In this respect, calcium phosphate cement is different from traditional bone substituents such as granules and blocks. Now, companies are introducing various kinds of calcium phosphate cements and are also widening their portfolio to fulfill the various requirements from customers (Table 1.4) [68, 125, 130-138], since calcium phosphate cement was firstly proposed 2 decades ago [139, 140].

They can be classified into two types of calcium phosphate cements depending on the Ca/P ratio in the starting composition. The first type is dry mixture of two calcium phosphates with larger and smaller Ca/P molar ratios than that of HA. The Ca-rich (base) and P-rich (acid) calcium phosphates can smoothly transform into apatite by the acid-base reaction with each other. The second type is the same Ca/P molar ratio before and after cement setting, called a conversion reaction. A typical example is combination of ACP and α-TCP, affording to CDHA after the setting. Although almost calcium phosphate cements transform into biological apatite, there are also some reports on brushite-type cements, which transform into brushite. These brushite cements have proved to be faster resorption than apatite cements in animal studies [138].

Table 1. 4. List of commercial calcium phosphate cmenets with their composition (when available)

Company	Cement name	Components	End-product
ETEX	α-BSM Embarc Biobon	*Powder*: ACP (50%), DCPD (50%) *Solution*: H_2O (unbuffered saline solution)	Apatite
Stryker-Leibinger Corp.	BoneSource	*Powder*: TTCP (73%), DCP (27%) *Solution*: H_2O, mixture of Na_2HPO_4 and NaH_2PO_4	Apatite
Teknimed	Cementek®	*Powder*: α-TCP, TTCP, Na Glycerophosphate *Solution*: H_2O, $Ca(OH)_2$, H_3PO_4	Apatite
	Cementek®LV	*Powder*: α-TCP, TTCP, Na Glycerophosphate, dimethylsiloxane *Solution*: H_2O, $Ca(OH)_2$, H_3PO_4	Apatite
Biomet	Calcibon® (previously called "Biocement D")	*Powder*: α-TCP (61%), DCP (26%), $CaCO_3$ (10%), PHA (3%) *Solution*: H_2O, Na_2HPO_4	Apatite
	Minix™	*Powder*: TTCP, α-TCP, $C_6H_5O_7Na_3{\cdot}2H_2O$ *Solution*: H_2O, $C_6H_8O_7$	Apatite
	QuickSet Minix™	*Powder*: not found *Solution*: not found	Apatite
Mitsubishi materials	Biopex®	*Powder*: α-TCP (75%), TTCP (20-18%), DCPD (5%), HA (0-2%) *Solution*: H_2O, sodium succinate, sodium chondroitin sulphate	Apatite
	Biopex®-R	*Powder*: α-TCP, TTCP, DCPD, HA, $Mg_3(PO_4)_2$, $NaHSO_3$ *Solution*: H_2O, sodium succinate, sodium chondroitin sulphate	Apatite
Kyphon	KyphOs™	*Powder*: α-TCP (77%), $Mg_3(PO_4)_2$ (14%), $MgHPO_4$ (4.8%), $SrCO_3$ (3.6%) *Solution*: H_2O, $(NH_4)_2HPO_4$ (3.5 M)	Apatite
Skeltal Kinetics	Callos™	*Powder*: not found[a] *Solution*: not found[a]	Apatite
Shanghai Rebone Biomaterials Co, Ltd	Rebone	*Powder*: TTCP, DCP *Solution*: H_2O	Apatite
Synthes-Norian	Norian® SRS Norian® CRS	*Powder*: α-TCP (85%), $CaCO_3$ (12%), MCPM (3%) *Solution*: H_2O, Na_2HPO_4	Apatite
	Norian® SRS Fast Set Putty Norian® CRS Fast Set Putty	*Powder*: not found[a] *Solution*: not found[a]	Apatite
	ChronOC™ Inject	*Powder*: β-TCP (73%), MCPM (21%), $MgHPO_4{\cdot}3H_2O$ (5%), $MgSO_4$ (<1%), $Na_4H_2P_2O_7$ (<1%) *Solution*: H_2O, sodium hyaluronate (0.5%)	Brushite
Kasios	Eurobone	*Powder*: β-TCP (98%), $Na_4P_2O_7$ (2%) *Solution*: H_2O, H_3PO_4 (3.0 M), H_2SO_4 (0.1 M)	Brushite
CalciphOs	VitalOs	*Component 1*: β-TCP (1.34 g), $Na_2H_2P_2O_7$ (0.025 g), H_2O, salts (0.05 M, pH 7.4 PBS solution) *Component 2*: MCPM (0.78 g), $CaSO_4{\cdot}2H_2O$ (0.39 g), H_2O, H_3PO_4 (0.05 M)	Brushite

[a] Not found in the literature or on the web.

During cement setting, calcium phosphates are firstly dissolved and precipitated around less soluble calcium phosphate particles, and the crystal grows and entangles with biological apatite, affording the mechanically rigid structure. Setting of these cements occurs mostly within 6 hours, yielding an 80% conversion to the final product and a compressive strength of 40-60 MPa [69, 116, 118-120, 125, 127, 128].

M. Bohner has claimed several directions as new trends of calcium phosphate

cements as follow; (i) study on basic properties (setting time and injectability), (ii) amorphous calcium phosphate, (iii) synthesis of granules and blocks and (iv) surgeon's needs [141]. Here, I briefly introduce feature of ACP, which strongly affect for the setting time and next transformation rate into apatite or brushite. Initially, ACP was obtained by precipitation. Recently, several authors synthesized amorphous-like calcium phosphate powders (it is called "amorphous calcium phosphate" and, not same but similar original ACP) by mechanical activation after high energy ball milling [142, 143]. As a result, "amorphise" or "micronise" calcium phosphate compound can be obtained from all crystalline phases regardless of the chemical composition such as Ca/P molar ratio. The advantage of this new technique compared to traditional precipitation method is two points: first, these new amorphous calcium phosphate powders require less mixing liquid than original calcium phosphate cements, leading to higher mechanical properties, second, the synthesis is more reproducible and mechanically activated calcium phosphate powders seem to be more stable against aging effects and recrystallization than original ACP. However, there is also very large risk of incorporating wear particles. Additionally, it is difficult to prevent the agglomeration during dry milling or the presence of organic residues during wet milling. Nevertheless, the possibility of using amorphous calcium phosphates opens up new perspective in term of fast setting time, fast transformation rate into apatite and incorporation of foreign ions in the structure.

1.2.3. Catalytic activity of calcium phosphates

The application of calcium phosphate can be expected for use as not only biomaterials but also catalysts. Some research groups have already reported on the potential application of calcium phosphate (especially nonstoichiometric HA) as catalysts. S. Sugiyama and co-workers studied the catalytic activity of HA successfully applied to the unique function of ion-exchange ability [4-6]. For example, HA with Ca^{2+} partially replaced by strontium ions showed oxidative dehydrogenation of ethane in the presence of tetrachloromethane. Direct synthesis of phenol from benzene has also been reported over HA containing both Ca^{2+} and Cu^{2+} ions in its cation portion. K. Mori and co-workers studied use of metal supported on HA, which showed high catalytic activity in oxidation of alcohols [7]. J. A. S. Bett and co-workers studied the application of nonstoichiometric HA itself [8-14]. For example, HA with a low Ca/P ratio showed a

lower activity to convert ethanol to ethylene or butanol to butene than popular catalysts such as zeolite and aluminum through dehydration process. Whereas nonstoichiometric HA with a high Ca/P ratio converted alcohol to aldehyde or ketone through dehydrogenation process. In such nonstoichiometric HA, the presence of acid and new base sites would be proposed due to the electrical imbalance caused by the loss of Ca^{2+} ions and/or the structural defect.

Recently, it has also been proposed that poorly crystallized HA shows both acidic and basic catalytic activities whether the Ca/P ratio is stoichiometric or not [15]. According to the report, the poorly crystallized HA with the Ca/P molar ratio of 1.52 converted ethanol to ethylene with 80% selectivity by dehydration. However, small amounts of acetaldehyde and/or diethyl ether, which are not formed on solid acid catalysts such as Al_2O_3 or zeolite, was also produced on such P rich HA, suggesting the presence of a large number of acid sites and even a small amount of base sites. In the same reaction, *n*-butanol was also obtained with Ca richer HA. When the Ca/P molar ratio was increased, the selectivity of ethylene was decreased and that of acetaldehyde was increased (Figure 1.10 [15]). Other alcohols sush as *n*-hexanol, *n*-octanol, *n*-decanol and corresponding branched alcohols were also formed with this HA with the Ca/P ratio of 1.64 under the reaction condition with different contact time or temperature (Figure 1.11) [15].

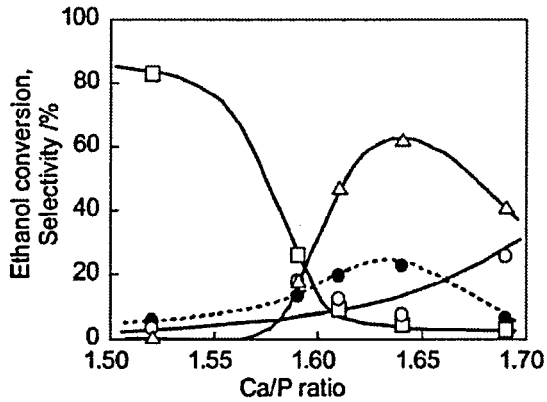

Figure 1.10. Relationship between Ca/P molar ratio of HA and ethanol conversion (conversion●) and selectivities of products. Selectivity to *n*-butanol, ethylene and acetaldehyde are shown as Δ, □ and ○, respectively.

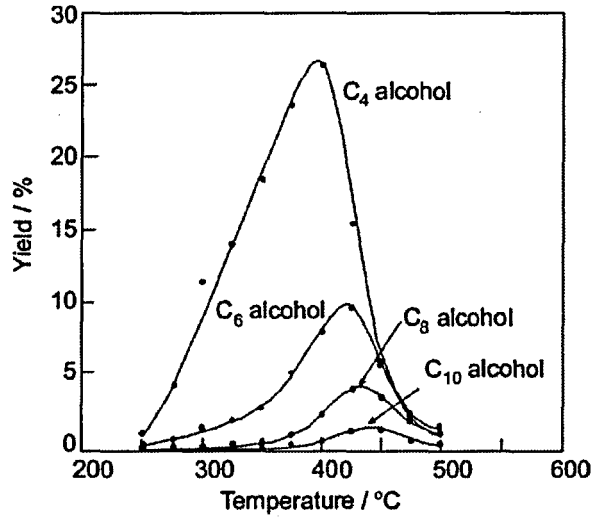

Figure 1.11. Effect of reaction temperature on yields of various alcohols from ethanol on HA with the Ca/P molar ratio of 1.64.

From these above reports, the potential catalytic ability of calcium phosphate itself with both acid and base sites which were strongly affected by Ca/P ratio and structural defect was demonstrated. However, the surface area of calcium phosphate with ionic bonded frameworks is lower (~100 m^2 g^{-1}) than covalently bonded inorganic materials. Thus, structural control of calcium phosphates for the improvement of their catalytic activity is absolutely one of most important problem.

1.3. Hybridization of calcium phosphate with organic molecules

1.3.1. Structural control of inorganic/organic composite materials

Structural control of inorganic materials has been opening up the potential as highly-functional materials to various fields such as absorbents, separations, catalysts, drug delivery agents, sensors and photonics. Structure of inorganic materials has easily been controlled by various kinds of methods at atomic level (~1.2 nm), but not nano- (2.0-50 nm) and macro- (50 nm~) ordered levels [144-149]. Therefore, the use of organic compounds as a template for the nano- and macro-ordered structural design of inorganic materials has attracted much attention over the last decade [150-154]. Polymers, surfactants and biomolecules, which possess self-assembling ability at nano- or macro-level, have been used as templates, affording to various kinds of structure such

as macro-ordered fibers [155], tubes [156], porous spheres (Figure 1.12) [157] and twisted ribbons [158] and nano-ordered porous materials [159-165] after removing the templates. These materials have noteworthy features to satisfy many demands from the various fields.

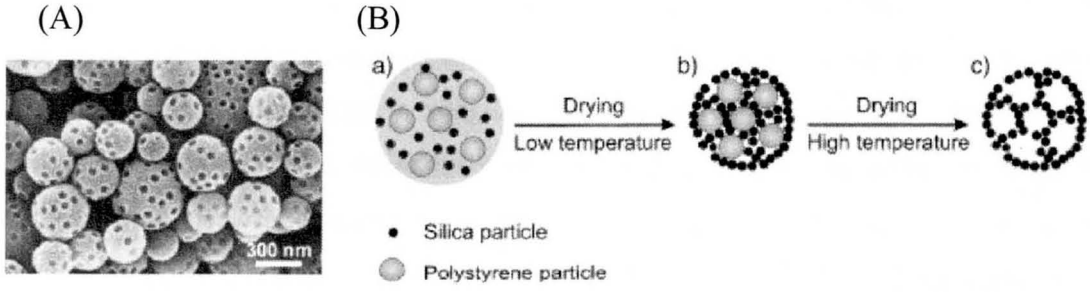

Figure 1.12. (A) SEM image of spherical silica powders, and (B) formation of a silica sphere with templated mesopores.

Nano-ordered porous material, which is commonly called mesoporous material with high surface area (~1000 m^2 g^{-1}) and narrow and tunable pore size distribution (2-10 nm), have been attractive candidate of research, since Japanese scientists and Mobil scientists separately reported the synthesis of mesoporous silicas (which are called FSM-16 and MCM-41, respectively) in the early 1990s [159, 162, 163]. These mesoporous silicas have strongly been hoped for using catalytic supports for reaction with larger molecules than micropores, because the large molecules cannot react in microporous catalysts such as zeolite. The frameworks of zeolites and zeolite-like microporous materials are atomically crystallized, whereas mesoporous silicas are nano-ordered materials, but atomically its frameworks are amorphous. Therefore, these two types of materials exhibit many different properties such as synthetic method, thermal stability and surface property. Mesoporous silicas can be obtained in shorter reaction time (within several days) and at lower reaction temperature (r.t.~130 °C) than zeolite (several days~even months, 80~300 °C). The morphologies of zeolites are strongly related to their structures and are difficult to control because zeolites are a kind of perfect crystal. In construct, mesoporous silicas exhibit various morphologies such as thin films, spheres, monoliths and fibers [166-168].

A large number of studies have been carried out to investigate the formation of mesostructures on the basis of surfactant self-assembly. The initial liquid-crystal

template mechanism reported by Mobil's scientists is essentially always true, because the pathways basically include almost all possibility [162, 163]. However, two pathways, which are cooperative self-assembly and true liquid-crystal templating processes, have been proposed (Figure 1.13) [169-172]. M. Davis and co-workers proposed a "silicate rod assembly" mechanism [173]. Two or three monolayers of silicate species first deposite on isolated surfactant micellar rods. The long surfactant-silicate rods spontaneously aggregate and eventually pack into a long-range ordered hexagonal arrangement. However, cooperative formation mechanism has been accepted by most researchers because of the difference of phase diagrams between self-assembled surfactant micelle and the mesostructured silicas prepared by the surfactant micelle as a template [174, 175].

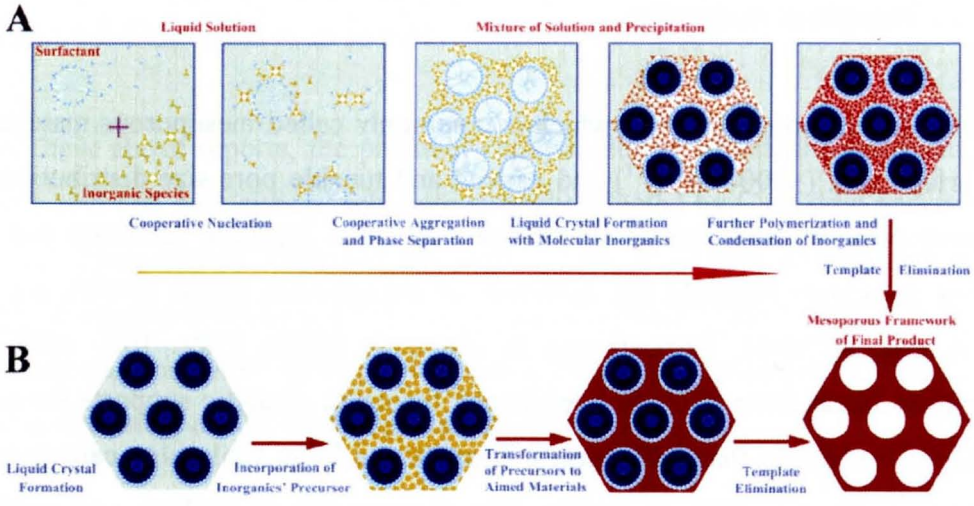

Figure 1.13. Two synthetic strategies of mesoporous materials: (A) cooperative self-assembly; (B) true liquid-crystal templating process.

1.3.2. Interaction between inorganic and organic species in composite material

Interactions at interface between inorganic and organic species during the formation of mesoporous materials have been studied by several research groups. Table 1.5 lists the proposed synthetic routes with surfactants and classical products [163, 171, 174-187]. G. D. Stucky and co-workers proposed four general synthetic routes, which are S^+I^-, S^-I^+, $S^+X^-I^+$ and $S^-X^+I^-$ (S^- = surfactant anions, S^+ = surfactant cations, I^- = inorganic precursor anions, I^+ = inorganic precursor cations, X^+ = cationic counterions and X^- = anionic counterions) [174, 175]. Under basic condition, silicate anions (I^-)

match with surfactant cations (S^+) through Coulomb forces (S^+I^-) [163, 176-180]. One of the examples of S^-I^+ interaction occurs between cationic Keggin ion (Al_{13}^{7+}) and anionic surfactant like dodecylbenzensulfonate salt [174]. In the synthesis of mesoporous silicates by $S^+X^-I^+$ interaction, X^- is halogen ions, SO_4^{2-} and NO_3^-. In strong acidic medium, initial $S^+X^-I^+$ interaction through Coulomb force, and the interaction gradually transform into the $(IX)^-S^+$ one [174, 177, 181].

Table 1. 5. Synthesis route to mesoporous materials with the emphasis on silicates

Route	Interactions	Symbols	Conditions	Classical products
S^+I^-	Electrostatic Coulomb force	S^+: cationic surfactants I^-: anionic silicate species	Basic	MCM-41, MCM-48, MCM-50, SBA-6, SBA-2, SBA-8, FDU-2, FDU-11, FDU-13, etc.
S^-I^+	Electrostatic Coulomb force	S^-: anionic surfactants $C_nH_{2n+1}COOH$, $C_nH_{2n+1}SO_3H$, $C_nH_{2n+1}OSO_2H$, $C_nH_{2n+1}OPO_2H$ I^+: tranditional metal ions, such as Al^{3+}	Aqueous	Mesoporous alumina, etc.
$S^+X^-I^+$	Electrostatic Coulomb force, double layer H bond	S^+: cationic surfactants I^-: anionic silicate species X^-: Cl^-, Br^-, I^-, SO_4^{2-}, NO_3^-	Acidic	SBA-1, SBA-2, SBA-3
$S^-X^+I^-$	Electrostatic Coulomb force, double layer H bond	S^-: anionic surfactants $C_nH_{2n+1}COOH$, $C_nH_{2n+1}SO_3H$, $C_nH_{2n+1}OSO_2H$, $C_nH_{2n+1}OPO_2H$ I^-: tranditional metal ions, WO_4^{2-}, $Mo_2O_7^-$ X^+: Na^+, K^+, Cr^{3+}, Ni^{2+}, etc.	Basic	W, Mo oxides
S^0I^0 (N^0I^0)	H bond	S^0: nonionic surfactants, oligomeric surfactants N^0: $C_nH_{2n+1}NH_2$ I^0: silicate species	Neutral	HMS, MSU, disordered worm-hole like mesoporous silicas
$S^0H^+X^-I^+$	Electrostatic Coulomb force, double layer H bond	S^0: nonionic surfactants I^+: silicate species X^-: Cl^-, Br^-, I^-, SO_4^{2-}, NO_3^-	Acidic, pH < ~2	SBA-*n* (*n* = 11, 12, 15 and 16), FDU-*n* (*n* = 1, 5 and 16), KIT-*n* (*n* = 5 and 6)

Hydrogen-bonding interaction mechanisms, denoted to S^0I^0 or N^0I^0, were also proposed by Pinnavaia and co-workers for preparing mesoporous silicates under neutral conditions [188, 189]. S^0 are nonionic surfactants, N^0 are neutral amines and I^0 are hydrated silicate oligomers from TEOS. Oligomeric alkyl PEO surfactant (S^0), triblock copolymers (S^0) and organic long-chain alkyl amines (N^0), such as primary alkylamines and *N*, *N*-dimethylalkylamines, have been used as nonionic surfactants, and these surfactants (S^0 and N^0) are probably partially protonated or charged. The synthesis of mesoporous silica SBA-15 was carried out under strongly acidic conditions by using triblock copolymer P123 as a template [163]. It is more likely a double-layer hydrogen-bonding of $S^0H^+X^-I^+$ interaction. These synthetic routes of mesoporous silicas

can be also applied to other inorganic components with covalently bonded frameworks such as metal oxides and metal phosphates [190-207]. However, understanding of the interaction between organic and inorganic species except silica has not been discussed in detail so far.

1.3.3. Previous study of mesostructured and mesoporous calcium phosphates

The syntheses of mesostructured and mesoporous calcium phosphates with ionitically bonded frameworks have also been investigated by several researchers (Table 1.6), [208-214]. G. A. Ozin and co-workers firstly reported the synthesis of lamellar mesostructured calcium phosphate which was alternatively stacked by inorganic and organic sheets using *n*-dodecylphosphate ($C_{12}H_{25}OPO_3H$) in water solvent system [208]. The micro-ordered structure of inorganic sheets is not assignable to crystalline calcium phosphates such as HA, DCPD and OCP but due to original phase of calcium *n*-dodecylphosphate salt. The syntheses of lamellar mesostructured calcium phosphates including the same structure of HA in inorganic sheets were separately reported by using $C_{12}H_{25}OPO_3H$ [208, 209] and sodium *n*-dodecylsulfate ($C_{12}H_{25}OSO_3Na$) [210] in water and/or ethanol solvent systems. Z. Y. Yung and co-workers reported the synthesis of lamellar mesostructured calcium phosphate using *n*-hexadecylamine in water solvent system [211]. Syntheses of wormhole-like mesoporous calcium phosphates using *n*-hexadecyltrimethylammonium bromide ($C_{16}H_{33}N(CH_3)_3Br$) and $EO_{99}PO_{65}EO_{99}$ (F127) were also reported by Y. Tokuda [212] and Y. F. Zhao [213], respectively. These inorganic frameworks include crystalline calcium phosphate phases such as DCPA or HA. Although TEM images of these mesoporous calcium phosphates showed wormhole-like mesopores, these surface areas were not described. S. M. Schmidt and co-workers also reported the synthesis of nanosized calcium phosphate rod with mesopores at the interparticles by using both $C_{12}H_{25}OPO_3H$ and $C_{16}H_{33}N(CH_3)_3Br$, and the BET surface area is 90 $m^2 g^{-1}$ [214].

Table 1. 6. Synthesis of mesostructured and mesoporous calcium phosphates

	Surfactants	Solvent	pH	Nano-ordered phases	Micro-ordered phases	Surface area /$m^2 g^{-1}$
Mesostructured calcium phosphate						
G A. Ozin et al.	$C_{12}H_{25}OPO_3H_2$	H_2O	8-9	Lamellar	[a]	-
G A. Ozin et al.	$C_{12}H_{25}OPO_3H_2$	H_2O	8-9	Lamellar	HA	-
S. Zhang et al.	$C_{12}H_{25}OPO_3H_2$	H_2O and EtOH	[b]	Lamellar	HA	-
Z. Y. Yung et al.	$C_{16}H_{33}NH_2$	H_2O	5	Lamellar	[b]	-
C. Liu et al.	$C_{12}H_{25}SO_3Na$	H_2O and EtOH	[b]	Lamellar	HA	-
Mesoporous calcium phosphate						
Y. Tokuda et al.	$C_{16}H_{33}N(CH_3)_3Br$	H_2O	[b]	Wormhole-like	DCPA	[b]
Y. F. Zhao et al.	$EO_{99}PO_{65}EO_{99}$(F127)	H_2O	12	Wormhole-like	HA	[b]
S. M. Schmidt et al.	$C_{12}H_{25}OPO_3H_2$ and $C_{16}H_{33}N(CH_3)_3Br$	H_2O	11.8	(nanosized rod)	DCPD, OCP	90 (BET)

[a] Original phase without crystalline calcium phosphate phases (DCPD, OCP, TCPs, HA, and so on)
[b] No data

The surfactant templating synthetic method of mesostructured and mesoporous calcium phosphates has not been achieved yet. Especially, understanding of interaction at interface between ionitically bonded inorganic frameworks and organic species on the synthesis of mesostructured calcium phosphates has not been discussed. Whereas numerous synthetic methods of composite material composed of self-assembled surfactants and amorphous inorganic species with covalently bonded frameworks have already been reported as precursor of mesoporous materials before removing of the surfactant molecules [159-207]. According to the reports, the hydrophilic head groups of surfactant can interact with inorganic species through electrostatic Coulomb force or weak H bond, and their structure is controlled by that of surfactant micelles. The structural control of the composite materials can be allowed by only structurally flexible amorphous inorganic frameworks with covalent bond. Therefore, it is not easy to apply the synthetic method for calcium phosphate with ionitically bonded frameworks. For the synthesis of composite materials of calcium phosphate and organic molecules, the most important point is how to suppress the crystallization of calcium phosphate species.

Freeze-drying method has been well-known to synthesize amorphous calcium phosphate. However, the reaction time is too short to complex calcium phosphate species and organic molecules in this method. Mixed solvent system of alcohol and water can be proposed as a candidate of another way for suppressing calcium phosphate species. In a reaction between calcium and phosphate ions, amorphous and/or poorly crystallized calcium phosphate firstly forms, and its structure recrystallizes into higher crystalline one through the repeat ionization and precipitation processes. Because the ionization can be inhibited in the alcohol/water mixed solvent system, this system

would be useful for the formation of calcium phosphate and organic molecule composite materials. Indeed, M. J. Larson and co-workers reported that poorly crystallized monetite (DCPA: $CaHPO_4$), which was anhydrated crystalline calcium phosphate generally precipitated at high temperature above 80 °C, was formed at room temperature instead of hydrated brushite (DCPD: $CaHPO_4 \cdot 2H_2O$) in the mixed solvent system of ethanol and water [215].

1.4. Objective of the thesis

In this research, I investigated the facile synthetic route of composite material of calcium phosphate with several kinds of simple organic molecules based on the concept of suppressing the crystallization of calcium phosphate frameworks, unlike previous mesostructured calcium phosphates including original crystalline calcium phosphate phases such as DCPD, DCPA, HA and OCP. This synthetic method has high potential for structural control of calcium phosphate at micro- and nano-ordered levels, because structure of organic molecules can affect that of calcium phosphate species. Organic molecules with carboxyl and/or amino groups, such as alkylamines, aliphatic acids and amino acids, are lined up as candidates due to the similarity to biomolecules. In Chapter 2, I investigated the synthesis of composite materials of calcium phosphate with *n*-alkylamines, and lamellar mesostructured calcium phosphates, which were alternatively stacked calcium phosphate and *n*-alkylamine sheets, can be obtained without any original crystalline calcium phosphate phases in the mixed solvent system of alcohol and water. On the basis of the result in Chapter 2, I demonstrated that composite materials of calcium phosphate with alkylamines were formed under the synthetic condition which is suppressing the original crystalline calcium phosphate formations. Lamellar mesostructured magnesium phosphate can also be obtained in the similar synthetic condition (Chapter 3). Lamellar mesostructured calcium phosphate can also be obtained using palmitic acid in mixed solvent system of ethanol and water, and it was demonstrated that composite material of calcium phosphate with carboxylic acid type organic molecule can also be obtained under the synthetic condition which is suppressing the original crystalline calcium phosphate formations (Chapter 4). In addition, wormhole-like mesostructured calcium phosphates can also be formed using

diamine-type (dodecyldiethylenetriamine) and dicarboxylic-type (*N*-lauroyl-L-glutamic acid) surfactants because layered structures were distorted by the surfactants with large head group. In Chapter 5, I studied the surface property on the mesoporous calcium phosphate prepared from wormhole-like mesostructured calcium phosphate after removing of the surfactant. In Chapter 6, I investigated the synthesis of composite material with amino acids which are the smallest units in biomolecules, and amorphous composite materials of calcium phosphate and amino acid can be obtained. The amorphous composite material can more fastly transform into hydroxyapatite than crystalline calcium phosphates in simulated body fluid (SBF). Calcium phosphate cement with the amorphous amino acid/calcium phosphate composite material can also be more smoothly transformed into apatite in SBF than additive-free calcium phosphate cement. On the basis of the results, I revealed the interactions between calcium phosphate species and organic molecules with amino and/or carboxylic acid groups and the characteristics of the composite materials constructed by calcium phosphate and organic molecule.

References

1 M. Jarcho, *Clin. Orthop. Relat. Res.*, 1981, **157,** 259.

2 P. Ducheyne and Q. Qiu, *Biomaterials,* 1999, **20,** 2287.

3 H. W. Kim, G. Georgiou, J. C. Knowles, Y. H. Koh and H. E. Kim, *Biomaterials,* 2004, **25,** 4203.

4 S. Sugiyama, T. Miyamoto, H. Hayashi and J. B. Moffat, *J. Mol. Catal.* A, 1998, **135**, 199.

5 B. Liptakova, M. Hronec and Z. Cvergrosova, *Catal, Today*, 2000, **61**, 143.

6 S. Sugiyama, H. Mitsuoka, T Shono, T. Moriga and H. Hayashi, *J. Chem. Eng. Jpn.*, 2003, **36**, 210.

7 K. Mori, T. Hara, T. Mizugaki, K. Ebitani and K. Kaneda, *J. Am. Chem. Soc.*, 2003, **125**, 11460.

8 J. A. S. Bett, L. G. Christner and W. K. Hall, *J. Am. Chem. Soc.*, 1967, 5135.

9 J. A. S. Bett and W. K. Hall, *J. Catal.* 1968, **10**, 105.

10 S. J. Joris and C. H. Amberg, *J. Phys. Chem.*, 1971, **75**, 3167.

11 C. L. Kibby, S. S. Lande and W. K. Hall, *J. Am. Chem. Soc.*, 1972, **94**, 214.

12 C. L. Kibby and W. K. Hall, *J. Catal.*, 1973, **31**, 65.

13 H. Monma, *J. Catal.*, 1982, **75**, 200.

14 Y. Matsumura and J. B. Moffat, *J. Chem. Soc., Faraday Trans.*, 1996, **92**, 1981

15 T. Tsuchida, S. Sakuma, T. Takeguchi and W. Ueda, *Ind. Eng. Chem. Res.*, 2006, **45**, 8634.

16 K. Kandori, A. Fudo and T Ishikawa, *Phys. Chem. Chem. Phys.*, 2000, **2**, 2015.

17 S. Aoki, A. Nakahira, H. Nakayama, K. Sakamoto, S. Yamaguchi, K. Suganuma, *J. Phys. Chem. Sol.*, 2004, **65**, 465.

18 J. G. Rio, P. Sanchez, P. J. Morando and D. S. Cicerone, *Chemosphere*, 2006, **64**, 1015.

19 Y. Hashimoto and T. Sato, *Chemosphere*, 2007, **69**, 1775.

20 K. Kandori, S. Tsuyama, H. Tanaka and T Ishikawa, *Colloids Surf.* B, 2007, **58**, 98.

21 P. H. Chen, Y. H. Tseng, Y. Mou, Y. M. Tsai, S. J. Guo, S. J. Huang, S. S. F. Yu and C. C. Chan, *J. Am. Chem. Soc.*, 2008, **130**, 2862.

22 J. Berzelius, *Ann. Chem. Pharmac.*, 1845, **53**, 286.

23 H. Hausen, *Acta. Acad. Abo. Ser.* B: *Mat. Phys. Mat. Natur. Teknik*, 1929, **5**, 62.

24 A. K. Lynn and W. Bonfield, *Acc. Chem. Res.*, 2005, **38**, 202.

25 D. R. Lide, The CRC hand book of chemistry and physics, 86th edn. CRC Press, Boca Raton, Florida, 2005, p. 2544.

26 R. Z. Legeros, Calcium phosphate in oral biology and medicine, Karger, Basel, 1991.

27 A. J. G. Notholt, R. P. Sheldon and D. F. Davidson, *Phosphate deposites of the world*, vol 2. Cambridge University Press, Cambridge, 1989.

28 P. Becker, In: *Fertilizer science and technology series*, 2nd edn. Marcel Dekker, New York p. 760.

29 A. A. Mirtchi, J. Lemaitre and N. Terao, *Biomaterials*, 1989, **10**, 475.

30 A. A. Mirtchi, J. Lemaitre and E. Munting, *Biomaterials*, 1989, **10**, 634.

31 O. Bermúdez, M. G. Boltong, F. C. M. Driessens and J. A. Planell, *J. Mater. Sci. Mater. Med.*, 1994, **5**, 67.

32 O. Bermúdez, M. G. Boltong, F. C. M. Driessens and J. A. Planell, *J. Mater. Sci. Mater. Med.*, 1994, **5**, 160.

33 F. C. M. Driessens, M. G. Boltong, O. Bermúdez, J. A. Planell, M. P. Ginebra and E. Fernández, *J. Mater. Sci. Mater. Med.*, 1994, **5**, 164.

34 S. Budavari, M. J. O'neil, A. Smith P. E. Heckelman and J. F. Kinneary, The Merck Index: an encycropedia of chemicals, drugs, and biological, 12th edn. Chapman & Hall, 1996, p. 1741.

35 J. J. Crall and J. M. Bjerga, *J. Oral. Pathol.*, 1987, **16**, 488.

36 J. S. Wefel and J. D. Harless, *J. Dent. Res.*, 1987, **66**, 1640.

37 P. M. Hoppenbrouwers, E. Groenendijik, N. R. Tewarie and F. C. M. Driessens, *J. Dent. Res.*, 1988, **67**, 1254.

38 A. Gaffar, J. Blake-Haskins and J. Mellberg, *Int. Dent. J.*, 1993, **43**, 81.

39 S. Cazalbou, C. Combes, D. Eichert and C. Rey, *J. Mater. Chem.*, 2004, **14**, 2148.

40 W. E. Brown, *Clin. Orthop.*, 1966, **44**, 205.

41 S. Kamakura, Y. Sasano, H. Honma, O. Suzuki, M. Kagayama and K. Motegi, *J. Dent. Res.*, 1999, **78**, 1682.

42 S. Kamakura, Y. Sasano, H. Honma, O. Suzuki, M. Kagayama and K. Motegi, *J. Dent. Res.*, 2001, **7**, 259.

43 F. Sargolzaei-Aval, A. Sobhani, M. R. Arab, S. A. Sarani and M. H. Heydari, Iran. *J. Med. Sci.*, 2004, **29**, 124.

44 O. Suzuki, S. Kamakura, T. Kitagiri, M. Nakamura, B Zhao, Y. Honda and R. Kamijo, *Biomaterials*, 2006, **27**, 2671.

45 A. A. Mirtchi, J. Lemaitre and E. Munting, *Biomaterials*, 1990, **11**, 83.

46 A. A. Mirtchi, J. Lemaitre and E. Munting, *Biomaterials*, 1991, **12**, 505.

47 J. Lemaitre, E. Munting, and A. A. Mirtchi, *Rev Stomatol Chir Maxillofac*, 1992, **93**, 163.

48 K. Ohkura, M. Bohner, P. Hardouin, J. Lemaitre, G. Pasquier and B. Flautu, *J. Biomed. Mater. Res.*, 1996, **30**, 193.

49 J. C. Elliot, In: Brès E, Hardouin P (eds) Les Matériaux en phosphate de calcium. Aspects fondamentaux. Sauramps Medical, Montpellier.

50 N. Rangavittal, A. R. Landa-Cánovas, J. M. González-Calbet and M. Vallet-Regi, *J. Biomed. Mater. Res.*, 2000, **51**, 660.

51 J. Y. Kim, R. R. Fenton, B. A. Hunter and B. J. Kennedy, *Austr. J. Chem.*, 2000, **53**, 679.

52 C. Hamanishi, K. Kitamoto, K. Ohura, S. Tanaka and Y. Doi, *J. Biomed. Mater. Res.*, 1996, **32**, 383.

53 W. Suchanek and M. Yoshimura, *J. Mater. Res.*, 1998, **13**, 94.

54 G. Willmann, *Adv, Eng, Mater.*, 1999, **1**, 95.

55 L. Sun, C. C. Berndt, K. A. Gross and A. Kucuk, *J. Miomed. Mater. Res.*, 2001, **58**, 570.

56 J. L. Ong and D. C. N. Chan, *Crit. Rev. Biomed. Eng*, 1999, **28**, 667.

57 R. G. Geesink, *Clin, Orthop, Rel, Res.*, 2002, **395**, 53.

58 L. L. Hench, *J. Am. Cream. Soc*, 1991, **74**, 1487.

59 L. L. Hench, *J. Am. Cream. Soc*, 1998, **81**, 1705.

60 R. Z. Legeros and J. P. Legeros, In: L. L. Hench and J. Wilson (eds) An introduction to bioceramics. World Scientific, London, p. 139.

61 M. Markovic, B. O. Fowler and M. S. Tung, *J. Res. Natl. Inst. Stand. Technol.*, 2004, **109**, 553.

62 P. Layrolle and A Lebugle, *Chem. Mater.*, 1994, **6**, 1996.

63 P. Layrolle and A Lebugle, *Chem. Mater.*, 1996, **8**, 134.

64 B. Yeong, X. Junmin and J. Wang, *J. Am. Cream. Soc*, 2001, **84**, 465.

65 M. L. Montero, A. Sáenz, J. G. Rodríguez, J. Arenas and V. M. Castaño, *J. Mater. Chem.*, 2006, **41**, 2141.

66 W. E. Brown and E. F. Epstein, *J. Res. Nat. Bur. Stand.*, 1965, **69A**, 547.

67 M. Ohtsuka, Y. Matsuda, Y. Suwa, J. L. Fox and W. I. Higuchi, *Chem. Pharm. Bull.*, 1993, **41**, 2055.

68 K. Kurashina. H. Kurita. M. Hirano. A. Kotani, C. P. Klein and K. de Groot, *Biomaterials*, 1997, **18**, 539.

69 Y. Fukase, E. D. Eanes, S. Takagi, L. C. Chow and W. E. Brown, *J. Dent. Res.*, 1990, **69**, 1852.

70 O. Bermúdez, M. G. Boltong, F. C. M. Driessens and J. A. Planell, *J. Mater. Sci. Mater. Med.*, 1994, **5**, 144.

71 L. C. Chow, *Nippon Seramikkusu Kyoukai Gakujutsu Ronbunshi*, 1991, **99**, 954.

72 J. D. Termine and E. D. Eanes, *Calcif. Tissue Res.* 1972, **10**, 171.

73 E. D. Eanes, J. D. Termine and M. U. Nylen, *Calcif. Tissue Res.* 1973, **12**, 143.

74 J. L. Meyer and E. D. Eanes, *Calcif. Tissue Res.* 1978, **28**, 59.

75 J. L. Meyer and E. D. Eanes, *Calcif. Tissue Res.* 1978, **28**, 209.

76 R. E. Wuthier, G. S. Rice, J. E. Wallace, R. L. Weaver, R. Z. LeGeros and E. D. Eanes, *Calcif. Tissue Int.* 1985, **37**, 401.

77 V. A. Sinyaev, E. S. Shustikova, L. V. Levchenko and A. A. Sedunov, *Inorg, Mater.*, 2001, **37**, 619.

78 G. Daculsi, J. M. Bouler and R. Z. Legeros, *Int. Rev. Cytology.*, 1997, **172**, 129.

79 D. Tadic, F. Peter and M. Epple, *Biomaterials*, 2002, *23*, 2553.

80 R. Z. Legeros, P. W. Brown and B. Constantz, Hydroxyapatite and related materials. CRC Press, Boca Raton, 1994, p. 3.

81 R. Z. Legeros, Z Kardiol (Suppl. 3):III/116.

82 A. Hesse and D. Heimbach, *World J. Urol.*, 1999, **17**, 308.

83 D. Skrtic, A. W. Hailer, S. Takagi, J. M. Antonucci and E. D. Eanes, *J. Dent. Res.*, 1996, **75**, 1679.

84 D. Skrtic, J. M. Antonucci and E. D. Eanes, *Dental. Mater.*, 1996, **12**, 295.

85 M. S. Park, E. D. Eanes, J. M. Antonucci and D. Skrtic, *Dental. Mater.*, 1998, **14**, 137.

86 D. Skrtic, J. M. Antoucci, E. D. Eanes, F. C. Eichmiller and G. E. Schumacher, *J. Biomed, Mater, Res.*, 2000, **53**, 381.

87 M. Julien, I. Khairoun, R. Z. LeGeros, S. Delplace, P. Pilet, P. Weiss, G. Daculsi, J. M. Bouler and J. Guicheux, *Biomaterials*, 2007, **28**, 956.

88 J. E. Harries, D.W. L. Hukins, C. Holt and S. S. Hasnain, *J. Cryst. Growth.*, 1987, **84**, 563.

89 M. G. Taylor, K. Simkiss, J. Simmons, L. N. Y. Wu and R.E. Wuthier, *Cell. Mol. Life Sci.*, 1998, **54**, 192.

90 F. Peters, K. Schwarz and M. Epple, *Thermochim, Acta*, 2000, **361**, 131.

91 K. Onuma and A. Ito, *Chem, Mater.*, 1998, **10**, 3346.

92 J. C. Heughebaert and G. Montel, *Calcif. Tissue Int.*, 1982, **34**, 103.

93 G. Daculsi, R. Z. LeGeros, E. Nery, K. Lynch and B. Kerebel, *J. Biomed. Res.*, 1989, **23**, 883.

94 R. Z. LeGeros, S. Lin, R. Rohanizadeh, D. Mijares and J. P. LeGeros, *J. Mater. Sci. Mat. Med.*, 2003, **14**, 201.

95 G. Daculsi, O. Laboux, O. Malard and P. Weiss, J. Mater. *Sci. Mater. Med.*, 2003, **14**, 195.

96 I. Alam, I. Asahina, K. Ohmamiuda and S. Enomoto, *J. Biomed, Mater, Res.*, 2001, **54**, 129.

97 M. Vallet-Regi and J. M. González-Calbet, *Progress Solid State Chem.*, 2004, **32**, 1.

98 D. McConnell, Apatite: its crystal chemistry, mineralogy, utilization, and biologic occurrences. Springer, New York, 1973, p. 111.

99 D. K. Smith, P. W. Brown, B. Constantz, Hydroxy apatite and related materials. CRC Press Inc., Boca Raton, Florida, 1994, p. 29.

100 A. I. Angelov, B. V. Levin, Y. D. Chernenko, Phosphate ore. A reference book (in Russian). Nedra busyness centre, Moscow, 2000, p. 120.

101 S. V. Dorozhkin, *J. Mater.Sci.*, 2007, **42**, 1061.

102 B. Wopenka and J. D. Pasteris, *Mater. Sci. Engin.* C 2005, **25**, 131.

103 J. D. Currey, Bone: structture and mechanics. Princeton Univ. Press, Princeton, 2002.

104 J. K. Rho, L. Kuhn-Spearing and P. Zioupos, *Med. Eng. Phys.* 1998, **20**, 92.

105 S. Mann, Biomimetic materials Chemistry, VCH, Weinheim, 1996.

106 N. M. Hancox, Biology of bone. Cambridge University Press, Cambridge, 1972.

107 R. B. Martin, *Mater. Sci. Forum*, 1999, **7**, 5.

108 G. Luquet, O. Testenière and F. Graf, in Chemistry and Biology of Mineralized Tissues, ed M. Goldberg, A. Boskey and C. Robinson, American Academy of Orthopaedic Surgeons, Rosemont, IL, USA, 2000, p. 7.

109 F. H. Jones, *Surface. Sci. Rep.*, 2001, **42**, 75.

110 D. F. Williams, The Williams dictionary of biomaterials. Liverpool University Press, Liverpool, 1999, p. 368.

111 J. F. Osborn and H. Newesely, Dental implants. CarlHansen Verlag, Munich, Germany, 1980, p. 111.

112 P. Ducheyne, *J. Biomed. Mater. Res.*, 1987, **21**, 219.

113 R. Z. Legeros and J. P. Legeros, *Key Engin. Mater.*, 2003, **3**, 240.

114 R. Z. Legeros and J. P. Legeros, Knochenersatzmaterialien und Waxhstumsfaktoren. Thieme, Stuttgart-New York, 1997, p. 180.

115 M. Bohner, *Injury*, 2000, **31**, 37.

116 B. R. Constantz, I. C. Ison, M. T. Fulmer, R. D. Posner, S. T. VanWagoner, J. Ross, S. A. Goldstein, J. B. Jupiter and D. I. Rosenthal, *Science*, 1995, **267**, 1796.

117 K. A. Gross and C. C. Berndt, Phosphates: geochemical, geobiological and materials importance. Series: Reviews in mineralogy and geochemistry, Mineralogical Society of America, Washington, DC, 2002, **48**, 631.

118 M. Bohner, *Eur. Spine. J.* 2001, **10**, 114.

119 C. E. Wilson, M. C. Kruyt, J. D. de Bruijn, C. A. van Bliitterswijk, F. C. Oner, A. J. Verbout and W. J. Dhert, *Biomaterials*, 2006, **27**, 302.

120 W. E. Brown and L. C. Chow, Cements research progress. American Ceramic Sciety, Weaterville, OH, 1986, p. 352.

121 S. Larsson and T. W. Bauer, *Clin. Orthop. Rel. Res.*, 2002, **395**, 23.

122 F. R. Dimaio, *Orthopedica*, 2002, **25**, 1399.

123 M. Bohner, U. Gbureck and J. E. Barralet, *Biomaterials*, 2005, **26**, 6423.

124 D. D. Weiss, M. A. Sachs and C. R. Woodard, *J. Long. Term. Eff. Med. Implants*, 2003, **13**, 41.

125 C. Lin, W. Shen, Y. Gu and L. Hu, *J. Biomed. Mater. Res.*, 1997, **35**, 75.

126 M. Otsuka, Y. Matsuda, Y. Suwa, J. L. Fox and W. I. Higuchi, *J. Biomed. Mater. Res.*, 1995, **29**, 25.

127 B. R. Constantz, I. C. Ison, M. T. Fulmer, R. O. Poser, S. T. Smith, M. VanWagoner, J. Ross, S. A. Goldstein and D. I. Rosenthal, *Science*, 1995, **267**, 1796.

128 J. Noetzel, A. M. Kielbassa, Schweizer Monatsschrift fur Zahnmedizin = Revue mensuelle suisse d'odonto-stomatologie = Rivista mensile svizzera di odontologia e stomatologia/SSO, 2005, **115**, 1148.

129 A. J. Ambard and L. Mueninghoff, *J. Prosthodontics*, 2006, **15**, 321.

130 A. Tofighi, S. Mounic, P. Chakravarthy, C. Rey and D. Lee, *Key, Eng. Mater.*, 2001, **192**, 769.

131 D. D. Lee, A. Tofighi, M. Aiolova, P. Chakravarthy, A. Catalano, A. Majahad and D. Knaack, *Clin. Orthop.*, 1999, **367**, 396.

132 W. E. Brown and L. C. Chow, US Patent Nr., 1985, 4518430.

133 L. C. Chow, S, Takagi, P. D. Costantino and C. D. Friedman, *Mater. Res. Soc. Symp. Proc.*, 1991, **179**, 3.

134 S. Goncalves, private communication.

135 I. Khairoun, F. C. M. Driessens, M. G. Boltong, J. A. Planell and R. Wenz, *Biomaterials*, 1999, **20**, 393.

136 S. Tanaka, T. Kishi, R. Shimogoryo, S. Matsuya and K. Ishikawa, *Dental. Mater. J.* 2003, **22**, 301.

137 E. Fernandez, J. A. Planell, S. M. Best and W. Bonfield, *J. Mater. Sci. Mater. Med.*, 1998, **9**, 789.

138 P. Frayssinet, M. Roudier, A. Lerch, J. L. Ceolin, E. Deprès and N. Rouquent, *J. Mater. Sci. Mater. Med.*, 2000, **11**, 811.

139 R. Z. LeGeros, A. Chohayeb and A. Shulman, *J. Dental, Res.*, 1982, **61**, 343.

140 W. E. Brown and L. C. Chow, *J. Dental. Res.*, 1983, **62**, 672.

141 M. Bohner, U. Gbureck and J. E. Barralet, *Biomaterials*, 2005, **26**, 6423.

142 A. Tofighi and C. Rey, US Patent application No US2003/0120351 A1.

143 U. Gbureck, O. Grolms, J. E. Barralet, L. M. Grover and R. Thull, *Biomaterials*, 2004, **24**, 4123.

144 J. H. van Esch and B. L. Freriga, *Angew. Chem.*, 2000, **112**, 2351.

145 D. J. Abdallah and R. G. Weiss, *Adv. Mater.*, 2000, **12**, 1237,

146 G. F. Swiegers and T. J. Malefetse, *Chem, Rev.*, 2000, **100**, 3483.

147 D. T. Bong, T. J. Malefetse, J. R. Granja and M. R. Ghadiri, *Angew. Chem.*, 2001, **113**, 1016.

148 L. J. Prins, D. N. Reinhoudt and P. Timmerman, *Angew. Chem.*, 2001, **113**, 2446.

149 B. J. Holliday and C. A. Mirkin, *Angew. Chem.*, 2001, **113**, 2076

150 N. K. Raman, M. T. Anderson and C. J. Brinker, *Chem. Mater.*, 1996, **8**, 1682.

151 S. Mann, S. L. Burkett, S. A. Davis, C. E. Fowler, N. H. Mendelson, S. D. Sims, D. Walsh and N. T. Whilton, *Chem. Mater.*, 1997, **9**, 2300.

152 L. A. Estroff and A. D. Hamilton, *Chem. Mater.*, 2001, **13**, 3227.

153 S. A. Davis, M. Brelmann, K. H. Rhodes, B. Zhang and S. Mann, *Chem. Mater.*, 2001, **13**, 3218.

154 R. A. Caruso and M. Antonietti, *Chem. Mater.*, 2001, **13**, 3272.

155 Y. Ono, Y. Kanekiyo, K. Inoue, J. Hojo, M. Nango and S. Shinkai, *Chem. Lett.*, 1999, 475.

156 F. Miyaji, S. A. Davis, J. P. H. Charmant and S. Mann, *Chem. Mater.*, 1999, **11**, 3021.

157 F. Iskandar, K. Mikrajuddin and K. Okuyama, *Nano. Lett.*, 2001, **1**, 231.

158 J. H. Jung, H. Kobayashi, M. Matsuda, T. Shimizu and S. Shinkai, *J. Am. Chem. Soc.*, 2001, **123**, 8785.

159 T. Yanagisawa, T. Shimizu, K. Kuroda and C. Kato, *Bull. Chem. Soc. Jpn.* 1990, **63,** 988.

160 S. Inagaki, Y. Fukushima and K. Kudoda, *J. Chem. Soc., Chem. Comm.*, 1993, 680.

161 S. Inagaki, A. Koiwai, N. Suzuki, Y. Fukushima and K. Kuroda, *Bull. Chem. Soc. Jpn.*, 1996, **69**, 1449.

162 C. T. Kresge, M. E. Leonowicz, W. J. Roth, J. C. Vartuli and J. S. Beck, *Nature,* 1992, **359,** 710.

163 S. Beck, J. C. Vartuli, W. J. Roth, M. E. Leonowicz, C. T. Kresge, K. D. Schmitt, C. T-W. Chu, D. H. Olson, E. W. Sheppard, S. B. McCullen, J. B. Higgins and J. L. Schlenker, *J. Am. Chem. Soc.*, 1992, **114,** 10834.

164 D. Y. Zhao, L. Feng, Q. Huo, N. Melosh, G. H. Fredrickson, B. F. Chmelka and G. D. Stucky, *Science,* 1998, **279,** 548.

165 Y. Wan and D. Y. Zhao, *Chem. Rev.*, 2007, **107**, 2821.

166 D. Y. Zhao, J. Y. Sun, Q. Z. Li and G. D. Stucky, *Chem. Mater.*, 2000, **12**, 275.

167 P. Y. Feng, X. H. Bu, G. D. Stucky and D. J. Pine, *J. Am. Chem. Soc.*, 2000, **122**, 994.

168 H. Lin and C. Y. Mou, *Acc. Chem. Res.*, 2002, **35**, 927.

169 A. Corma, *Chem. Rev.*, 1997, **97**, 2373.

170 F. Schüth and W. Schmidt, *Adv. Mater.*, 2002, **14**, 629.

171 J. Y. Jing, C. P. Mehnert and M. S. Wong, *Angew. Chem., Int. Ed.*, 1999, **38**, 56.

172 F. Schüth, *Chem. Mater.*, 2001, **13**, 3184.

173 C. Y. Chen, S. Q. Xiao and M. E. Davis, *Microporous. Mater.* 1995, **4**, 1.

174 Q. S. Huo, D. I. Margolese, U. Ciesla, P. Y. Feng, T. E. Gier, P. Sieger, R. Leon. P. M. Petroff, F. Schüth and G. D. Stucky, *Nature*, 1994, **368**, 317.

175 Q. S. Huo, D. I. Margolese, U. Ciesla, D. Demuth, P. Y. Feng, T. E. Gier, P. Sieger, A. Firouzi, B. F. Chelka, F. Schüth and G. D. Stucky, *Chem. Mater*, 1994, **6**, 1176.

176 Y. Sakamoto, M. Kaneda, O. Terasaki, D. T. Zhao, J. M. Kim, G. D. Stucky, H. J. Shim and R. Ryoo, *Nature*, 2000, **408**, 449.

177 Q. S. Huo, D. I. Margolese and G. D. Stucky, *Chem. Mater.*, 1996, **8**, 1147.

178 D. Y. Zhoa, Q. S. Huo, J. L. Feng, J. M. Kim, Y. J. Ham and G. D. Stucky, *Chem. Mater.*, 1999, **11**, 2668.

179 S. D. Shen, Y. Q. Li, Z. D. Zhang, J.Fan, B. Tu, W. Z. Zhou and D. Y. Zhao, *Chem. Commun.*, 2002, 2212.

180 S. D. Shen, A. E. Garcia-Bennett, Z. Liu, Q. Y. Lu, Y. F. Shi, Y. Yan, C. Z. Yu, W. C. Liu, Y. Cai, O. Terasaki and D. Y. Zhao, *J. Am. Chem. Soc.*, 2005, **127**, 6780.

181 Q. S. Huo, R. Leon, P. M. Petroff and G. D. Stucky, *Science*, 1995, **268**, 1324.

182 S. Che, A. E. Garcia-Bennett, T. Yokoi, K. Sakamoto, H. Kunieda, O. Terasaki and T. Tatsumi, *Nat. Mater.*, 2003, **2**, 801.

183 S. Che, Z. Liu, K. Sakamoto, H. Kunieda, O. Terasaki and T. Tatsumi, *Nature*, 2004, **429**, 281.

184 T. Yokoi, H. Yoshitake and T. Tatsumi, *Chem. Mater.*, 2003, **15**, 4536.

185 A. E. Garcia-Bennett, K. Miyasaka, O. Terasaki and S. Che, *Chem. Mater.*, 2004, **16**, 3597.

186 A. E. Garcia-Bennett, N. Kupferschmidt, N. Sakamoto, S. Che and O. Terasaki, *Angew. Chem., Int. Ed.*, 2005, **44**, 5317.

187 C. B. Gao, Y. Sakamoto, K. Sakamoto, O. Terasaki and S. Che, *Angew. Chem., Int. Ed.*, 2006, **45**, 4295.

188 S. A. Bagshaw, E. Prouzet and T. J. Pinnavaia, *Science*, 1995, **269**, 1242.

189 P. T. Tanev and T. J. Pinnavaia, *Science*, 1995, **267**, 865.

190 P. Behrens, *Angew. Chem., Int. Ed.*, 1996, **35**, 515.

191 A. Sayari and P. Liu, *Micropor. Mater.*, 1997, **12**, 149.

192 M. Tiemann and M. Fröba, *Chem. Mater.*, 2001, **13**, 3211.

193 T. Kimura, *Micropor. Mesopor. Mater.*, 2005, **77**, 97.

194 C. Yu, B. Tian and D. Zhao, *Curr. Opin. Solid State Mater. Sci.*, 2003, **7**, 191.

195 Q. Gao, R. Xu, J. Chen, R. Li, S. Li, S. Qui and Y. J. Yue, *Chem. Mater.*, 1997, **9**, 457.

196 T. Kimura, Y. Sugawara and K, Kuroda, *Chem. Mater.*, 1999, **11**, 508.

197 N. K. Mal, M. Fujiwara, S. Ichikawa and K. Kuraoka, *J. Ceram. Soc. Jpn.*, 2002, **110**, 890.

198 N. K. Mal, S. Ichikawa and M. Fujiwara, *Chem. Commun.*, 2003, 872.

199 M. Roca, J. E. Haskouri, S. Cabrera, A. Beltrán-Porter, J. Alamo, D. Beltrán-Porter, M. D. Macros and P, Amorós, *Chem. Commum.*, 1998, 1883.

200 S. Dasgupta, M. Agarwal and A. Datta, *J. Mater. Chem.*, 2002, **12**, 162.

201 J. Jiménez-Jiménez, P. Maireles-Torres, P. Olivera-Pastor, E. Rodríguez-Castellón, A. Jiménez-López, D, J, Jones and J. Rozière, *Adv. Mater.*, 1998, **10**, 812.

202 D. J. Jones, G. Aptel, M. Brandhorst, M. Jacquin, J. Jiménez-Jiménez, A. Jiménez-López, P. Maireles-Torres, I. Piwonski, E. Rodríguez-Castellón, J. Zajac and J. Rozière, *J. Mater. Chem.*, 2000, **10**, 1957.

203 A. Bhaumik and S Inagaki, *J. Am. Chem. Soc.*, 2001, **123**, 691.

204 X. Guo, W. Ding, X. Wang and Q. Yan, *Chem. Commun.*, 2001, 709.

205 J.-S. Chang, S.-E. Park, Q. Gao, G. Férey and A. K. Cheetham, *Chem. Commun.*, 2001, 859.

206 A. Tarafdar, S. Biswas, N. K. Pramanik and P. Pramanik, *Micropor. Mesopor. Mater.*, 2006, **89**, 204.

207 N. K. Mal, S. Ichikawa and M. Fujiwara, *Chem. Commun.*, 2002, 112.

208 G. A. Ozin, N. Varaksa, N. Coombs, J. E. Davies, D. D. Perovic and M. Ziliox, *J. Mater. Chem.*, 1997, **7**, 1601.

209 S. Zhang, Y. Wang, K. Wei, X. Liu, J. Chen and X. Wang, *Mater. Lett.*, 2007, **61**, 1341.

210 C. Liu, X. Ji and G. Cheng, *Appl. Surf. Sci.*, 2007, **253**, 6840.

211 Z. Y. Yuan, J. Q. Liu and L. M. Peng, *Langmuir*, 2002, **18**, 2450.

212 Y. Tokuoka, Y. Ito, K. Kitahara, Y. Niikura, A. Ochiai and N. Kawashima, *Chem. Lett.*, 2006, **35**, 1220.

213 Y. F. Zhao and J. Ma, *Micorpor. Mesopor. Mater.* 2005, **87**, 110.

214 S. M. Schmidt, J. McDonald, E. T. Pineda, A. M. Verwilst, Y. Chen, R. Josephs and A. E. Ostafin, *Micorpor. Mesopor. Mater.* 2006, **94**, 330.

215 M. J. Larson, A. Thorsen and S. J. Jensen, *Calcif Tissue Int.*, 1985, **37**, 189.

Chapter 2

Synthesis of lamellar mesostructured calcium phosphates using *n*-alkylamines as structure-directing agents in alcohol/water mixed solvent systems

2.1. Introduction

Calcium phosphate compounds with biocompatibility have been widely applied to biomaterials such as bone prosthesis and adsorbents for biomolecules [1-3]. Hydroxyapatite that is one of crystalline calcium phosphate compounds has actually used as artificial bone in practical clinic [4]. However, patients who need a medical treatment of their fractures with synthetic bones must bear his privation for a long time until the complete curing of the bone tissue because of the low physical strength between bionic and original bones [5]. Composites of inorganic calcium phosphate and organic collagen have drawn much attention as artificial bone and scaffold materials [6, 7] because the presence of collagen promotes the crystallization of the calcium phosphate. Therefore, many research groups have investigated the potential applications of the inorganic-organic composite materials and their robust achievements have been already verified [8-10]. Such composite materials are applicable not only to bone prosthesis but also to a model system of inorganic-organic hybrid materials including precursors of porous materials prepared using some organic molecules and assemblies as structure directing agents.

The preparation of ordered mesoporous materials has been conducted by using amphiphilic organic molecules which are self-organized in aqueous solutions and their hydrophilic headgroups are interacted with soluble inorganic species [11-14]. The mesoporous materials have some specific features such as high surface area and high adsorption capacity including uniformity and periodicity of tunable mesopores [15-17], which are widely applicable to adsorbents and catalytic supports [18-21]. Crystalline calcium phosphates used as adsorbents have showed relatively low

surface areas (~100 m^2 g^{-1}) so far. The value is obviously inferior to those of surfactant-templated mesoporous materials [22-24]. Recently, bioactive mesoporous silica whose surfaces were covered with apatite layer grown in simulated body fluid was reported as a high capacity vessel for drug delivery and scaffold materials [25]. The paper also suggested the potential application of mesoporous calcium phosphate as biomaterials.

Synthetic procedures of ordered mesoporous materials have been advanced by some strategies to control mesostructures [26, 27], compositions [28-32], and so on mainly through the investigation on silica-based materials. Inorganic-organic mesostructured composites act as precursors of ordered mesoporous materials formed through self-assembly of surfactant molecules attached with inorganic species and condensation of the inorganic species [15-17]. The surfactant-templating method has applied to the synthesis of other mesoporous solids, leading to the successful preparation of a large number of mesoporous and mesostructured metal oxides and phopshates [28-46]. However, it is quite difficult to synthesize surfactant-templated mesoporous materials composed of pure calcium phosphates because the inorganic frameworks are connected through ionic bonds between Ca^{2+} and phosphate ions. Some research groups have commented only the possibility to form lamellar mesostructured calcium phosphates [47-52]. In general, it is recognized that calcium phosphate-based materials with ionic frameworks are more preferentially crystallized than other covalently bonded phosphate-based materials. Actually, in the previous reports on the synthesis of mesostructured calcium phosphates using surfactants, crystallization of calcium phosphate species could not be suppressed and then mesostructured precursors composed of calcium phosphates were not obtained except for lamellar phases. Even the formation of the lamellar phases is not proved by powerful analyses such as TEM so distinctly.

In this Chapter, I firstly investigated the synthesis of a lamellar mesostructured calcium phosphate using *n*-hexadecylamine under the synthetic condition to suppress the crystallization of calcium phosphates. As the result, a lamellar mesostructured calcium phosphate without any original crystalline calcium phosphate phases can be obtained in the ethanol and water mixed solvent systems. I also investigated the effects of the synthetic conditions such as alcohol/water molar ratio, Ca/P molar ratio, reaction

temperature, the kind of alcohol, and the alkyl chain length of *n*-alkylamine in more detail on the formation of the lamellar mesostructured calcium phosphate.

2.2. Experimental

2.2.1. Materials

All the *n*-alkylamines (*n*-$C_nH_{2n+1}NH_2$, n = 8, 10, 12, 16, and 18) were obtained from Tokyo Kasei Kogyo Co. Phosphoric acid (85% H_3PO_4), aqueous solution of ammonia (25% NH_3), and calcium acetate monohydrate ($Ca(OAc)_2 \cdot H_2O$) were obtained from Wako Chemical Co. Aliphatic alcohols such as methanol (MeOH), ethanol (EtOH), *n*-propanol (PrOH) and *n*-butanol (BuOH) were also purchased from Wako Chemical Co. and used without further purification. Calcium hydroxide ($Ca(OH)_2$) was obtained from Kanto Chemical Co.

2.2.2. Synthesis of mesostructured calcium phosphate

Lamellar mesostructured calcium phosphate was prepared as follows. *n*-Alkylamine and 85% H_3PO_4 were added to a mixed solvent of alcohol and water. A white slurry mixture was obtained after stirring over 1 h. $Ca(OAc)_2 \cdot H_2O$ and 25% NH_3 were added to the white slurry mixture under vigorous stirring and the stirring was maintained for 15 min. The starting mixture ($Ca(OAc)_2$: H_3PO_4 : *n*-$C_nH_{2n+1}NH_2$: $0.5NH_3$: 40*n*-$C_nH_{2n+1}OH$: $40H_2O$) was statically kept for another 5 days at room temperature. The product was filtered, washed with EtOH repeatedly, and air-dried.

2.2.3. Characterization

X-ray diffraction (XRD) patterns were obtained by using a Rigaku RINT 2000 with graphite monochromatized Cu Kα radiation (40 kV, 30 mA). The compositions were measured by inductively coupled plasma atomic emission spectroscopy (ICP-AES, Seiko SPS 7700). Thermogravimetric (TG) analyses were conducted by using a Seiko TG/DTA320 thermal analyser. Transmission electron microscopic (TEM) images were taken by a JEOL JEM-2010 microscope, operated at 200 kV. ^{31}P MAS NMR spectra were obtained by using a Bruker DRX-400 spectrometer with a 7 mm zirconia rotor at a resonance frequency of 161.9 MHz with a spinning rate of 6

kHz. The spectra were accumulated with 4.5 μs pulses and 40 s recycle delay. 85% H_3PO_4 aqueous solution was used as a chemical shift reference. ^{13}C CP/MAS NMR spectra were also collected by using the same spectrometer at 100.7 MHz with a spinning rate of 4 kHz, 6.8 μs pulses, and 15 s recycle delay. Tetramethylsilane was used as a chemical shift reference. Scanning electron microscopic (SEM) images were taken by a JEOL JSM-6320FS to observe morphology of the products.

2.3. Results and discussion

The crystallization of calcium phosphate formed through rapid reaction between Ca^{2+} and phosphate ions is dramatically fast than other inorganic compounds constructed by covalent bond. Indeed, there are few reports on the preparation of amorphous calcium phosphate before its transformation into more stable crystalline phases [54]. Since interaction between surfactant molecules and phosphate ions is lost by the formation of discrete crystalline calcium phosphates, it is necessary to control mesostructures of calcium phosphates before rapid formation of crystalline calcium phosphates. Accordingly, I suggest a two-step reaction. Alkylammonium phosphates are utilized as intermediates [55] and reacted with calcium sources under conditions that keep ionic bonds between alkylammonium and phosphate ions during generation of mesostructured calcium phosphates.

2.3.1. Synthesis conditions

The synthesis of lamellar mesostructured calcium phosphate was carried out by using *n*-$C_{16}H_{33}NH_2$ in the mixed solvent of ethanol (EtOH) and water. The starting mixtures were prepared by mixing 85% H_3PO_4, $Ca(OAc)_2 \cdot H_2O$, and 25% NH_3 in the mixed solvent with the different molar ratios of EtOH and water. The composition of the starting mixtures was presented as $Ca(OAc)_2$: H_3PO_4 : *n*-$C_{16}H_{33}NH_2$: $0.5NH_3$: $80(EtOH+H_2O)$. The XRD patterns of the products prepared in the presence and absence of *n*-$C_{16}H_{33}NH_2$ are shown in Figure 2.1. Even when the synthesis was conducted in the presence of *n*-$C_{16}H_{33}NH_2$, a hydrated product such as brushite ($CaHPO_4 \cdot 2H_2O$) was mainly observed in the aqueous system (Figure 2.1(A)(a)) [56]. Brushite was also obtained in the absence of the surfactant in the aqueous system (Figure 2.1(B)(a)). With the increase in the amount of EtOH in the

reaction systems containing n-$C_{16}H_{33}NH_2$, the peaks due to brushite disappeared (Figure 2.1(A)(b)-(d)), indicating that the formation of brushite is suppressed in the $EtOH/H_2O$ systems.

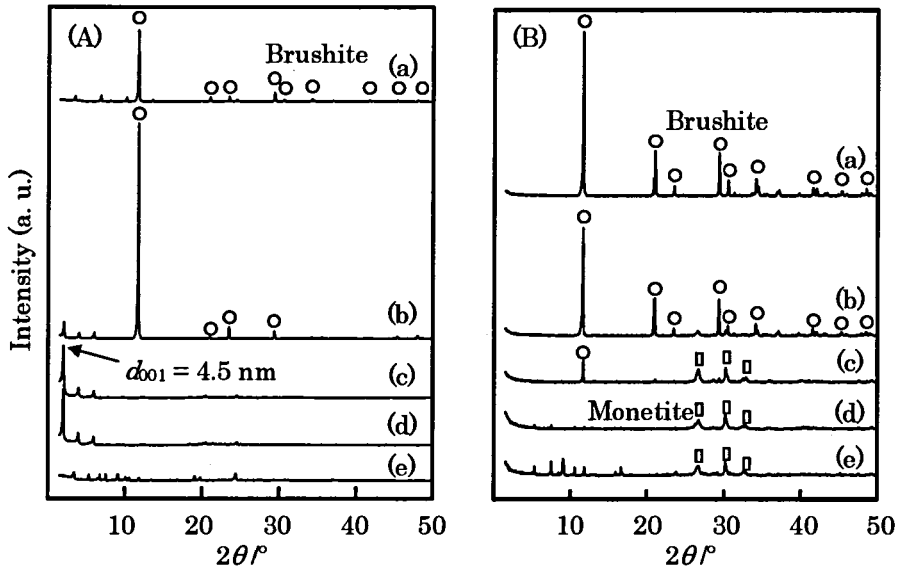

Figure. 2.1. XRD patterns of the products obtained (A) with and (B) without $C_{16}H_{33}NH_2$. $EtOH/H_2O$ ratio: (a) 0/100, (b) 25/75, (c) 50/50, (d) 75/25 and (e) 96/4.

The synthesis of crystalline calcium phosphates in the $EtOH/H_2O$ systems without surfactant was already reported and the preferential formation of brushite is suppressed by using EtOH as a co-solvent [57]. Therefore, similar synthesis was also conducted in the absence of the surfactant. Peaks due to brushite disappeared gradually by increasing the amount of EtOH in the reaction systems without n-$C_{16}H_{33}NH_2$ (Figure 2.1(B)(a)-(d)). Peaks due to monetite ($CaHPO_4$) that is one of anhydrous calcium phosphate phases appeared by increasing the amount of EtOH (Figure 2.1(B)(c)-(e)). In contrast, a peak with the d-spacing of 4.5 nm and the higher order diffractions that are possibly assignable to lamellar phases appeared in low diffraction angles of the reaction systems with n-$C_{16}H_{33}NH_2$ (Figure 2.1(A)(b)-(d)). The formation of lamellar mesostructured calcium phosphate was confirmed further by TEM observation, showing clear striped patterns (Figure 2.2). The results reveal that the lamellar mesostructured calcium phosphate can be obtained in the mixed solvent systems [53]. It is considered that further increase of the amount of EtOH was not useful for the reaction between $Ca(OAc)_2$ and H_3PO_4

because $Ca(OAc)_2 \cdot H_2O$ could not be dissolved in the mixtures (Figure 2.1(A)(e) and (B)(e)). Accordingly, only lamellar hexadecylammonium phosphate [(n-$C_{16}H_{33}NH_3^+$)($H_2PO_4^-$)] was formed in the ethanolic system containing n-$C_{16}H_{33}NH_2$ (Figure 2.1(A)(e)).

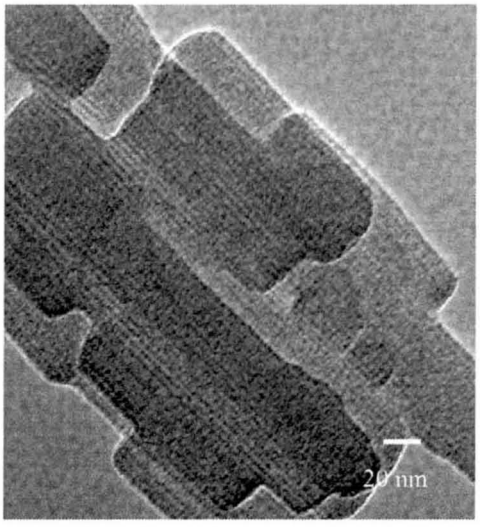

Figure 2.2. TEM image of lamellar mesostructured calcium phosphate obtained with $EtOH/H_2O$ (50/50).

2.3.2. Effect of Ca/P molar ratio

Lamellar mesostructured calcium phosphates were synthesized under the conditions with different Ca/P molar ratios in the starting mixtures. The composition of the starting mixture was $0.7–1.5Ca(OAc)_2$: H_3PO_4 : n-$C_{16}H_{33}NH_2$: $0.5NH_3$: $80(EtOH+H_2O)$. The $EtOH/H_2O$ molar ratio was simultaneously changed with the variation in the Ca/P molar ratio under the condition with the fixed H_2O/Ca molar ratio (40) in the reaction system. The XRD patterns of the products obtained at the Ca/P molar ratios of 0.7–1.5 in the starting mixtures are shown in Figure 2.3. In the products obtained at the Ca/P molar ratios ranging from 0.7 to 1.0, the peaks observed at 2θ = 1.5–6.0° are corresponded to the formation of lamellar mesostructured calcium phosphate (d_{001} = 4.5 nm) (Figure 2.3(A)(a)-(c)). Several peaks, almost of which at higher diffraction angles have not been assigned yet, were also observed in high diffraction angles (Figure 2.3(B)(a)-(c)). Some of the peaks are considered to be due to the ordering in the calcium phosphate framework of the

lamellar phase. With the further increase in the Ca/P molar ratio from 1.2 to 1.5, the peaks at 2θ = 15–25° (Figure 2.3(B)(d)-(e)) as well as the peaks assignable to the lamellar mesostructuted calcium phosphate disappeared (Figure 2.3(A)(d)-(e)) although small broad peaks assignable to initial crystalline hydroxyapatite phase appeared at 2θ = 26 and 32° (Figure 2.3(B)(d)-(e)) [54-58]. The result indicates that the formation of the lamellar mesostructured calcium phosphate occurred at the Ca/P molar ratios from 0.7 to 1.0 because the hydroxyapatite phase was formed preferentially at higher Ca/P molar ratios than 1.0. Hydroxyapatite ($Ca_{10}(PO_4)_6(OH)_2$) known as anhydrate crystalline calcium phosphate was formed in the non-aqueous solvent system under the calcium-rich conditions.

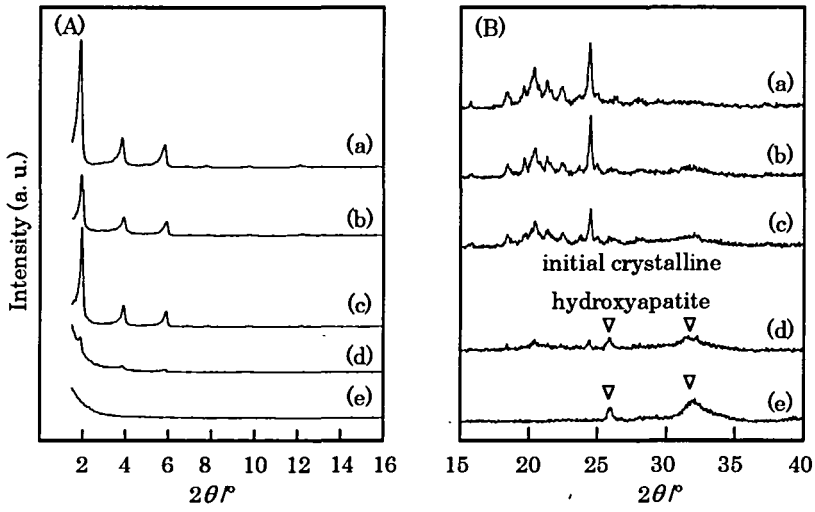

Figure 2.3. XRD patterns at (A) low and (B) high angles of the products obtained at various Ca/P ratios: (a) 0.7, (b) 0.9, (c) 1.0, (d) 1.2 and (e) 1.5.

When the composition of the starting mixture was changed into $0.7Ca(OAc)_2$: H_3PO_4 : n-$C_{16}H_{33}NH_2$: $0.5NH_3$: 40EtOH : $40H_2O$, however, lamellar mesostructured calcium phosphate was obtained with the slight formation of brushite. The result would be caused by the H_2O-rich condition (H_2O/Ca molar ratio of 40/0.7) because the presence of H_2O in the reaction system is necessary for controlling the dissolution of the calcium source. The ^{31}P MAS NMR measurements were applied to get further information on the calcium phosphate frameworks and the spectra of the products prepared by changing the Ca/P molar ratios in the range of 0.7–1.5 in the starting mixtures are shown in Figure 2.4. In the ^{31}P MAS NMR

spectrum of the product obtained at Ca/P = 0.7, three peaks were observed at 2.1, 0.4, and −1.7 ppm (Figure 2.4(b)). In compared with the spectrum of (n-$C_{16}H_{33}NH_3^+$)($H_2PO_4^-$) (Figure 2.4(a)), the small peak at 0.4 ppm is considered to be assigned to P atoms in the similar salt. With the increase in the Ca/P molar ratio, the intensity of the shoulder peak at around −1.7 ppm decreased gradually while that of the peak at 2.1 ppm was enhanced (Figure 2.4(b)-(e)). The ^{31}P MAS NMR spectra were also measured with ^{1}H-^{31}P cross-polarization (CP) technique (not shown here). The intensity of the peak at 2.1 ppm was not enhanced in the ^{31}P CP/MAS NMR spectrum, being consistent with the lack of protons neighboring to P atoms in the calcium phosphate framework. However, the CP enhancement was observed for the product obtained at Ca/P = 0.9, revealing the presence of two PO_4 units, probably, $[PO_4]^{3-}$ and $[HPO_4]^{2-}$ or $[H_2PO_4]^-$, are present in the framework of the lamellar mesostructured calcium phosphate [59, 60].

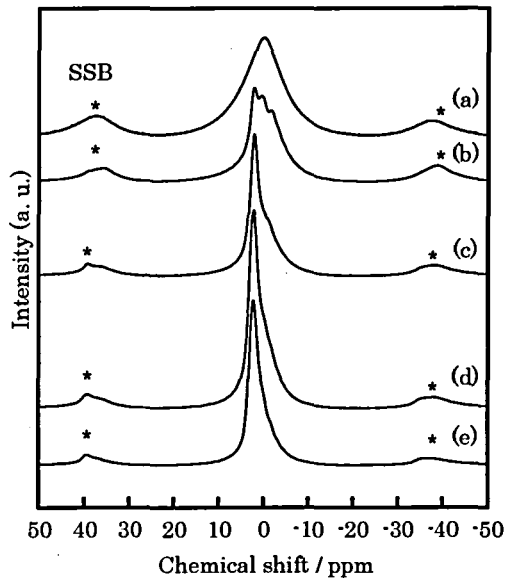

Figure 2.4. ^{31}P MAS NMR spectra of lamellar mesostructured calcium phosphates obtained at different Ca/P ratios: (a) [$C_{16}H_{33}NH_3^+$][$H_2PO_4^-$], (b) 0.7, (c) 0.9, (d) 1.0 and (e)1.2.

2.3.3. Effect of the reaction temperature

The synthesis was also conducted at different temperatures under the condition with the composition of $Ca(OAc)_2$: H_3PO_4 : n-$C_{16}H_{33}NH_2$: $0.5NH_3$: 40EtOH :

$40H_2O$. After the starting mixture was stirred for 15 min, the mixture was aged at room temperature, 50 or 70 °C statically. The XRD patterns of the products prepared at room temperature, 50 and 70 °C are shown in Figure 2.5. Although all of the XRD patterns showed the formation of lamellar mesostructured calcium phosphates, the d_{001} values (4.0 nm) of the lamellar phases obtained by heating at 50 and 70 °C were smaller than that of the lamellar phase (4.5 nm) at room temperature (Figure 2.5(a)-(c)). In addition, the products obtained by heating contained monetite and the amount of that was increased by elevating the synthetic temperature [61]. None of typical striped patterns characteristic for lamellar mesostructured materials were found in the TEM images of the products obtained at 50 and 70 °C. Additional experiment was carried out to get more information about this phase. After each product (0.5 g) was stirred at 60 °C for 5 h in EtOH (150 g), filtered, and washed with EtOH at 60 °C, only the peaks in the low diffraction angles disappeared completely. It is reasonable to be considered that this phase would not be lamellar but organic, probably a moiety of *n*-hexadecylamine and/or $(n\text{-}C_{16}H_{33}NH_3^+)(H_2PO_4^-)$. The crystallization of monetite would occur more preferentially than that of the lamellar mesostructured calcium phosphate at higher temperatures. The result exhibits that the control of the reaction temperature enables to suppress the crystallization of monetite under the condition, being strongly useful for the mesostructural control of calcium phosphates.

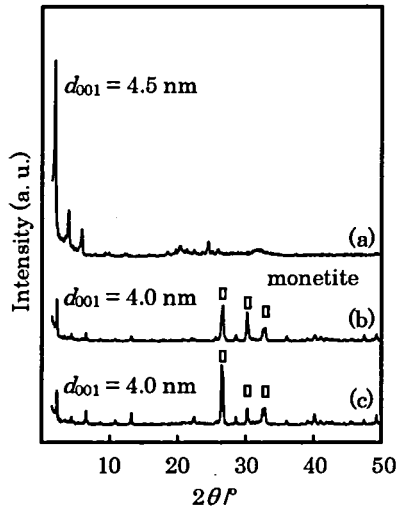

Figure 2.5. XRD patterns of the products prepared at (a) room temperature, (b) 50 and (c) 70 °C.

The synthetic regions that several calcium phosphates could be obtained under synthetic conditions with various EtOH/H_2O and Ca/P molar ratios at r.t. are schematized in Scheme 2.1. In the region of higher Ca/P molar ratio than 1.0, the predominant formation of hydroxyapatite occurred in the mixed solvent system regardless of the EtOH/H_2O molar ratio. When the Ca/P molar ratio was lower than 1.0, brushite was formed in the H_2O-rich system. The reaction between (n-$C_{16}H_{33}NH_3^+$)($H_2PO_4^-$) and calcium source did not occurred in pure EtOH system. At higher aging temperature than r.t., monetite was formed. In the synthetic region that the formations of crystalline calcium phosphates were suppressed by the control of synthetic conditions, the lamellar mesostructured calcium phosphate could be formed. This result strongly indicates that the interaction between hexadecylammonium and phosphate ions must be maintained to obtain the lamellar mesostructured calcium phosphate during the reaction of Ca^{2+} ions and hexadecylammonium phosphate (Scheme 2.2).

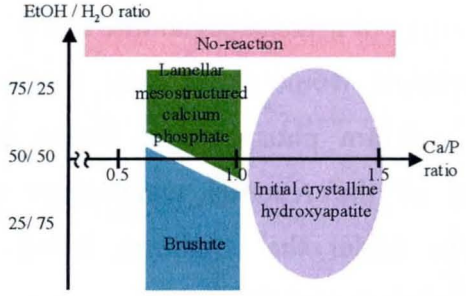

Scheme 2.1. The synthetic region of lamellar mesostructured calcium phosphates at room temperature.

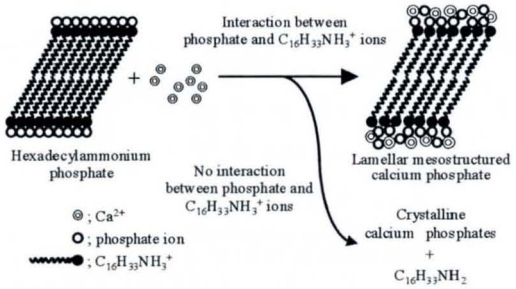

Scheme 2.2. Proposed formation route of lamellar mesostructured calcium phosphate.

2.3.4. Effect of alcohol as co-solvent

Effect of co-solvents was investigated by using a series of aliphatic alcohols. The composition of the starting mixture was $Ca(OAc)_2$: H_3PO_4 : *n*-$C_{16}H_{33}NH_2$: $0.5NH_3$: 80($ROH+H_2O$), R = CH_3, C_2H_5, C_3H_7, and C_4H_9. The ROH/H_2O molar ratio was changed from 0/100 to 96/4. The mixture of lamellar mesostructured calcium phosphate and brushite was obtained at the $MeOH/H_2O$ molar ratio of 25/75. The formation of brushite was suppressed with an increase in the amount of MeOH, leading to the successful preparation of pure lamellar phase in the range of $MeOH/H_2O$ molar ratio from 40/60 to 75/25. In the cases of the $PrOH/H_2O$ and $BuOH/H_2O$ systems, pure lamellar mesostructured calcium phosphate could be obtained at ROH/H_2O of 75/25. Under the conditions in the range of ROH/H_2O molar ratio from 50/50 to 25/75, only brushite was formed in both of the systems. The formation of brushite was also suppressed by increasing the amount of MeOH, PrOH and BuOH as well as EtOH. However, there is a difference in the range of the ROH/H_2O molar ratio to afford lamellar mesostructured calcium phosphate.

The results are schematically summarized in Figure 2.6. Lamellar phases were formed under restricted ROH/H_2O molar ratios in the reaction systems using aliphatic alcohols having longer alkyl chains. Actually, the range of the $EtOH/H_2O$ molar ratio affording pure lamellar mesostructured calcium phosphate was narrower than that of the $MeOH/H_2O$ molar ratio. As ROH with longer alkyl chains is not mixed with H_2O because hydrophobicity of the alcohol becomes strong, the reaction system seems to be relatively analogous to aqueous systems, which has a tendency to provide hydrated crystalline calcium phosphate phase such as brushite. Therefore, the effective range of the ROH/H_2O molar ratio becomes narrow with an increase in the alkyl chain length of alcohol, which prevent from the formation of lamellar mesostructured calcium phosphate. The results indicate that the kind of alcohol is also important for controlling the solubility of the calcium source and the preferential formation of crystalline calcium phosphate phases. The TEM images of the mesostructured calcium phosphates obtained by using a series of ROH in the mixed solvent systems with ROH/H_2O of 75/25 and 50/50 are shown in Figure 2.7. Stripe patterns were clearly observed for all the products obtained at ROH/H_2O of

75/25 (Figure 2.7(a), (d)-(f)). However, in addition to the stripe patterns (Figure 2.7(b)), disordered stripe patterns were slightly observed for the product obtained at MeOH/H_2O of 50/50 (Figure 2.7(c)). The SEM observation of the products was also conducted and the images of the products obtained at ROH/H_2O of 75/25 are shown in Figure 2.8. Morphologies of the lamellar mesostructured calcium phosphates were plate-like and the size increased gradually by using ROH with longer alkyl chains, revealing that the particle size of the lamellar phases is controllable in the mixed solvent systems according to the alkyl chain length of alcohol.

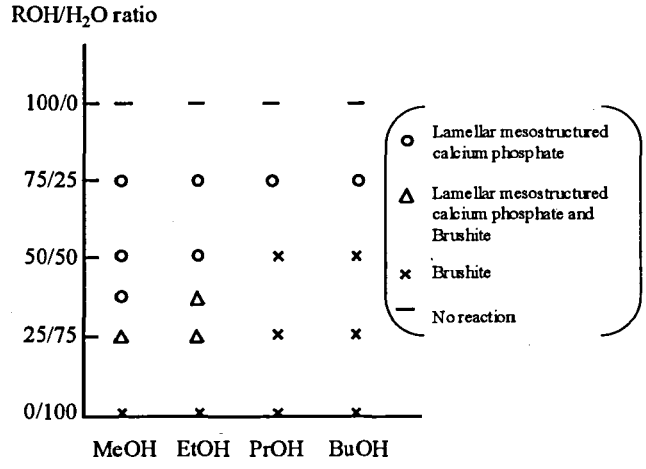

Figure 2.6. Effect of aliphatic alcohol on synthesis of lamellar mesostructured calcium phosphate with *n*-$C_{16}H_{33}NH_2$.

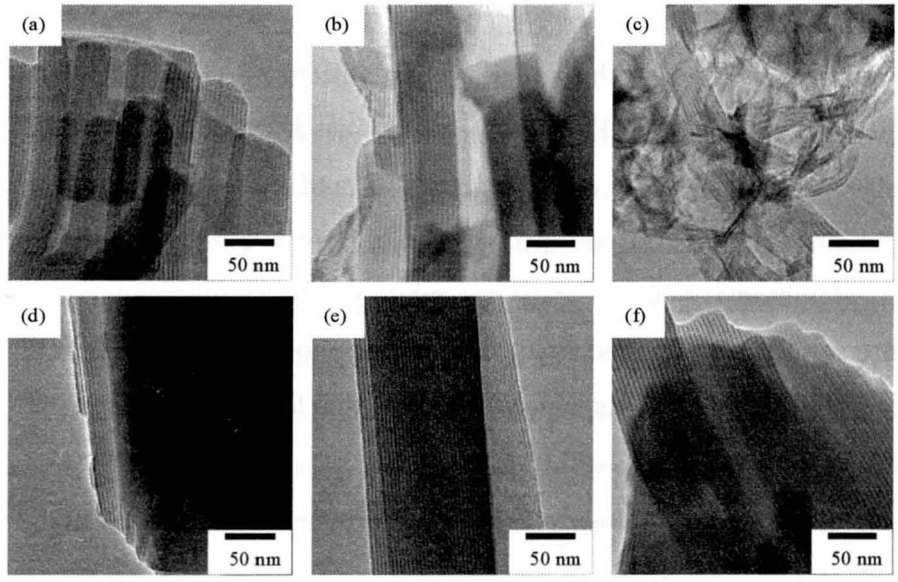

Figure 2.7. TEM images of lamellar mesostructured calcium phosphates obtained in the ROH/H_2O systems. (a) MeOH/H_2O (75/25), (b) and (c) MeOH/H_2O (50/50), (d) EtOH /H_2O (75/25), (e) PrOH /H_2O (75/25) and (f) BuOH /H_2O (75/25).

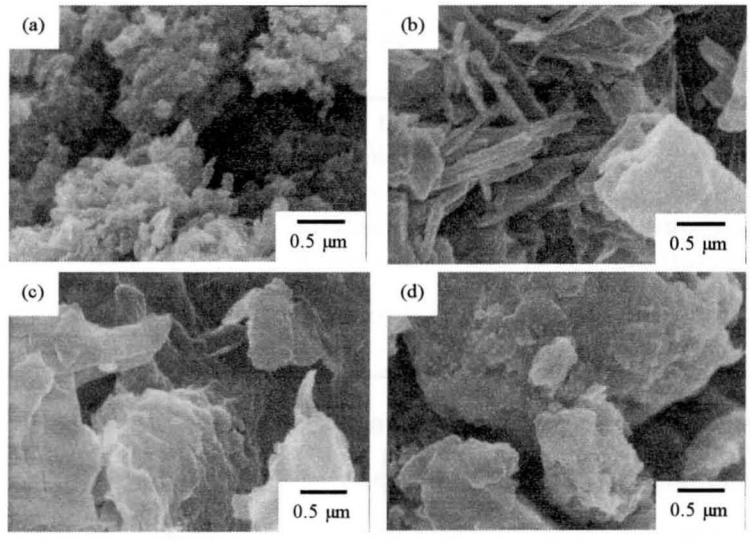

Figure 2.8. SEM images of lamellar mesostructured calcium phosphates obtained in the ROH/H_2O (75/25) systems: (a) MeOH, (b) EtOH, (c) PrOH and (d) BuOH.

2.3.5. Possible structure of lamellar mesostructured calcium phosphate

On the basis of the ^{31}P MAS NMR results, it is considered that the framework structure of the lamellar mesostructured calcium phosphate contains two phosphate

units. The elemental analysis showed that Ca/P molar ratios in the frameworks were almost consistent with those in the corresponding starting mixtures. Thermogravimetric curve of the lamellar mesostructured compound with the Ca/P molar ratio of 1.0 is shown in Figure 2.9. Main mass losses of 23.0 and 28.7 mass % were observed below 200 °C and between 200 and 600 °C, which correspond to dehydration and combustion of organic moiety, respectively. After the lamellar phase was calcinated at 600 °C for 10 h, a white solid was obtained. The XRD peaks of the white solid were assigned to a calcium pyrophosphate ($Ca_2P_2O_7$) (Figure 2.10). On the basis of the mass loss below 600 °C, the formula could be presented as $(C_{16}H_{33}NH_3^+)_{0.6}Ca^{2+}(HPO_4^{2-})_{0.4}(PO_4^{3-})_{0.6}$.

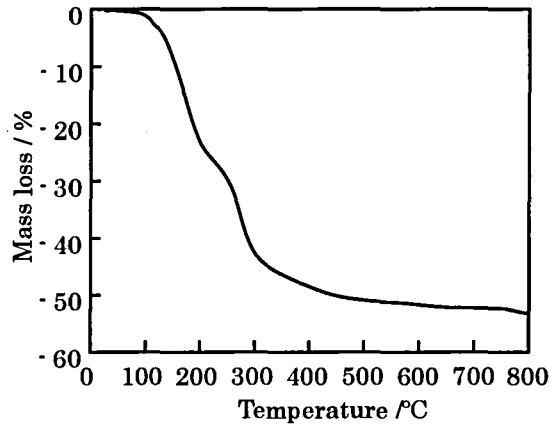

Figure 2.9. Thermogravimetric curve of lamellar mesostructured calcium phosphate with Ca/P molar ratio of 1.0.

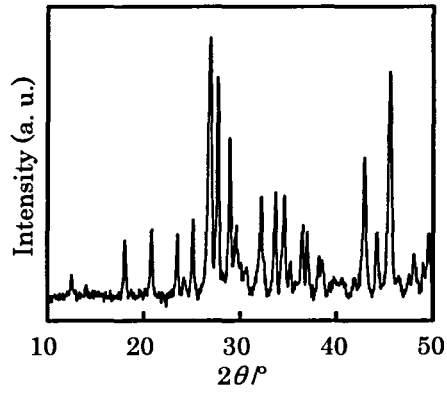

Figure 2.10. XRD pattern of the calcined product of lamellar mesostructured calcium phosphate with the Ca/P molar ratio of 1.0 at 600 °C.

Lamellar mesostructured calcium phosphates were prepared by using *n*-alkylamines with different alkyl chain lengths as structure-directing agents. Calcium hydroxide was used as a calcium source instead of calcium acetate monohydrate, because the products containing both of lamellar mesostructured calcium phosphate (main product) and alkylammonium phosphate salt (byproduct) were obatined by using *n*-$C_nH_{2n+1}NH_2$ except for using *n*-$C_{16}H_{33}NH_2$ when calcium acetate monohydrate was used. The XRD patterns of the products obtained from a series of starting mixtures with $Ca(OH)_2$: H_3PO_4 : *n*-$C_nH_{2n+1}NH_2$ (*n* = 8–18) : 40EtOH : $40H_2O$ are shown in Figure 2.11. The patterns contained the peaks due to both unreacted calcium hydroxide and lamellar mesostructured calcium phosphate. The d_{100} values corresponding to the lamellar phases were changed in the range of 2.8–4.8 nm (2.8 nm for *n* = 8, 3.4 nm for *n* = 10, 3.7 nm for *n* = 12, 4.5 nm for *n* = 16, and 4.8 nm for *n* = 18). Conformation of the alkyl chains of the surfactant molecules (*n*-hexadecylamine) in the lamellar mesostructured calcium phosphate was investigated by ^{13}C CP/MAS NMR. The ^{13}C CP/MAS NMR spectrum of the lamellar mesostructured calcium phosphate obtained from the starting mixture with the composition of $Ca(OAc)_2$: H_3PO_4 : *n*-$C_{16}H_{33}NH_2$: $0.5NH_3$: 40EtOH : $40H_2O$ are shown in Figure 2.12. Several peaks due to carbon atoms in *n*-hexadecylamine were observed and the peak at 32 ppm can be assigned to carbon atoms in all-*trans* methylene (-CH_2-) chains [62, 63]. Figure 2.13 shows the relation between the d_{100} spacing and the number of carbon atoms in the alkyl chains of the *n*-alkylamines. In accordance with the correlation, a slope of the straight line was calculated to be 0.185 nm/CH_2. Since the distance between two adjacent carbon atoms are expressed as 0.127 nm/CH_2 in an all-*trans* alkyl chains [64], the alkyl chains are arranged in the lamellar phases as double layers with a tilt angle of ca. 46°. Also, the wall thickness of the mesostructured calcium phosphates was estimated to be ca. 1.2 nm.

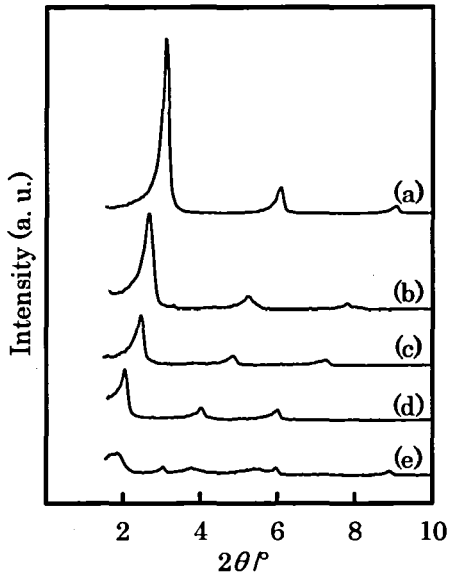

Figure 2.11. XRD patterns of lamellar mesostructured calcium phosphates prepared using (a) n-$C_8H_{17}NH_2$, (b) n-$C_{10}H_{21}NH_2$, (c) n-$C_{12}H_{25}NH_2$, (d) n-$C_{16}H_{33}NH_2$ and (e) n-$C_{18}H_{37}NH_2$.

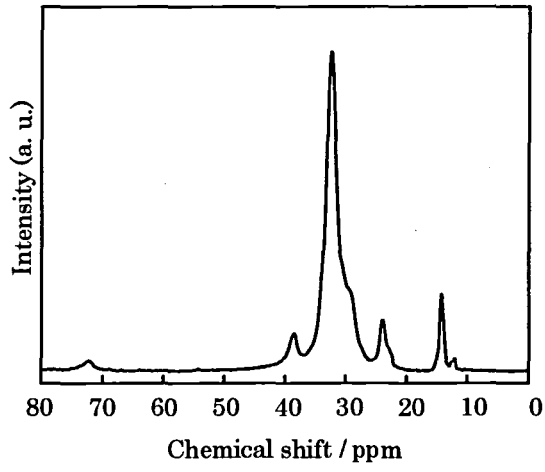

Figure 2.12. ^{13}C CP/MAS NMR spectrum of lamellar mesostructured calcium phosphate obtained from the starting mixture of $Ca(OAc)_2$: H_3PO_4 : n-$C_{16}H_{33}NH_2$: $0.5NH_3$: $40EtOH$: $40H_2O$.

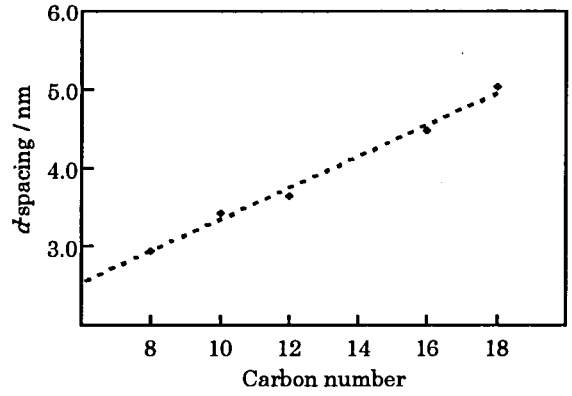

Figure 2.13. Relationship between *d*-spacing and carbon number in the alkyl chain of *n*-alkylamine.

2.4. Conclusions

Lamellar mesostructured calcium phosphates constructed through ionic bonds were successfully synthesized by using *n*-alkylamines as structure-directing agents under a wide variety of conditions. Morphology of lamellar mesostructured calcium phosphates was also controlled by changing the alkyl chain length of alcohol used as co-solvents. It was mainly important for synthesis of the lamellar mesostructured calcium phosphates to control both solubility of calcium source and crystallization of calcium phosphate species. The controlled synthesis is possible in the mixed solvent systems of alcohols and water that allows the interaction between the surfactant molecules and calcium phosphate species and the suppression of the discrete crystallization of calcium phosphate species. These materials are promising as biomaterials such as bone prosthesis and adsorbents for biomolecules, and the crystallization and solubility controlled synthesis will open the new route to obtain mesostructured materials whose frameworks are constructed by ionic bonds.

References

1 M. Jarcho, *Clin. Orthop. Relat. Res.*, 1981, **157,** 259.

2 P. Ducheyne and Q. Qiu, *Biomaterials,* 1999, **20,** 2287.

3 H. W. Kim, G. Georgiou, J. C. Knowles, Y. H. Koh and H. E. Kim, *Biomaterials,* 2004, **25,** 4203.

4 S. F. Hulbert, F. A. Young, R. S. Mathews, J. J. Klawitter, C. D. Talbert and F. H. Stelling, *J. Biomed. Mater. Res.*, 1970, **4,** 433.

5 K. De Groot, C. De Putter, P. Smitt and A. Driessen, *Sci. Ceram.*, 1981, **11,** 433.

6 J. D. Hartgerink, E. Beniash and S. I. Stupp, *Science,* 2001, **294,** 1684.

7 M. Kikuchi, S. Itoh, S. Ichinose, K. Shinomiya and J. Tanaka, *Biomaterials,* 2001, **22,** 1705.

8 H. Cölfen and S. Mann, *Angew. Chem., Int. Ed.,* 2003, **42,** 2350.

9 G. A. Silva, C. Czeisler, K. L. Niece, E. Beniash, D. A. Harrington, J. A. Kessler and S. I. Stupp, *Science,* 2004, **27,** 1352.

10 J. A. A. W. Elemans, A. E. Rowan and R. J. M. Nolte, *J. Mater. Chem.*, 2003, **13,** 2661.

11 T. Yanagisawa, T. Shimizu, K. Kuroda and C. Kato, *Bull. Chem. Soc. Jpn.* 1990, **63,** 988.

12 S. Inagaki, Y. Fukushima and K. Kudoda, *J. Chem. Soc., Chem. Comm.*, 1993, 680.

13 C. T. Kresge, M. E. Leonowicz, W. J. Roth, J. C. Vartuli and J. S. Beck, *Nature,* 1992, **359,** 710.

14 S. Beck, J. C. Vartuli, W. J. Roth, M. E. Leonowicz, C. T. Kresge, K. D. Schmitt, C. T-W. Chu, D. H. Olson, E. W. Sheppard, S. B. McCullen, J. B. Higgins and J. L. Schlenker, *J. Am. Chem. Soc.*, 1992, **114,** 10834.

15 D. Zhao, L. Feng, Q. Huo, N. Melosh, G. H. Fredrickson, B. F. Chmelka and G. D. Stucky, *Science,* 1998, **279,** 548.

16 X. S. Zhao, G. Q. Lu and G. J. Millar, *Ind. Eng. Chem. Res.*, 1996, **35**, 2075.

17 P. Selvam, S. K. Bhatia and C. G. Sonwane, *Ind. Eng. Chem. Res.*, 2001, **40**, 3237.

18 A. Sayari, *Chem. Mater.*, 1996, **8,** 1840.

19 A. Corma, *Chem. Rev.*, 1997, **97,** 2373.

20 A. Taguchi and F. Schüth, *Micropor. Mesopor. Mater.*, 2005, **77**, 1.

21 F. Schüth, *Angew. Chem., Int. Ed.,* 2003, **42,** 3604.

22 H. Monma, *Inorg. Mater.*, 1995, **2,** 401.

23 L. M. Rodriguez-Lorenzo and M. Vallet-Regi, *Chem. Mater.*, 2000, **12,** 2460.

24 M. Uota, H. Arakawa, N. Kitamura, T. Yoshimura, J. Tanaka and T. Kijima, *Langmuir,* 2005, **21,** 4724.

25 M. Vallet-Regí, L. Ruiz-González, I. Izquierdo-Barba and J. M. González-Calbet, *J. Mater, Chem.*, 2006, **16,** 26.

26 Q. Huo, R. Leon, P. M. Petroff and G. D. Stucky, *Science,* 1995, **268,** 1324.

27 Q. Huo, D. I. Margolese and G. D. Stucky, *Chem. Mater.*, 1996, **8,** 1147.

28 P. Behrens, *Angew. Chem., Int. Ed.*, 1996, **35,** 515.

29 A. Sayari and P. Liu, *Micropor. Mater.*, 1997, **12,** 149.

30 F. Schüth, *Chem. Mater.*, 2001, **13,** 3184.

31 M. Tiemann and M. Fröba, *Chem. Mater.*, 2001, **13,** 3211.

32 T. Kimura, *Micropor. Mesopor. Mater.*, 2005, **77,** 97.

33 C. Yu, B. Tian and D. Zhao, *Curr. Opin. Solid State Mater. Sci.*, 2003, **7,** 191.

34 Q. Gao, R. Xu, J. Chen, R. Li, S. Li, S. Qui and Y. J. Yue, *Chem. Mater.*, 1997, **9,** 457.

35 T. Kimura, Y. Sugawara and K, Kuroda, *Chem. Mater.*, 1999, **11,** 508.

36 N. K. Mal, M. Fujiwara, S. Ichikawa and K. Kuraoka, *J. Ceram. Soc. Jpn.*, 2002, **110,** 890.

37 N. K. Mal, S. Ichikawa and M. Fujiwara, *Chem. Comm.*, 2003, 872.

38 M. Roca, J. E. Haskouri, S. Cabrera, A. Beltrán-Porter, J. Alamo, D. Beltrán-Porter, M. D. Macros and P, Amorós, *Chem. Comm.*, 1998, 1883.

39 S. Dasgupta, M. Agarwal and A. Datta, *J. Mater. Chem.*, 2002, **12,** 162.

40 J. Jiménez-Jiménez, P. Maireles-Torres, P. Olivera-Pastor, E. Rodríguez-Castellón, A. Jiménez-López, D, J, Jones and J. Rozière, *Adv. Mater.*, 1998, **10,** 812.

41 D. J. Jones, G. Aptel, M. Brandhorst, M. Jacquin, J. Jiménez-Jiménez, A. Jiménez-López, P. Maireles-Torres, I. Piwonski, E. Rodríguez-Castellón, J. Zajac and J. Rozière, *J. Mater. Chem.*, 2000, **10,** 1957.

42 A. Bhaumik and S Inagaki, *J. Am. Chem. Soc.*, 2001, **123,** 691.

43 X. Guo, W. Ding, X. Wang and Q. Yan, *Chem. Comm.*, 2001, 709.

44 J.-S. Chang, S.-E. Park, Q. Gao, G. Férey and A. K. Cheetham, *Chem. Comm.*, 2001, 859.

45 A. Tarafdar, S. Biswas, N. K. Pramanik and P. Pramanik, *Micropor. Mesopor. Mater.*, 2006, **89,** 204.

46 N. K. Mal, S. Ichikawa and M. Fujiwara, *Chem. Comm.*, 2002, 112.

47 G. A. Ozin, N. Varaksa, N. Coombs, J. E. Davies, D. D. Perovic and M. Ziliox, *J. Mater. Chem.*, 1997, **7,** 1601.

48 I. Soten and G. A. Ozin, *J. Mater. Chem.*, 1999, **9,** 703.

49 J. Yao, W. Tjandra, Y. Z. Chen, K. C. Tam, J. Ma and B. Soh, *J. Mater. Chem.*, 2003, **13,** 3053.

50 S. M. Schmidt, J. McDonald, E. T. Pineda, A. M. Verwilst, Y. Chen, R. Josephs and A. E. Ostefin, *Micropor. Mesopor. Mater.*, 2006, **94,** 330.

51 Y. Tokuoka, Y. Ito, K. Kitahara, Y. Niikura, A. Ochiai and N. Kawashima, *Chem. Lett.*, 2006, **35,** 1220.

52 Y. F. Zhao and J. Ma, *Micropor. Mesopor. Mater.*, 2005, **87,** 110.

53 N. Ikawa, Y. Oumi, T. Kimura, T. Ikeda and T. Sano, *Chem. Lett.*, 2006, **35,** 948.

54 E. D. Eanes, I. H. Gillessen and A. S. Posner, *Nature,* 1965, **208,** 365.

55 S. R. J. Oliver and G. A. Ozin, *J. Mater. Chem.*, 1988, **8,** 1081.

56 G. R. Sivakumar, E. K. Girija, S. N. Karukura and C. Subramanian, *Cryst. Res. Technol.*, 1998, **33,** 197.

57 M. J. Larson, A. Thorsen and S. J. Jensen, *Calcif Tissue Int.*, 1985, **37,** 189.

58 S. Kim, H. S. Ryu, H. Shin, H. S. Jung and K. S. Hong, *Mater. Chem. Phys.*, 2005, **91,** 500.

59 W. P. Aue, A. H. Roufosse, M. J. Glimcher and R. G. Griffin, *Biochemistry,* 1984, **23,** 6110.

60 J. L. Miquel, L. Facchini, A. P. Legrand, C. Rey and J. Lemaitre, *Colloids Surfaces,* 1990, **45,** 427.

61 K, Furuichi, Y. Oaki and H. Imai, *Chem. Mater.*, 2006, **18,** 229.

62 R. Simonutti, A. Comotti, S. Bracco and P. Sozzani, *Chem. Mater.*, 2001, **13,** 771.

63 F. Kooli, L. Mianhui, S. F. Alshahateet, F. Chen and Z. Yinghuai, *J. Phys. Chem. Solids,* 2006, **67,** 926.

64 A. I. Kitaigorodskii, *Molecular Crystals and Molecules,* Academic Press, New York, 1973.

Chapter 3

Understanding of the formation of mesostructured alkylammonium-alkaline earth metal phosphates composed of ionic frameworks

3.1. Introduction

Metal phosphates and the alkylamine (n-$C_nH_{2n+1}NH_2$: $n \leq 6$) -intercalated materials are widely applied in the research fields such as catalysts, adsorbents, biomaterials, and electrical conductors [1-8]. Mesostructural control of metal phosphates by using alkylamines with longer alkyl chains (n-$C_nH_{2n+1}NH_2$: $n \geq 10$) is quite interesting to extend the possible applications. Alkaline earth metal phosphates are also attractive materials according to the characteristic features such as ion-exchange capacity, high adsorption capacity, biocompatibility, catalytic activity, and molecular sieving [9-12]. However, their mesostructural controls have hardly been developed so far.

Ordered mesoporous silicas which are strongly expected as catalyst supports and adsorbents can be obtained through condensation of silicate species interacted with alkyltrimethylammonium surfactants [13, 14]. Since the discovery of the mesoporous silicas, there have been a large number of reports on the synthesis of inorganic-organic composites using amphiphilic organic molecules [15-26]. The self-assembling ability of the organic molecules is quite useful for the mesostructural control of inorganic solids and then a wide variety of periodic mesoporous materials are obtained by successful removal of the organic assemblies [15-21]. The synthetic strategy is considered to be widely applicable for the preparation of other inorganic solids such as metal oxides and phosphates [22-26]. Nevertheless, non-silica-based mesoporous materials cannot be synthesized without some efforts even by using surfactants because the favorable formation of their crystalline phases leads to the lowering of the charge of frameworks that does not allow possible interaction with surfactant molecules.

In the case of alkaline earth metal phosphates, it is quite difficult to control whether phosphate anions are interacted with cationic surfactants or alkaline earth metal cations

because the crystallization between the inorganic species generally occurs very fast. Therefore, the mesostructural control of alkaline earth metal phosphates has not been realized until recently. Although it is considered that layered *n*-alkylammonium phosphates potentially act as intermediates to obtain mesostructured metal phosphates through the appropriate control of the interactions on one another [27], the route has not been applicable to the preparation of mesostructured alkaline earth metal phosphates. In Chapter 2, I actually demonstrated the synthetic route of a lamellar mesostructured calcium phosphate from *n*-alkylammonium phosphate under the synthetic condition to suppress the identical crystallization of calcium and phosphate ions [28].

In this Chapter, I report the successful synthesis of a composite material constructed by magnesium phosphate sheets and *n*-hexadecylammonium ions in the EtOH/H_2O mixed solvent system. I also discuss the influences of synthetic conditions such as the kind of alkali source, EtOH/H_2O molar ratio, and Mg/P molar ratio in the starting mixture on the formation of the composite material for further understanding ionically bonded mesostructured materials. In my preliminary study, mesostructured barium and strontium phosphates have never been obtained by the same synthetic method because the metal cations are strongly interacted with phosphate anions (not with protonated alkylamines). The insights including the present and previous results on the synthesis of lamellar mesostructured magnesium and calcium phosphates are important for understanding the formation of mesostructured alkaline earth metal phosphates, which provide a facile synthetic route of mesostructured materials with ionic frameworks.

3.2. Experimental

3.2.1. Materials

n-Hexadecylamine (*n*-$C_{16}H_{33}NH_2$) and aqueous solution of tetramethylammonium hydroxide (26% TMAOH) were obtained from Tokyo Kasei Kogyo Co. Phosphoric acid (85% H_3PO_4), aqueous solution of ammonia (25% NH_3), magnesium acetate tetrahydrate ($Mg(OAc)_2 \cdot 4H_2O$), and ethanol (EtOH) were obtained from Wako Chemical Co. Aqueous solution of tetraethylammonium hydroxide (35% TEAOH) was obtained from Sigma-Aldrich.

3.2.2. Synthesis of a lamellar mesostructured magnesium phosphate

In a typical synthesis, *n*-$C_{16}H_{33}NH_2$ (2.41 g, 10 mmol) and 85% H_3PO_4 (1.15 g, 10 mmol) were added to a mixed solvent of EtOH (27.6 g, 600 mmol) and H_2O (1.48 g, 82 mmol) and then a white slurry was obtained immediately. After stirring for 1 h, 26% TMAOH (1.75 g, 5 mmol) and $Mg(OAc)_2 \cdot 4H_2O$ (1.93 g, 9 mmol) were added to the white slurry under stirring and the stirring was kept for 0.5 h. The mixture with a composition of 0.9$Mg(OAc)_2$: H_3PO_4 : *n*-$C_{16}H_{33}NH_2$: 0.5TMAOH : 60EtOH : 20H_2O was stayed statisically for 24 h and then the resultant solid product was filtered, washed with EtOH repeatedly, and air-dried. The chemical composition in the stating mixtures was changed in the range of 0.5–1.5$Mg(OAc)_2$: H_3PO_4 : *n*-$C_{16}H_{33}NH_2$: 0.5alkali (NH_3, TMAOH, TEAOH) : 20–60EtOH : 20–60H_2O. The detailed synthesis conditions are listed in Table 3.1.

3.2.3. Characterization

X-ray diffraction (XRD) patterns were obtained by using a Bruker AXS D8 ADVACE with graphite monochromatized Cu Kα radiation. Transmission electron microscopic (TEM) images were taken by a JEOL JEM-2010 microscope, operated at 200 kV. Scanning electron microscopic (SEM) images were taken by a JEOL JSM-6320FS. ^{31}P MAS NMR spectra were obtained by using a Bruker DRX-400 spectrometer with a 7 mm zirconia rotor at a resonance frequency of 162.0 MHz with a spinning rate of 9 kHz. The spectra were accumulated with 4.5 μs pulse (π/2) and 10 s recycle delay. 85% H_3PO_4 aqueous solution was used as a chemical shift reference. ^{13}C CP/MAS NMR spectra were also collected by using the same spectrometer at 100.7 MHz with a spinning rate of 4 kHz, 6.1 μs pulse (π/2), and 10 s recycle delay. Adamantane was used as a chemical shift reference. The chemical compositions were measured by inductively coupled plasma atomic emission spectroscopy (ICP-AES, Seiko SPS 7700). Thermogravimetric (TG) analysis was conducted by using a Seiko TG/DTA320 thermal analyser.

Table 3. 1. Synthesis conditions of mesostructured magnesium phosphates

Run	Starting mixture		Product	
	Chemical composition/mol ratio Mg /P /$C_{16}NH_2$ /Alkali /EtOH /H_2O	Alkali source	phase	*d*-spacing / nm
1	0.9/1.0/1.0/0.5/60/20	TMAOH	LMMP	4.1
2	0.9/1.0/1.0/-/60/20	Non	LMMP, Salt	4.1, 2.7
3	0.9/1.0/1.0/0.5/60/20	Ammonia	Lamellar, Salt	5.1, 2.7
4	0.9/1.0/1.0/0.5/60/20	TEAOH	LMMP	4.1
5	0.9/1.0/1.0/0.5/20/60	TMAOH	LMMP, Newberyite	4.1
6	0.9/1.0/1.0/0.5/40/40	TMAOH	LMMP, Newberyite	4.1
7	0.5/1.0/1.0/0.5/60/20	TMAOH	LMMP, Salt	4.1, 2.7
8	0.8/1.0/1.0/0.5/60/20	TMAOH	LMMP, Salt	4.1, 2.7
9	1.0/1.0/1.0/0.5/60/20	TMAOH	LMMP, Salt	4.1, 2.7
10	1.2/1.0/1.0/0.5/60/20	TMAOH	LMMP	5.7
11	1.5/1.0/1.0/0.5/60/20	TMAOH	Amorphous	-

$C_{16}NH_2$: *n*-hexadecylamine, LMMP: lamellar mesostructured magnesium phosphate
Salt: *n*-hexadecylammonium phosphate salt, Temp. = room temperature, Time = 24 h

3.3. Results and discussion

3.3.1. Synthesis of a lamellar mesostructured magnesium phosphate

A composite material of magnesium phosphate sheets and *n*-hexadecylammonium (*n*-$C_{16}H_{33}NH_3^+$) ions was prepared through the reaction between magnesium acetate tetrahydrate ($Mg(OAc)_2 \cdot 4H_2O$) and phosphoric acid (H_3PO_4) in a basic $EtOH/H_2O$ mixed solution. The pH value of the solution was adjusted by the addition of tetramethylammonium hydroxide (TMAOH). A typical XRD pattern of the composite material, so called a lamellar mesostructured magnesium phosphate, is shown in Figure 3.1.

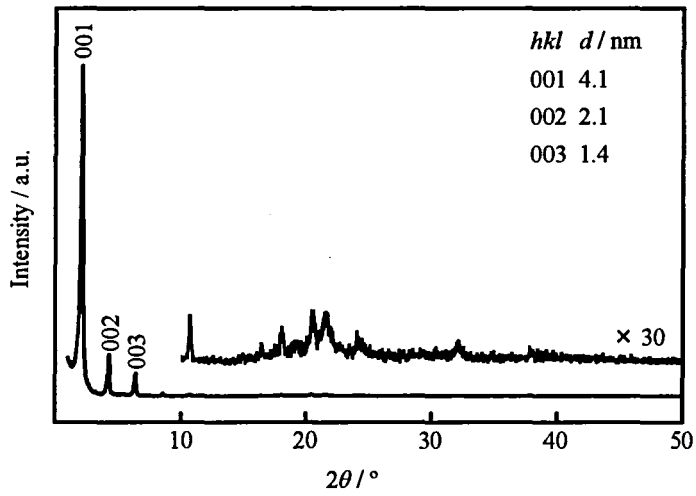

Figure 3.1. XRD pattern of a lamellar mesostructured magnesium phosphate.

A peak at the *d*-spacing of 4.1 nm and the higher order diffraction peaks were observed and those are due to a lamellar phase. The formation of the lamellar phase was also confirmed by TEM (Figure 3.2); clear striped patterns with a repeat distance of 4.0 nm were observed. Small peaks observed at 2θ = 15–35° are not assignable to well-known crystalline magnesium phosphates such as newberyite ($MgHPO_4 \cdot 3H_2O$), phosphorrösslerite ($MgHPO_4 \cdot 7H_2O$), farringtonite ($Mg_3(PO_4)_2$), and so on [29]. It is considered that the peaks at 2θ = 15–35° are due to the crystal structure of the composite material because the SEM image of the lamellar mesostructured material only exhibits aggregates of plate-like crystals with 0.2–0.8 μm in size (Figure 3.3).

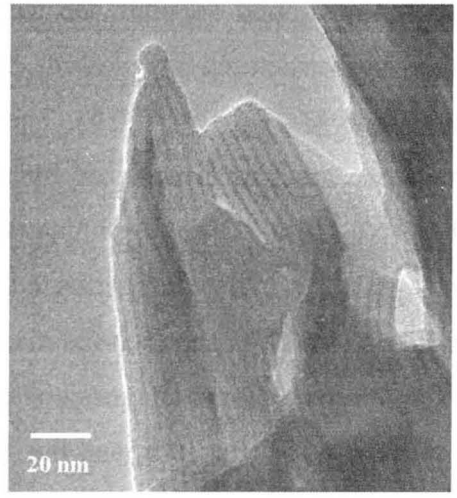

Figure 3.2. TEM image of a lamellar mesostructured magnesium phosphate.

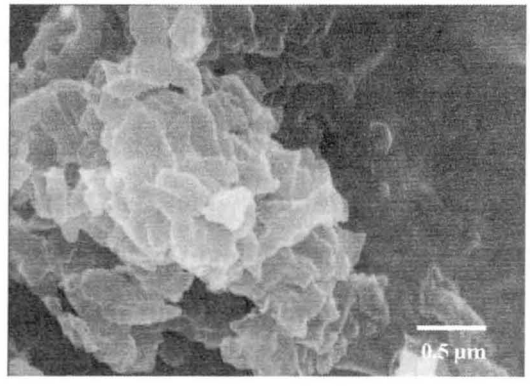

Figure 3.3. SEM image of a lamellar mesostructured magnesium phosphate.

The chemical formula of the composite material was investigated by ICP, ^{31}P MAS NMR, and TG. The Mg/P molar ratio of the composite material was ca. 0.5. The ^{31}P MAS NMR spectra are shown in Figure 3.4. Two peaks were observed at 5.4 and −0.8 ppm and those peaks were also detected at similar positions by the cross-polarization (CP) technique. The ^{31}P MAS NMR data reveal that two PO_4 units containing OH groups are present in the magnesium phosphate sheets. In the ^{13}C CP/MAS NMR spectrum of the composite material (Figure 3.5), several peaks assignable to carbon atoms in the alkyl chain of *n*-$C_{16}H_{33}NH_2$ were observed. The peak at 32 ppm can be assigned to $C_{4\text{-}13}$ atoms in all-*trans* methylene chains. A broadening of the peak due to C_1 atom in the α position of the ammonium moiety is due to the restricted conformation of *n*-$C_{16}H_{33}NH_2$ between magnesium phosphate sheets [30]. In addition, a peak due to TMA cations was not observed at around 55 ppm. On the basis of the results, it is considered that the lamellar mesostructured magnesium phosphate is composed of *n*-$C_{16}H_{33}NH_3^+$, two PO_4 units, and Mg^{2+} (Mg/P = 0.5). The TG curve of the lamellar mesostructured magnesium phosphate was categorized by three regions (Figure 3.6). Adsorbed EtOH and/or H_2O (6.0 mass %) were eliminated below 80 °C. The mass losses of the surfactant and the water molecules generated from the condensation of hydroxyl group were observed up to 600 °C and the total mass loss was calculated to be ca. 52 mass %. The lamellar mesostructured magnesium phosphate was calcined at temperatures in the range of 200–750 °C for 10 h, and the XRD patterns are shown in Figure 3.7. With an increase in temperature, the peak of the lamellar mesostructured magnesium phosphate were gradually disappeared below 300 °C. There were no XRD peaks in the XRD pattern of the product calcined between 300 and 600 °C. Taking into account the fact that metal diphosphites such as nickel and calcium diphosphites show no XRD peaks and are formed as precursors of metal pyrophosphates [31-33], the product might be magnesium diphosphite ($Mg(PO_3)_2$) compound. In the case of the products calcined at higher temperatures, the XRD peaks due to magnesium pyrophosphate ($Mg_2P_2O_7$) actually appeared and the intensity increased with elevating the calcination temperatures. By including the result that the *n*-$C_{16}H_{33}NH_2/PO_4$ molar ratio was calculated to be 1.0 by TG, the chemical formula of the lamellar mesostructured magnesium phosphate was represented as (*n*-$C_{16}H_{33}NH_3^+$)$Mg^{2+}(HPO_4^{2-})(H_2PO_4^-)$.

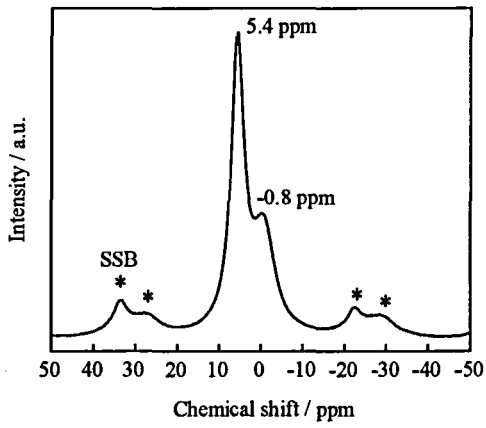

Figure 3.4. ^{31}P MAS NMR spectrum of a lamellar mesostructured magnesium phosphate.

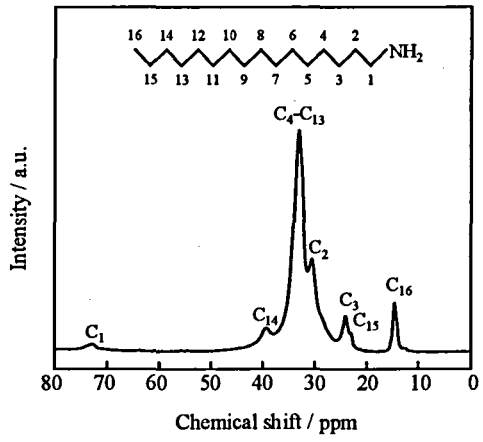

Figure 3.5. ^{13}C CP/MAS NMR spectrum of a lamellar mesostructured magnesium phosphate.

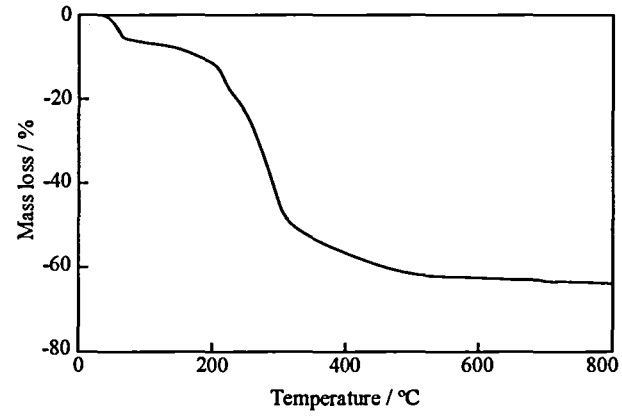

Figure 3.6. TG curve of a lamellar mesostructured magnesium phosphate.

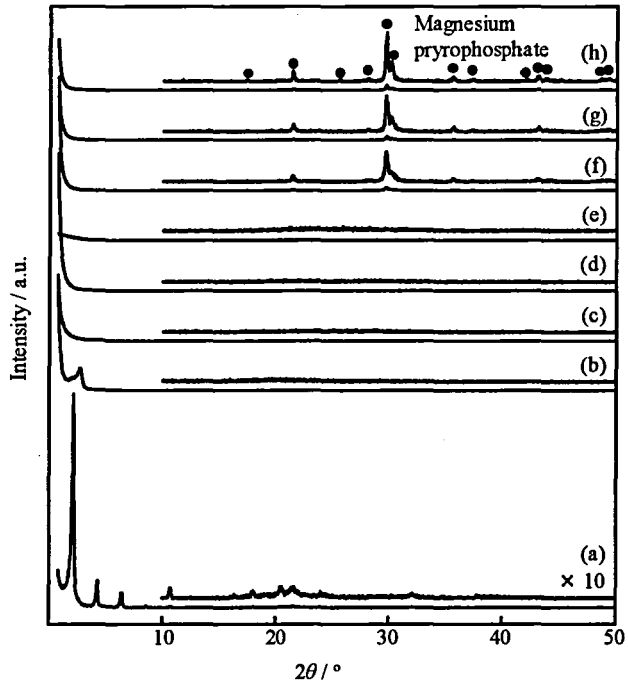

Figure 3.7. XRD patterns of (a) a lamellar mesostructured magnesium phosphate and the products obtained after calcination at (b) 200, (c) 300, (d) 400, (e) 600, (f) 650, (g) 700, and (h) 750 °C.

3.3.2. Effects of the synthesis conditions

3.3.2.1. Effect of the alkali source

The lamellar mesostructured magnesium phosphate was prepared by using different alkali sources. The composition of the starting mixture was $0.9Mg(OAc)_2$: H_3PO_4 : n-$C_{16}H_{33}NH_2$: 0.5alkali : 60EtOH : $20H_2O$. Aqueous solutions of ammonia, TMAOH,

and TEAOH were used as alkali sources. When the similar synthesis was conducted under an alkali-free condition, a lamellar phase was obtained as a main product (Figure 3.8(a)). However, *n*-hexadecylammonium phosphate salt (n-$C_{16}H_{33}NH_3^+$)($H_2PO_4^-$) was also co-existed as an impurity that is actually eliminated by an EtOH treatment [27]. After 0.5 g of the resultant solid was stirred in 150 g of EtOH at 60 °C for 5 h, filtered, and washed with EtOH at 60 °C, the impurity was removed completely.

The XRD pattern of the product prepared in the presence of ammonium ions showed a peak at the *d*-spacing of 5.1 nm (Figure 3.8(b)). Small peaks due to (n-$C_{16}H_{33}NH_3^+$)($H_2PO_4^-$) were still observed in the XRD pattern and the peak the *d*-spacing of 5.1 nm disappeared after the EtOH treatment. The synthesis with ammonia was also conducted at the Mg/P molar ratio of 1.0 in the stating mixture. The product contained not only the lamellar mesostructured magnesium phosphate but also struvite ($MgNH_4PO_4 \cdot 6H_2O$) because of the strong affinity between magnesium phosphate species and ammonium ions [29]. Therefore, it was found that pure lamellar mesostructured magnesium phosphate was obtained under the basic conditions with TMAOH and TEAOH (Figure 3.8(c), (d)).

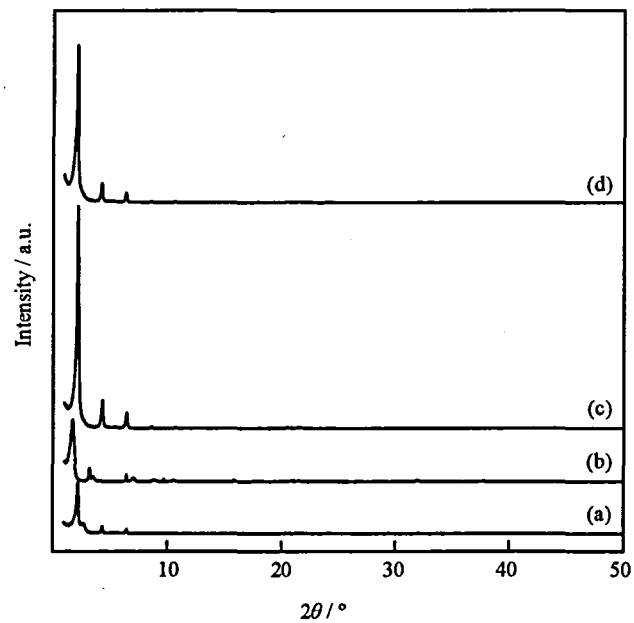

Figure 3.8. XRD patterns of the products obtained in the presence of various alkali sources of (a) alkali-free, (b) ammonia solution, (c) TMAOH, and (d) TEAOH.

3.3.2.2. Effect of the EtOH/H_2O molar ratio

The synthesis of the lamellar mesostructured magnesium was carried out under the conditions with compositions of 0.9$Mg(OAc)_2$: H_3PO_4 : *n*-$C_{16}H_{33}NH_2$: 0.5TMAOH : 80(EtOH+H_2O). The EtOH/H_2O molar ratio was varied in the range between 25/75, 50/50, and 75/25. The XRD patterns of the products prepared by using the basic mixed solvent systems with the EtOH/H_2O molar ratio of 25/75, 50/50 and 75/25 are shown in Figure 3.9. The lamellar mesostructured magnesium phosphate was obtained under the water rich condition (EtOH/H_2O = 25/75) with the formation of a hydrated crystalline magnesium phosphate newberyite ($MgHPO_4 \cdot 3H_2O$) (Figure 3.9(a)). The intensity of the peaks due to the lamellar phase increased slightly under the condition with EtOH/H_2O = 50/50 but newberyite was still present as a byproduct (Figure 3.9(b)). The XRD peaks due to newberyite disappeared under the EtOH rich condition (EtOH/H_2O = 75/25) and then lamellar mesostructured magnesium phosphate was obtained without impurities (Figure 3.9(c)). The results suggest that the absence of H_2O suppresses the formation of hydrated magnesium phosphates such as newberyite.

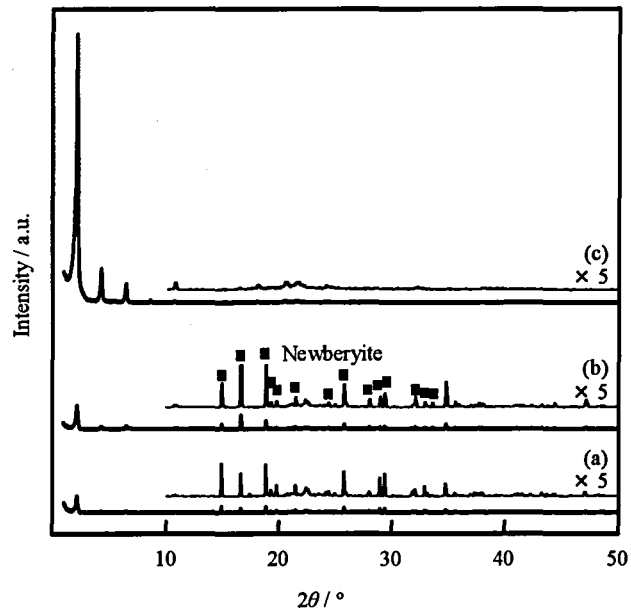

Figure 3.9. XRD patterns of the products prepared in various EtOH/H2O molar ratios of (a) 25/75, (b) 50/50, and (c) 75/25.

3.3.2.3. Effect of the Mg/P molar ratio

The lamellar mesostructured magnesium phosphate was prepared under the condition with various Mg/P molar ratios. The composition of the starting mixture was 0.5−1.5$Mg(OAc)_2$: H_3PO_4 : *n*-$C_{16}H_{33}NH_2$: 0.5TMAOH : 60EtOH : 20H_2O. Both the lamellar mesostructured magnesium phosphate and (*n*-$C_{16}H_{33}NH_3^+$)($H_2PO_4^-$) were obtained at lower Mg/P molar ratios (Figure 3.10(a)). The peak intensity due to the lamellar mesostructured magnesium phosphate increased with the increase in the amount of magnesium (Figure 3.10(a)-(c)). The peaks due to (*n*-$C_{16}H_{33}NH_3^+$)($H_2PO_4^-$) disappeared under the condition with the Mg/P molar ratio of 0.9. Even when the synthesis was conducted at a higher Mg/P molar ratio (1.0), (*n*-$C_{16}H_{33}NH_3^+$)($H_2PO_4^-$) was obtained again (Figure 3.10(d)). With the further increase of the Mg/P molar ratios (1.2−1.5), the XRD peaks due to the lamellar mesostructured magnesium phosphate disappeared with the broadening of the high angle XRD peaks due to the framework structure (Figure 3.10(e)-(f)). It was obvious that portion of Mg^{2+} ions eluted in the resultant mixture because there was the difference in the Mg/P molar ratios between the starting mixture and the composite material. The solubility of Mg^{2+} ions can be controlled by both the amount of the H_2O in the mixed solvent system and the pH value of the starting mixture prepared by using TMAOH and TEAOH as alkali sources.

3.3.3. Understanding of the formation of mesostructured alkaline earth metal phosphates with ionic frameworks

The crystallization of magnesium phosphates was suppressed by controlling pH value, Mg/P molar ratio, and EtOH/H_2O molar ratio in the starting mixture. Solubility of Mg^{2+} ions can be controlled according to the pH value of the starting mixture. The formation of hydrated magnesium phosphates such as newberyite ($MgHPO_4 \cdot 3H_2O$) can be suppressed by controlling the EtOH/H_2O molar ratio in the reaction mixtures. However, it is strongly demanded that pH adjusting agents do not participate in the formation of crystalline magnesium phosphate. Ammonia was not used as an alkali source because ammonium-type struvite ($MgNH_4PO_4 \cdot 6H_2O$) was preferentially formed under the condition. When the synthesis was carried out under conditions with low Mg/P molar ratios, undesirable (*n*-$C_{16}H_{33}NH_3^+$)($H_2PO_4^-$) were obtained with the formation of

objective lamellar phases.

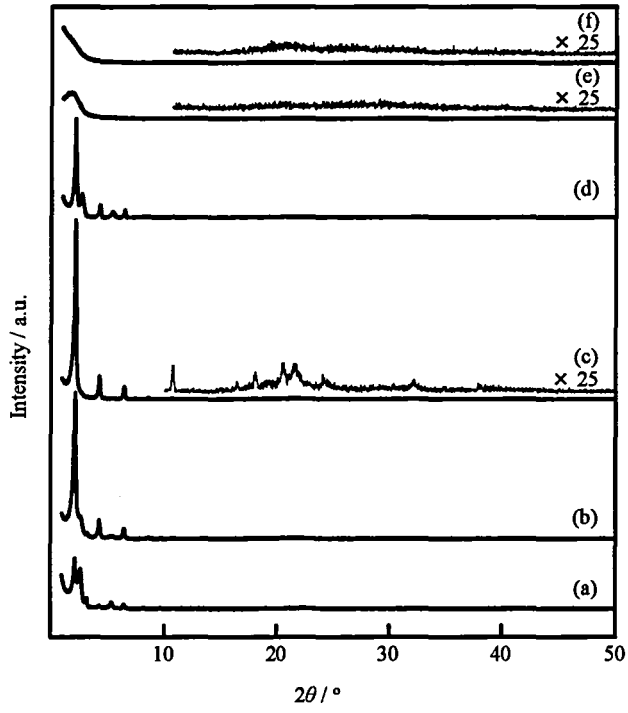

Figure 3.10. XRD patterns of the products obtained from various Mg/P molar ratios in the starting gel composition of (a) 0.5, (b) 0.8, (c) 0.9, (d) 1.0, (e) 1.2, and (f)1.5.

The synthetic region of lamellar mesostructured magnesium phosphate is narrower than that of calcium phosphate because of the difference in the solubility between Mg^{2+} and Ca^{2+} ions. Pure mesostructured materials can be obtained under a condition with the Mg/P molar ratio (0.9) and the EtOH/H_2O molar ratio (75/25). In the case of calcium phosphate, the solubility and crystallization controlled synthesis are also important to synthesize a lamellar mesostructured calcium phosphate without impurities. In compared with a lamellar mesostructured magnesium phosphate, lamellar mesostructured calcium phosphate is formed under wider conditions with the Ca/P molar ratios (0.7-1.0) and the EtOH/H_2O molar ratio (50/50-75/25). When barium and strontium phosphates were synthesized in the similar ethanol/water systems containing surfactants, mesostructured materials have never been obtained under any conditions because of stronger interactions of phosphates with the metal species than those with Ca^{2+} and Mg^{2+} ions.

On the basis of all the results on the mesostructural control of alkaline earth metal phosphates, I can summarize that one of the most important points to synthesize mesostructured alkaline earth metal phosphates is how to keep the interaction between ionically bonded inorganic sheets and alkylammonium ions, which is strongly related to the suppression of the formation of crystalline metal phosphate minerals and the control of the solubilities of reactants and products. The crystalline phases are formed very fast through the reaction between metal cations and phosphate anions, leading to the breaking the electrostatic interaction between alkylammonium cations and phosphate anions. The resultant minerals are hydrates and ammonium-type materials. Therefore, it should be considered whether water and ammonia are useful or not as solvent and regulator for the preparation of mesostructured alkaline earth metal phosphates, respectively.

3.4. Conclusions

A lamellar mesostructured magnesium phosphate was synthesized using *n*-$C_{16}H_{33}NH_2$ under the controlled conditions to avoid the formation of hydrated and ammonium-type alkaline earth metal phosphate minerals. Effects of several synthetic conditions such as the kind of alkali source, the EtOH/H_2O molar ratio, and the Mg/P molar ratio in the starting mixture were investigated in detail. Consequently, I can totally understand the formation of the mesostructured magnesium phosphates composed of ionic frameworks in detail, leading to further understanding of the formation of mesostructured alkaline earth metal phosphates with ionic frameworks. The insights are also quite useful for understanding the formation of mesostructured metal phosphates with covalent bonds in the presence of surfactants and will lead to the development of their facile synthetic methods.

References

1 J. B. Moffat, *Catal. Rev.*, 1978, **18**, 199.

2 C. Criado and J. R. R. Barrado, *Solid State Ionics*, 1993, **61**, 139.

3 A. De Stefanis, G. Perez and A. A. G. Tomlinson, *J. Mater. Chem.*, 1994, **4**, 959.

4 G. Alberti, M. Casciola, U. Costantino and R. Vivani, *Adv. Mater.*, 1996, **8**, 291.

5 A. K. Cheetham, G. Férey and T. Loiseau, *Angew. Chem., Int. Ed.*, 1999, **38**, 3269.

6 A. Clearfield, *Progr. Inorg. Chem.*, 1998, **47**, 47.

7 G. Cao, H. G. Hong and T. Mallouk, *Acc. Chem. Res.*, 1992, **25**, 420.

8 M. Ogawa and K. Kuroda, *Chem. Res.*, 1995, **95**, 399.

9 M. Jarcho, *Clin. Orthop. Relat. Res.*, 1981, **157**, 259.

10 H. W. Kim, G. Georgiou, J. C. Knowles, Y. H. Koh and H. E. Kim, *Biomaterials*, 2004, **25**, 4203.

11 S. Popovics, N. Rajendran and M. Penko, *ACI Mater. J.*, 1987, **81**, 64.

12 L. E. de-Bashan and Y. Bashan, *Water Res.*, 2004, **38**, 4222.

13 C. T. Kresge, M. E. Leonowicz, W. J. Roth, J. C. Vartuli and J. S. Beck, *Nature*, 1992, **359**, 710.

14 S. Beck, J. C. Vartuli, W. J. Roth, M. E. Leonowicz, C. T. Kresge, K. D. Schmitt, C. T-W. Chu, D. H. Olson, E. W. Sheppard, S. B. McCullen, J. B. Higgins and J. L. Schlenker, *J. Am. Chem. Soc.*, 1992, **114**, 10834.

15 Q. Huo, R. Leon, P. M. Petroff and G. D. Stucky, *Science*, 1995, **268**, 1324.

16 Q. Huo, D. I. Margolese and G. D. Stucky, *Chem. Mater.*, 1996, **8**, 1147.

17 T. Yanagisawa, T. Shimizu, K. Kuroda and C. Kato, *Bull. Chem. Soc. Jpn.*, 1990, **63**, 988.

18 S. Inagaki, Y. Fukushima and K. Kudoda, *J. Chem. Soc., Chem. Commun.*, 1993, 680.

19 D. Zhao, L. Feng, Q. Huo, N. Melosh, G. H. Fredrickson, B. F. Chmelka and G. D. Stucky, *Science*, 1998, **279**, 548.

20 X. S. Zhao, G. Q. Lu and G. J. Millar, *Ind. Eng. Chem. Res.*, 1996, **35**, 2075.

21 P. Selvam, S. K. Bhatia and C. G. Sonwane, *Ind. Eng. Chem. Res.*, 2001, **40**, 3237.

22 P. Behrens, *Angew. Chem., Int. Ed.*, 1996, **35**, 515.

23 A. Sayari and P. Liu, *Micropor. Mater.*, 1997, **12**, 149.

24 F. Schüth, *Chem. Mater.*, 2001, **13**, 3184.

25 M. Tiemann and M. Fröba, *Chem. Mater.*, 2001, **13**, 3211.

26 T. Kimura, *Micropor. Mesopor. Mater.*, 2005, **77**, 97.

27 S. R. J. Oliver and G. A. Ozin, *J. Mater. Chem.*, 1998, **8**, 1081.

28 N. Ikawa, Y. Oumi, T. Kimura, T. Ikeda and T. Sano, *Chem. Lett.*, 2006, **35**, 948.

29 JCPDS card numbers: newberyite; 00-035-0780, phosphorrösslerite; 00-019-0761, farringtonite; 00-033-0876, struvite; 00-036-1491

30 R. Simonutti, A. Comotti, S. Bracco and P. Sozzani, *Chem. Mater.*, 2001, **13**, 771.

31 A. Goñi, J. Rius, M. Insausti, L. Lezama, J. L. Pizarro, M. I. Arriortua and T. Rojo, *Chem. Mater.*, 1996, **8**, 1052.

32 C. B. A. Lima and C. Airoldi, *Solid State Sci.*, 2002, **4**, 1321.

33 C. B. A. Lima and C. Airoldi, *Solid State Sci.*, 2004, **4**, 1245.

Chapter 4

Structural control of mesostructured calcium phosphates using amine- and carboxylic acid-type surfactants

4.1. Introduction

Calcium phosphate compounds have attracted much attention for applications to biomaterials because of the unique properties such as the selective adsorption ability for biomolecules, biocompatibility, and ion-exchange ability [1-7]. High surface areas and large pore volumes have generally been demanded for uses in adsorbents, and moreover the control of pore size expands the possibility of the calcium phosphate compounds for the selective adsorption of nanometer-sized biomolecules. Actually, many researchers have tried to control morphologically and structurally for improving calcium phosphates [8-10] as excellent adsorbents and catalysts. Composite materials of calcium phosphates and biomolecules such as collagen and bone morphogenetic protein have been focused and applied to artificial bones. Both of carboxyl and amino groups in such biomolecules play an important role in the formation of apatite in our body, because calcium phosphate species can interact with functional groups of the organic molecules at the inorganic-organic interfaces.

There have been a large number of reports on the structural control of silicas in nanometer scale through the interaction with surfactant molecules that can be self-assembled in aqueous solutions [11-17]. Cationic surfactants have mainly been used to prepare mesophase silicates, affording periodic mesoporous silicas with high surface areas, tunable mesopores, and large pore volumes after the removal of the surfactants. Surfactant templating has also been useful for the mesostructural control of metal oxides and phosphates composed of covalently bonded non-silica-based frameworks [18-23], as well as silica. However, similar templating of ionic inorganic materials such as calcium phosphates has not been developed so far. This is related to the difficulty to balance the interactions of phosphate species with calcium ions and

amine-type headgroups in surfactant molecules simultaneously. Several research groups have reported the synthesis of mesostructured calcium phosphates mainly using surfactants serving as cationic molecules [24-35], but it is difficult to prepare pure mesostructured calcium phosphate without byproducts such as crystalline calcium phosphates (brushite, monetite, tricalcium phosphates, apatite, and so on.) because calcium ions and phosphate species show a tendency to be strongly interacted each other and then such crystalline byproducts are formed in aqueous solutions. In Chapter 2, I described that a lamellar mesostructured calcium phosphate was successfully synthesized without byproducts using *n*-hexadecylamine in the ethanol/water ($EtOH/H_2O$) system [36-38]. Interaction between *n*-hexadecylamine and phosphate species during the generation of the ionic interaction between calcium ions and phosphate species can be maintained in the $EtOH/H_2O$ system which suppresses the formation of a hydrated crystalline calcium phosphate (brushite). The mixed solvent system of alcohol and water is also expected for controlling the crystallinity of calcium phosphates because the $EtOH/H_2O$ system is useful for the synthesis of low crystalline and/or amorphous calcium phosphates [39, 40].

Only lamellar mesostructured calcium phosphate constructed by ionic frameworks was successfully prepared using *n*-hexadecylamine presenting as a cationic species in the presence of water as described above [36-38] and I demonstrated that the synthetic method was vaguely applied to the synthesis of lamellar mesostructured magnesium phosphate (Chapter 3) [41]. Anionic surfactant templating of silica has also been reported [42-44]; organosilane compounds with amino and ammonium groups that fulfill as cationic species in aqueous solutions play an important role in the generation of the interaction between silicate species and anionic surfactant molecules. Anionic headgroups in the surfactants cannot directly be interacted with silicate species, but silicate species are fixed through the formation of siloxane bonds in the frameworks. Many kinds of other interactions between inorganic species and surfactant molecules have been reported [45]. In case of calcium phosphates, it is considered that direct interaction of calcium cations with anionic surfactant molecules is possible during the formation of ionic inorganic frameworks. Accordingly, both of anionic and cationic surfactants will be available for the mesostructural controlling of calcium phosphate materials, which is quite important for further understanding various interactions at the

inorganic-inorganic (I-I) and inorganic-organic (I-O) interfaces in surfactant templating of inorganic solids.

In this Chapter, I investigate to control interactions of headgroups in carboxylic acid-type and amine-type surfactants during the formation of mesostructured calcium phosphates, leading to the development of surfactant templating of calcium phosphates as a candidate of inorganic solids with ionic frameworks. On the basis of the insights, wormhole-like mesostructured calcium phosphates are obtained using chemically designed surfactant molecules such as carboxylic acid-type *N*-lauroyl-L-glutamic acid and amine-type 4-dodecyldiethylenetriamine with large headgroups, while the use of palmitic acid and *n*-hexadecylamine with simple functional groups leads to the formation of lamellar mesostructured calcium phosphates.

4.2. Experimental

4.2.1. Materials.

N-lauroyl-L-glutamic acid ($C_{11}H_{23}CONHCH(CO_2H)C_2H_4CO_2H$) was supplied by Ajinomoto Co., Inc. Palmitic acid ($C_{15}H_{31}CO_2H$), *n*-hexadecanethiol ($C_{16}H_{33}SH$), *n*-hexadecyltrimethylammonium bromide ($C_{16}H_{33}N(CH_3)_3Br$), and 1-chlorohexadecane ($C_{16}H_{33}Cl$) were obtained from Tokyo Kasei Kogyo Co. Phosphoric acid (85% H_3PO_4), calcium acetate monohydrate ($Ca(OAc)_2 \cdot H_2O$), ethanol (EtOH), and ethylenediamine ($NH_2C_2H_4NH_2$) were obtained from Wako Chemical Co. Diammonium hydrogenphosphate ($(NH_4)_2HPO_4$) was obtained from Nacalai Tesque Co. 4-Dodecyldiethylenetriamine ($C_{12}H_{25}N(C_2H_4NH_2)_2$: 80%) and tetramethylammonium hydroxide (TMAOH) pentahydrate ($(CH_3)_4NOH \cdot 5H_2O$) were obtained from ACROS. Calcium diisopropoxide ($Ca(O^iPr)_2$) was obtained from Kojundo Chemical Lab. Co. According to the literature [46], *n*-hexadecylethylenediamine ($C_{16}H_{33}NHC_2H_4NH_2$) was prepared by the reaction between $C_{16}H_{33}Cl$ and $NH_2C_2H_4NH_2$.

4.2.2. Synthesis of mesostructured calcium phosphates using anionic surfactants.

Mesostructured calcium phosphates were prepared using palmitic and *N*-lauroyl-L-glutamic acids as anionic surfactants. In a typical synthesis using *N*-lauroyl-L-glutamic acid, $Ca(O^iPr)_2$ (1.58 g) and *N*-lauroyl-L-glutamic acid (4.87 g) were added to a mixed solvent of EtOH (5.0 g) and H_2O (14.4 g) and then a white slurry

was obtained after stirring for 2 h. $(NH_4)_2HPO_4$ (0.79 g) was added to the white slurry under stirring and the stirring was kept for 2 h. The resultant mixture was filtered, washed with EtOH, and air-dried. The composition of the mixture was $Ca(O^iPr)_2$: $0.6(NH_4)_2HPO_4$: $1.5C_{11}H_{23}CONHCH(CO_2H)C_2H_4CO_2H$ (pH = 5.5). In a synthesis using palmitic acid, the starting mixture ($1.5C_{15}H_{31}CO_2H$: 11EtOH : $80H_2O$, pH = 9.7) was prepared by the same procedure.

4.2.3. Synthesis of mesostructured calcium phosphates using amine-type surfactants.

Mesostructured calcium phosphates were prepared using $C_{12}H_{25}N(C_2H_4NH_2)_2$ and $C_{16}H_{33}NHC_2H_4NH_2$ acting as cationic surfactants in aqueous solutions. In a typical synthesis with 4-dodecyldiethylenetriamine, 85% H_3PO_4 (0.58 g), pentahydrated TMAOH (0.09 g), and 80% 4-dodecyldiethylenetriamine (0.85 g) were added to EtOH (30.0 g) and then a white slurry was obtained after stirring for 2 h. A clear aqueous solution of $Ca(OAc)_2$ (0.88 g) was added to the white slurry under stirring and the stirring was kept for 30 min. The resultant mixture was filtered, washed with EtOH, and air-dried. The compositions of the mixtures were $0.5Ca(OAc)_2{\cdot}H_2O$: H_3PO_4 : 0.5TMAOH : $0.5C_{16}H_{33}NHC_2H_4NH_2$: 60EtOH : $20H_2O$ (pH = 6.9) and $Ca(OAc)_2{\cdot}H_2O$: H_3PO_4 : 0.5TMAOH : $0.5C_{12}H_{25}N(C_2H_4NH_2)_2$: 130EtOH : $30H_2O$ (pH = 5.4). The synthesis using $C_{16}H_{33}N(CH_3)_3Br$ as a cationic surfactant was also conducted to investigate interactions at the interfaces between calcium phosphate frameworks and surfactant molecules.

4.2.4. Characterization.

X-ray diffraction (XRD) patterns were obtained by using a Bruker AXS D8 ADVANCE with graphite monochromatized Cu Kα radiation (40 kV, 30 mA). Transmission electron microscopic (TEM) images were taken by a JEOL JEM-2010 microscope, operated at 200 kV. ^{13}C CP/MAS NMR spectra were obtained by using a Bruker DRX-400 spectrometer with a 7 mm zirconia rotor at a resonance frequency of 100.7 MHz with a spinning rate of 4 kHz. The spectra were accumulated with a 90 ° pulse width of 6.8 μs and 15 s recycle delay. Tetramethylsilane was used as a reference. ^{31}P MAS NMR spectra were also collected with the same spectrometer at 161.9 MHz with a spinning rate of 6 kHz, a 90 ° pulse width of 4.5 μs, and 10 s recycle delay. 85%

H_3PO_4 aqueous solution was used as a reference. FT-IR spectra were recorded on JEOL JIR-7000 spectrometer with 2 cm^{-1} resolution using KBr disc method. The compositions were measured by inductively coupled plasma atomic emission spectroscopy (ICP-AES, Seiko SPS 7700) and thermogravimetric (TG) analysis (Seiko TG/DTA320 thermal analyzer).

4.3. Results and discussion

4.3.1. Synthesis of mesostructured calcium phosphates using anionic surfactants.

Mesostructured calcium phosphates were synthesized using palmitic ($C_{15}H_{31}CO_2H$) and *N*-lauroyl-L-glutamic acid ($C_{11}H_{23}CONHCH(CO_2H)C_2H_4CO_2H$) as anionic surfactants in the mixed solvent system of ethanol and water. The XRD pattern of the product prepared using palmitic acid showed three peaks in low diffraction angles assignable to (001), (002), and (003) reflections of a lamellar structure with the d_{001} spacing of 4.4 nm (Figure 4.1(a)). Several peaks were also observed in high diffraction angles, which cannot be assigned to peaks due to crystalline calcium phosphates such as brushite, monetite, and hydroxyapatite [47]. The TEM image of the product exhibited clear striped patterns typically observed for lamellar mesostructured materials (Figure 4.2(a)). The ^{13}C CP/MAS NMR spectrum of the lamellar product showed several peaks, all of which were assignable to carbon atoms in palmitic acid (Figure 4.3(a)). A peak at 32 ppm can be assigned to carbon atoms of all-*trans* methylene groups in the alkyl chain and several peaks between 180 and 190 ppm are due to carboxyl groups in palmitic acid. The ^{31}P MAS NMR spectrum of the lamellar product showed a sharp peak centered at 1.6 ppm (Figure 4.3(c)). The FT-IR spectrum of the lamellar product showed that sharp and broad peaks corresponding to ionized ($-CO_2^-$) and unionized ($-CO_2H$) carboxyl groups were observed at 1540 and 1724 cm^{-1}, respectively (Figure 4.4(a)) [48], with the peaks due to methyl and methylene groups in the range of 2800–3000 cm^{-1}.

The XRD pattern of the product prepared using *N*-lauroyl-L-glutamic acid showed a peak with the *d* spacing of 3.8 nm in the 2θ region lower than 5° without any obvious peaks in high diffraction angles, suggesting the formation of a mesostructured product composed of amorphous frameworks (Figure 4.1(b)) [49]. A wormhole-like structure

was observed by TEM (Figure 4.2(b)), supporting that the mesostructural ordering of calcium phosphate was affected by the molecular structure of surfactants used. The ^{13}C CP/MAS NMR spectrum of the mesostructured product showed several peaks assignable to carbon atoms in *N*-lauroyl-L-glutamic acid (Figure 4.3(b)). A peak at around 30 ppm can be assigned to carbon atoms of methylene groups in the alkyl chain. Broad peaks due to carboxyl and amide groups in the surfactant were observed between 170 and 190 ppm. In the FT-IR spectrum, the peaks corresponding to methyl and methylene groups were observed in the range of 2800–3000 cm^{-1} (Figure 4.4(b)). The FT-IR spectrum also contained a peak at around 1590 cm^{-1} with a shoulder peak at 1716 cm^{-1} assignable to ionized ($-CO_2^-$) and unionized ($-CO_2H$) carboxyl groups, respectively [50, 51]. A broad peak due to N-H stretching vibration of amide groups were also observed at 3200–3600 cm^{-1}. The ^{31}P MAS NMR spectrum of the product showed a broad peak centered at 1.3 ppm (Figure 4.3(d)). The result indicates the presence of P atoms with only one environment even in amorphous calcium phosphate frameworks. On the basis of the results by ICP and TG (Figure 4.5(a)), the composition of the product was $0.36C_{11}H_{23}CONH(CO_2H)C_2H_4CO_2H : 1.00CaO : 0.26P_2O_5$.

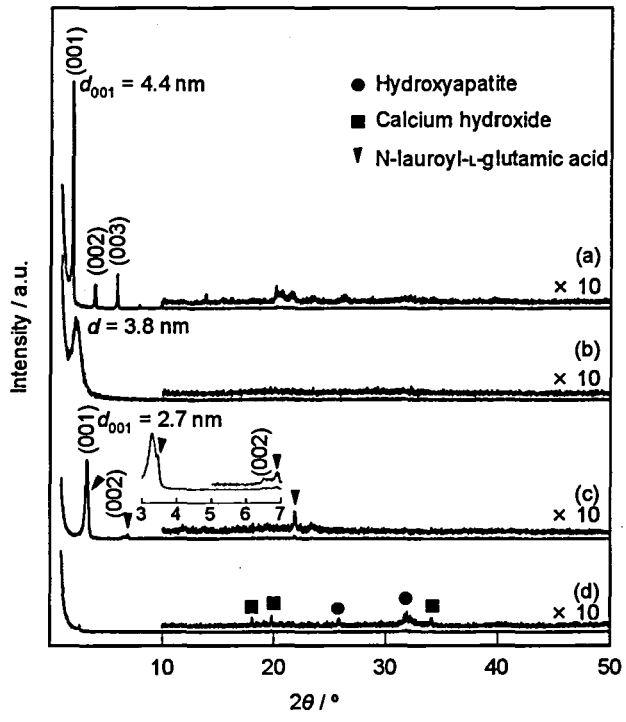

Figure 4.1. XRD patterns of the mesostructured products prepared using (a) palmitic and (b) *N*-lauroyl-L-glutamic acids, (c) the intermediate obtained without phosphoric acid by the reaction between *N*-lauroyl-L-glutamic acid and $Ca(O^iPr)_2$, and (d) the mesostructured product prepared using n-hexadecanethiol.

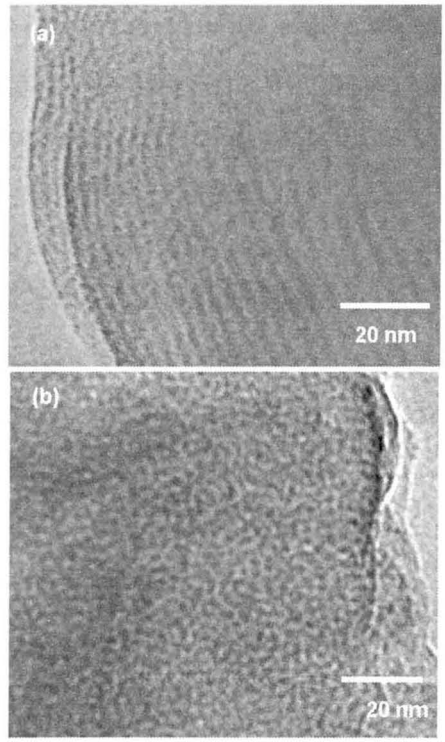

Figure 4.2. TEM images of the mesostructured products prepared using (a) palmitic and (b) *N*-lauroyl-L-glutamic acids.

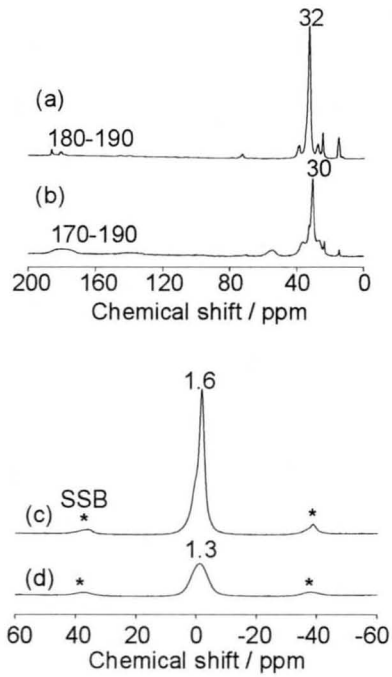

Figure 4.3. (a, b) ^{13}C CP/MAS and (c, d) ^{31}P MAS NMR spectra of the mesostructured products with (a, c) lamellar and (b, d) wormhole-like structures.

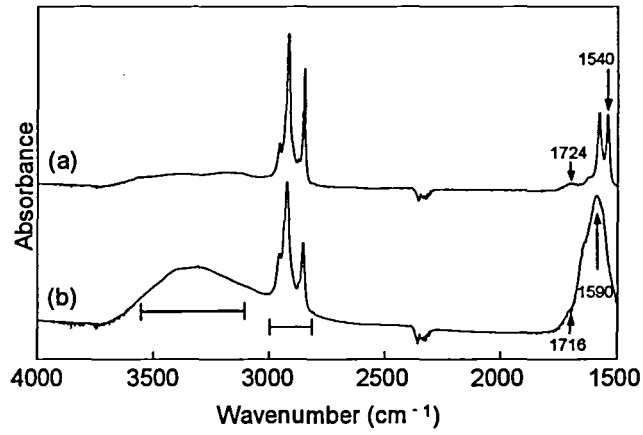

Figure 4.4. FT-IR spectra of the mesostructured products prepared using (a) palmitic and (b) *N*-lauroyl-L-glutamic acid s.

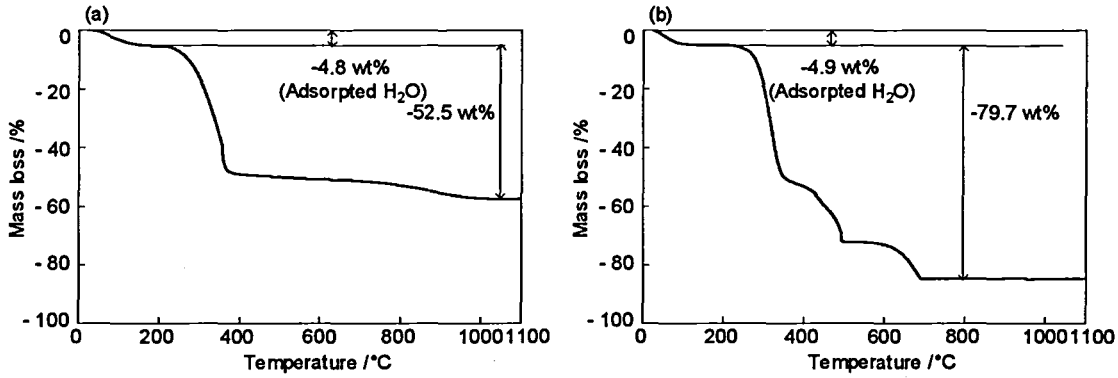

Figure 4.5. TG curves of (a) the mesostructured product prepared using *N*-lauroyl-L-glutamic acid and (b) the intermediate obtained without phosphoric acid.

4.3.2. Formation of lamellar and wormhole-like mesostructured calcium phosphates prepared using anionic surfactants.

A lamellar mesostructured calcium phosphate was obtained using palmitic acid. Similar product with a lamellar structure was obtained even without phosphoric acid (this kind of the product is called as intermediate hereafter) and the structure of the intermediate was not changed by subsequent reaction with phosphoric acid.

On the basis of the ICP and TG data (Figure 4.6), the compositions of the final lamellar product and the intermediate were $0.70C_{15}H_{31}CO_2H$: $1.00CaO$: $0.29P_2O_5$ and $1.95C_{15}H_{31}CO_2H$: $1.00CaO$, respectively. The headgroup of palmitic acid is very small and then the lamellar mesostructured calcium phosphate is formed (Scheme 4.1(a)). The XRD pattern of the intermediate obtained by the reaction between *N*-lauroyl-L-glutamic acid and $Ca(O^iPr)_2$ (without phosphoric acid) was different from that of the final

product with a wormhole-like structure showing only one peak in low diffraction angles. The XRD pattern of the intermediate showed two peaks assignable to (001) and (002) reflections of a lamellar structure with the d_{001} spacing of 2.7 nm in addition to three peaks due to residual *N*-lauroyl-L-glutamic acid. The lamellar structure of the intermediate was directly observed by TEM (Figure 4.7), being also supported by the result that the d_{001} spacing (2.7 nm) was increased to 3.8 nm by swelling in *n*-decyl alcohol. The mesostructured calcium phosphate with a wormhole-like structure was formed after the reaction with phosphate species. It is considered that the transformation of the lamellar intermediate into the wormhole-like structure is caused through the release of *N*-lauroyl-L-glutamic acid during the reaction with phosphate anions to balance the whole change. On the basis of the TG analysis of the intermediate, the composition was $1.27C_{11}H_{23}CONHCH(CO_2H)C_2H_4CO_2H$: 1.00CaO (Figure 4.5(b)). In comparison with that of the final product with the wormhole-like structure ($0.36C_{11}H_{23}CONH(CO_2H)C_2H_4CO_2H$: 1.00CaO : $0.26P_2O_5$), the excess amount of *N*-lauroyl-L-glutamic acid is present, being good agreement with the XRD result. The lamellar structure of the intermediate was distorted by the reaction with phosphoric acid that induces both of the elimination of *N*-lauroyl-L-glutamic acid and the transformation into the wormhole-like structure because of the larger headgroup of *N*-lauroyl-L-glutamic acid than that of palmitic acid (Scheme 4.1(b)). It is difficult to associate the formation of wormhole-like structure with the phase behavior of *N*-lauroyl-L-glutamic acid because of the presence of alcohols such as ethanol and isopropanol [52].

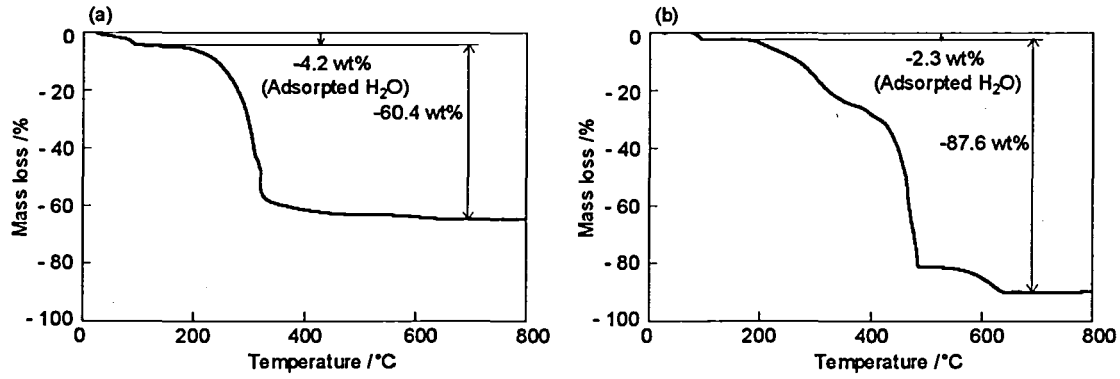

Figure 4.6. TG curves of (a) the mesostructured product prepared using palmitic acid and (b) the intermediate obtained without phosphoric acid by reaction between palmitic acid and $Ca(O^iPr)_2$.

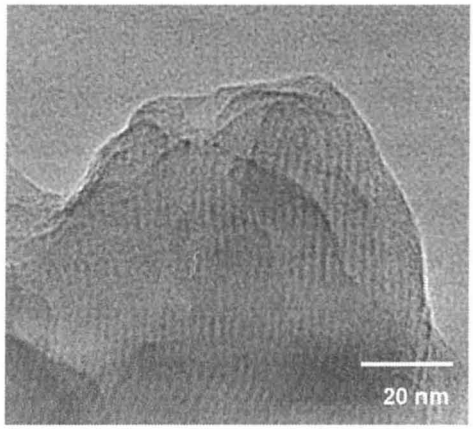

Figure 4.7. TEM image of the intermediate obtained (without phosphoric acid) by the reaction between *N*-lauroyl-L-glutamic acid and $Ca(O^iPr)_2$.

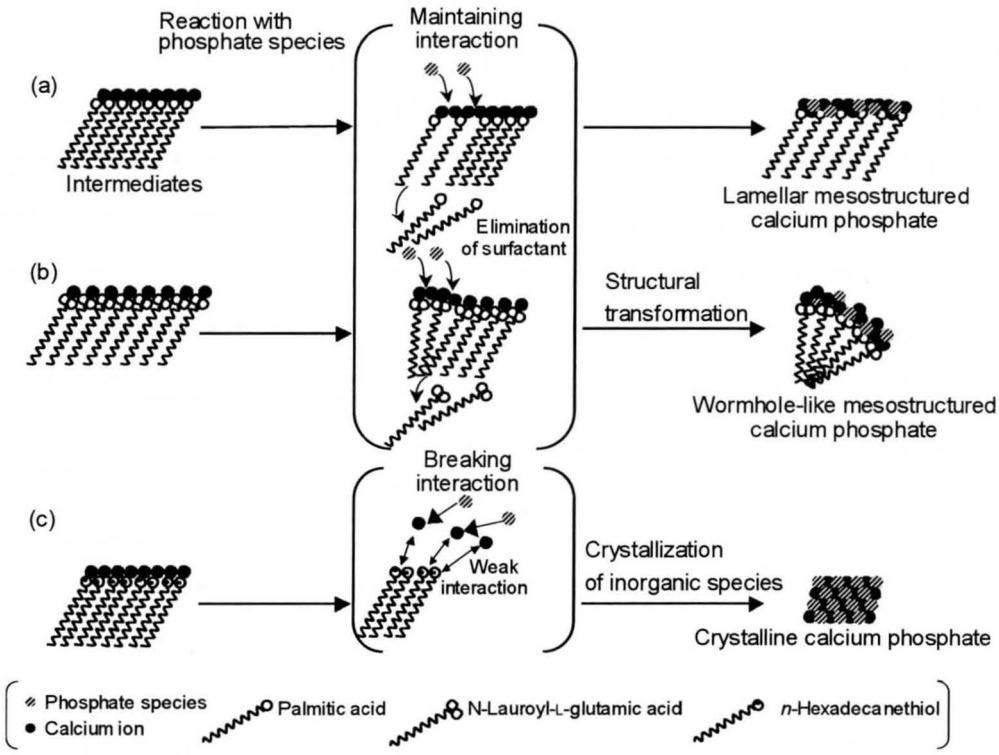

Scheme 4.1. Formation of (a) lamellar and (b) wormhole-like mesostructured products prepared respectively using palmitic acid and *N*-lauroyl-L-glutamic acid, and (c) crystalline calcium phosphate in the presence of n-hexadecanethiol.

On the basis of the FT-IR results, both carboxylic acid-type surfactants were mainly ionized in the mesostructured calcium phosphates. Considering the chemical compositions, all the calcium ions are not interacted with the anionic carboxyl groups, and interact with phosphate ions to afford calcium phosphate species in the mesostructured products. Such calcium phosphates are exchangeable by other ions such as F^-, Cl^-, Br^-, I^- and OH^- [53] which are not present in the present systems. A peak due to OH^- was not observed at around 3570 cm^{-1} in the FT-IR spectra [54]. Consequently, the mesostructured calcium phosphates are constructed by calcium ions and phosphate units with both ionized and unionized carboxylic acid-type surfactant molecules.

4.3.3. Interaction between anionic surfactants and calcium phosphates.

The preparation using *n*-hexadecanethiol ($C_{16}H_{33}SH$), as well as anionic palmitic and *N*-lauroyl-L-glutamic acids, was conducted in the mixed solvent system to investigate interactions between anionic surfactants and inorganic species. Several XRD peaks due to low crystalline hydroxyapatite [55] and calcium hydroxide ($Ca(OH)_2$) were observed (Figure 4.1(d)). Mesostructured calcium phosphate was not obtained using *n*-hexadecanethiol because of a weak interaction with inorganic species (Scheme 4.1(c)).

Interactions at the inorganic-inorganic (I-I) and inorganic-organic (I-O) interfaces during the formation of mesostructured calcium phosphates are summarized in Scheme 4.2. Anionic surfactant molecules are normally interacted with cationic species such as calcium ions. As described above, a lamellar intermediate was formed by the reaction between *N*-lauroyl-L-glutamic acid and $Ca(O^iPr)_2$. After the reaction with phosphoric acid, the intermediate was transformed into a wormhole-like calcium phosphate. In this case, interaction of calcium ions with carboxyl groups in *N*-lauroyl-L-glutamic acid is concurrent during further reaction between calcium ions and phosphate species (Scheme 4.2(a)). In the lamellar mesostructured calcium phosphate prepared using palmitic acid, similar formation mechanism is applied because of the presence of carboxyl group in palmitic acid (Scheme 4.2(a)). In contrast, the interaction between *n*-hexadecanethiol and inorganic species is so weak that *n*-hexadecanethiol is not useful for mesostructural control and leads to the formation of crystalline calcium phosphates (Scheme 4.2(b)).

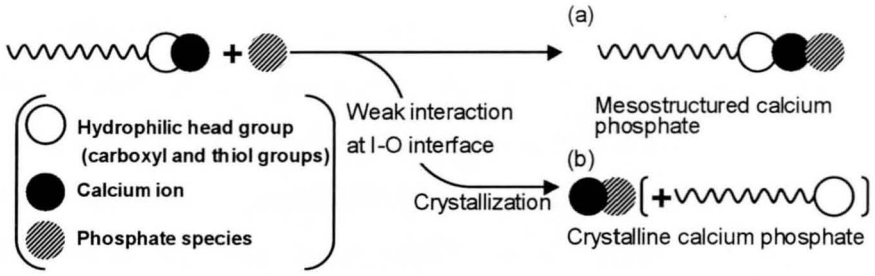

Scheme 4.2. Interactions at the I-I and I-O interfaces during the formations of mesostructured calcium phosphates prepared using carboxylic acid- and thiol-type surfactants.

4.3.4. Synthesis of mesostructured calcium phosphates using amine-type surfactants.

Calcium phosphates were synthesized using amine-type surfactants such as 4-dodecyldiethylenetriamine ($C_{12}H_{25}N(C_2H_4NH_2)_2$) and *n*-hexadecylethylenediamine ($C_{16}H_{33}NH(C_2H_4)NH_2$) in the EtOH/$H_2O$ system. The XRD pattern of the product prepared using 4-dodecyldiethylenetriamine showed only one peak with the *d* spacing of 4.4 nm in low diffraction angles without any obvious peaks in high diffraction angles (Figure 4.8(a)), as in the case using *N*-lauroyl-L-glutamic acid, and a wormhole-like structure was observed by TEM (Figure 4.9(a)). The ^{13}C CP/MAS NMR spectrum of the mesostructured product showed several peaks assignable to carbon atoms in 4-dodecyldiethylenetriamine (Figure 4.10(a)). A peak at around 32 ppm can be assigned to methylene groups in the alkyl chain. A broad peak centered at 47 ppm is due to ethylene groups located between primary and tertiary amino groups. The ^{31}P MAS NMR spectrum of the mesostructured product showed a broad peak centered at 1.2 ppm, indicating that phosphorus atoms are present in amorphous frameworks (Figure 4.10(c)). The FT-IR spectrum of the mesostructured product showed broad peaks due to ammonium groups in the range of 2800-3300 cm^{-1} and two peaks corresponding to neutral primary amine groups at 1580 and 1650 cm^{-1} (Figure 4.11) [56]. The composition of the mesostructured product was calculated by the TG and ICP data as $0.16C_{12}H_{25}N(C_2H_4NH_2)_2 : 0.95CaO : 0.5P_2O_5$ (Figure 4.12).

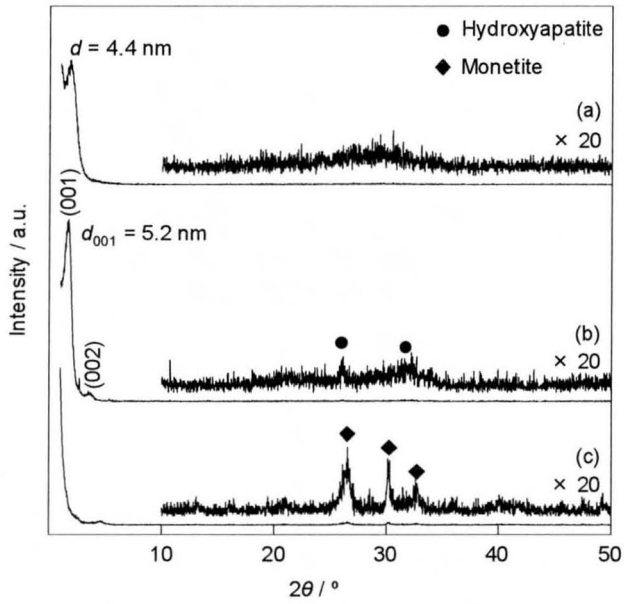

Figure 4.8. XRD patterns of mesostructured products prepared using (a) 4-dodecyldiethylenetriamine, (b) *n*-hexadecylethylenediamine, and (c) *n*-hexadecyltrimethylammonium bromide.

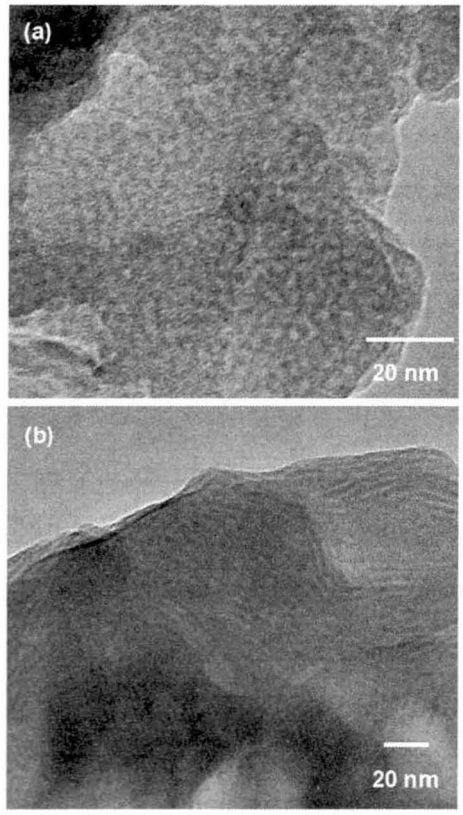

Figure 4.9. TEM images of mesostructured products prepared using (a) 4-dodecyldiethylenetriamine and (b) *n*-hexadecylethylenediamine.

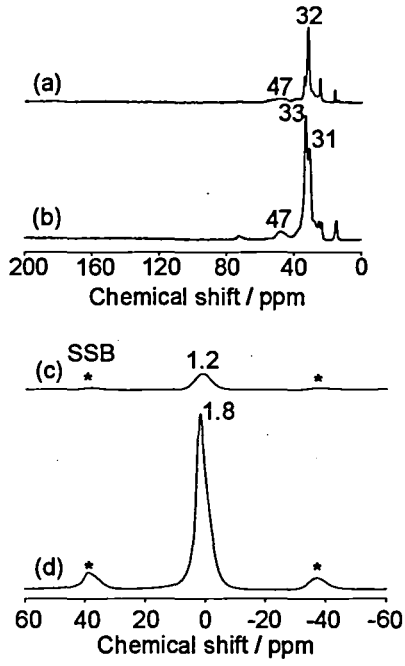

Figure 4.10. (a, b) ^{13}C CP/MAS NMR and (c, d) ^{31}P MAS NMR spectra of mesostructured products prepared using (a, c) 4-dodecyldiethylenetriamine and (b, d) *n*-hexadecylethylenediamine.

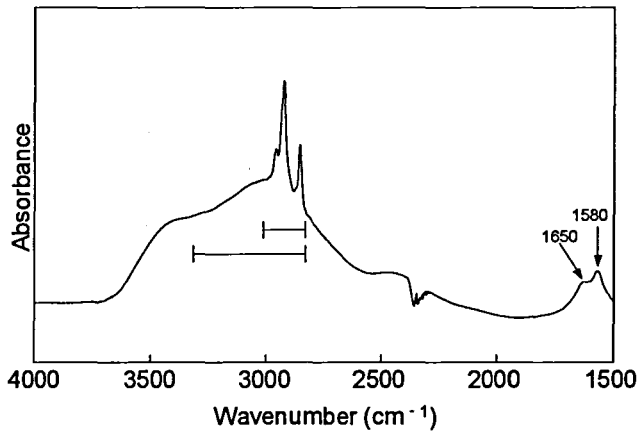

Figure 4.11. FT-IR spectrum of the mesostructured product prepared using 4-dodecyldiethylenetriamine.

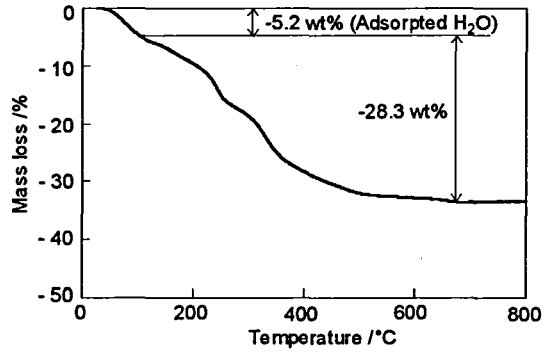

Figure 4.12. TG curve of the mesostructured product prepared using 4-dodecyldiethylenetriamine.

The XRD pattern of the product prepared using *n*-hexadecylethylenediamine showed two peaks in low diffraction angles assignable to (001) and (002) reflections of a lamellar structure with the d_{001} spacing of 5.2 nm (Figure 4.8(b)). Two small peaks at 2θ = 26 and 32° due to hydroxyapatite were observed in high diffraction angles. The TEM image of the mesostructured product showed a distorted striped pattern, suggesting the formation of a lamellar mesostructured calcium phosphate that is not stacked so regularly whole the structure (Figure 4.9(b)). The ^{13}C CP/MAS NMR spectrum of the mesostructured product showed several peaks assignable to carbon atoms in *n*-hexadecylethylenediamine (Figure 4.10(b)). Peaks originating from methylene groups in the alkyl chain were observed at around 31 and 33 ppm. A broad peak at around 47 ppm is due to the ethylene spacer located between primary and secondary amino groups. The ^{31}P MAS NMR spectrum of the mesostructured product showed a sharp peak at 1.8 ppm (Figure 4.10(d)).

4.3.5. Interaction between amine-type surfactants and calcium phosphates.

Interactions at the I-I and I-O interfaces during the formation of the mesostructured calcium phosphates are summarized in Scheme 4.3. In the preparation of a lamellar mesostructured calcium phosphate using *n*-hexadecylamine in the EtOH/H_2O mixed solvent system [36-38], the interaction of phosphate species with primary amino groups was maintained to some extent during the generation of new interaction between phosphate species and calcium ions because of the strong interaction between phosphate species and primary amino groups. However, brushite was formed in the water solvent system in spite of the presence of *n*-hexadecylamine, indicating the interaction at the I-I

interface was stronger than the I-O interface. The interaction at the I-I interface is weaken in the EtOH/H_2O mixed solvent system due to suppress the formation of crystalline calcium phosphates. The wormhole-like mesostructured calcium phosphate is constructed by calcium ions, phosphate species, and dodecyldiethylenetriamine molecules mainly with two primary ammonium groups.

As shown in Scheme 4.4, the formation of the wormhole-like structure depends on the molecular structure of 4-dodecyldiethylenetriamine with a headgroup much larger than amino group in *n*-hexadecylamine useful for the preparation of a lamellar mesostructured product (Scheme 4.4(a, b)). In case using *n*-hexadecylethylenediamine, the d_{001} spacing (5.2 nm) is larger than those observed for other mesostructured calcium phosphates synthesized using *n*-hexadecylamine (4.4 nm) [36-38] and 4-dodecyldiethylenetriamine (4.4 nm). This would be related to the reactivities of amino and ammonium groups with phosphate species. Secondary amino group in the diammonium ions is not interacted with phosphate species and then the surfactant molecules behave as stick-like molecules with repulsion of the secondary amino groups close to one another in the organic assemblies, possibly affording a distorted lamellar phase with a large d_{001} spacing (Scheme 4.4(c)). The preparation using *n*-hexadecyltrimethylammonium bromide (C_{16}TMABr) was also conducted in the similar synthetic condition. The XRD pattern of the product showed several peaks due to a byproduct (monetite) in high diffraction angles (Figure 4.8(c)). The use of C_{16}TMABr is not appropriate for the formation of mesostructured calcium phosphates because phosphate species are not interacted with quaternary ammonium groups so strongly (Scheme 4.4(d)). In the calcium phosphate-surfactant systems, only primary amino groups in surfactants are available for the formation of mesostructured calcium phosphates to interact with phosphate species strongly and to keep the interaction during the further reaction with calcium ions.

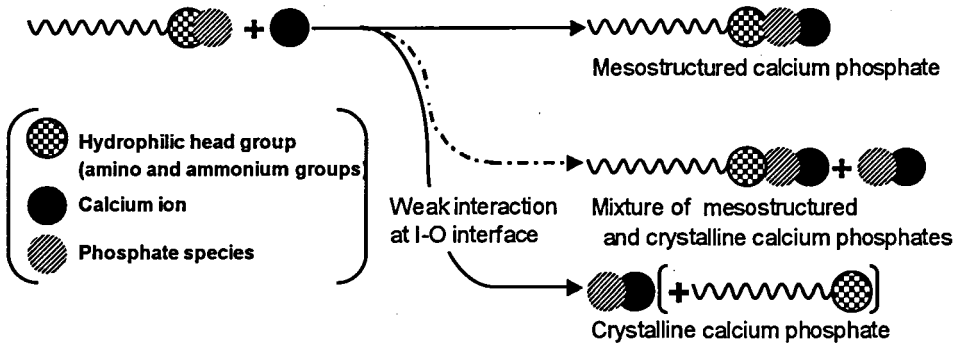

Scheme 4.3. Interactions at the I-I and I-O interfaces during the formations of mesostructured calcium phosphates prepared using amine- and ammonium-type surfactants.

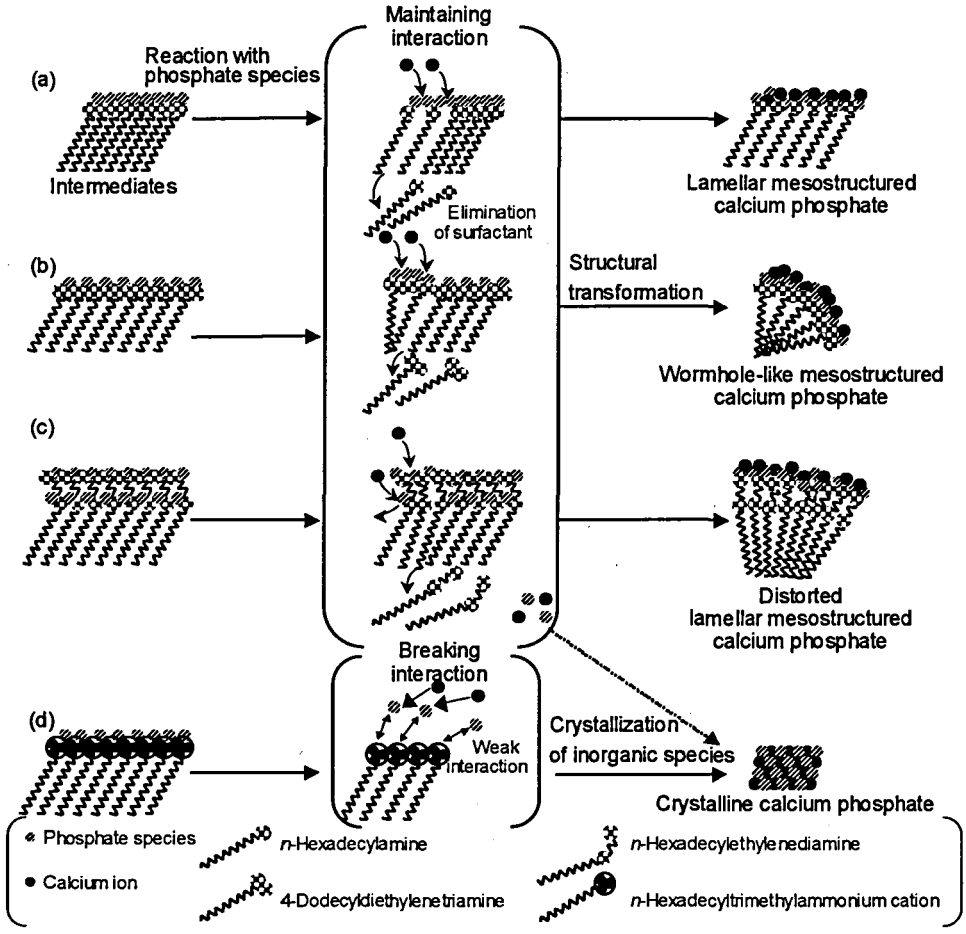

Scheme 4.4. Formation of (a) lamellar, (b) wormhole-like and (c) distorted lamellar mesostructured products respectively prepared using *n*-hexadecylamine, 4-dodecyldiethylenetriamine and *n*-hexadecylethylenediamine, and (d) crystalline calcium phosphates in the presence of *n*-hexadecyltrimethylammonium bromide.

4.3.6. Ca/P molar ratio of mesostructured calcium phosphates.

Calcium phosphate compounds are classified according to the Ca/P molar ratios. The Ca/P molar ratio of a lamellar mesostructured calcium phosphate prepared from the starting mixture (Ca/P = 1.0) containing *n*-hexadecylamine with amino group is lower than 1.0 [38]. Even when 4-dodecyldiethylenetriamine was used as amine-type surfactant, the Ca/P molar ratio of wormhole-like mesostructured product was almost 1.0. Crystalline hydroxyapatite (Ca/P = 1.67) was formed under the Ca-rich conditions (Ca/P = 1.2~) because the interaction of phosphate species with amino groups is disturbed by the excess amount of calcium ions. In contrast, a Ca-rich mesostructured calcium phosphate (Ca/P = 1.7) can be obtained using palmitic acid, indicating that calcium ions can interact with carboxyl groups in the presence of the small amount of phosphate species. Similarly, wormhole-like mesostructured calcium phosphate with much larger Ca/P molar ratio (Ca/P = 1.9) was obtained using *N*-lauroyl-L-glutamic acid. The synthetic method using surfactants with carboxyl and amino groups has a potential to control the Ca/P molar ratio of mesostructured calcium phosphates.

4.4. Conclusions

Mesostructured calcium phosphates were successfully synthesized using palmitic and *N*-lauroyl-L-glutamic acids as anionic surfactants and 4-dodecyldiethylenetriamine as a cationic surfactant in EtOH/H_2O mixed solvent systems. Interactions of carboxyl and primary amino groups in the surfactants with inorganic species are important for the synthesis of mesostructured calcium phosphates whose mesostructures and Ca/P molar ratios are strongly affected by the molecular structures of the surfactants. The insights on the interactions at the inorganic-inorganic (I-I) and inorganic-organic (I-O) interfaces has showed a potential for the mesostructural control of ionically bonded inorganic solids, which is quite important for understanding various interactions at the I-I and I-O interfaces in surfactant templating of inorganic solids. The controlled synthesis will allow the synthesis of inorganic-organic composite materials of calcium phosphates and biomolecules such as collagen and proteins for improving designed artificial bones.

References

1 H. Oonishi, L. L. Hench, J. Wilson, F. Sugihara, E. Tsuji, S. Kushitani and H. Iwaki, *J. Biomed. Mater. Res.*, 1999, **44**, 31.

2 K. J. L. Burg, S. Porter and J. F. Kellam, *Biomaterials*, 2000, **21**, 2347.

3 M. Vallet-Regí and J. M. González-Calbet, *Progr. Solid State Chem.*, 2004, **32**, 1.

4 L. Le Guéhennec, P. Layrolle and G. Daculsi, *Eur. Cell. Mater.*, 2004, **8**, 1.

5 A. M. Pietak, J. W. Reid, M. J. Stott and M. Sayer, *Biomaterials*, 2007, **28**, 4023.

6 A. El-Ghannam, *Expert Rev. Med. Devices*, 2005, **2**, 87.

7 V. Karageorgiou and D. Kaplan, *Biomaterials*, 2005, **26**, 5474.

8 L. M. Rodríguez-lorenzo and M. Vallet-Regí, *Chem. Mater., 2000*, **12**, 2460.

9 S. A. Catledge, M. D. Fires, Y. K. Vohra, W. R. Lacefield, J. E. Lemons, S. Woodard and R. Venugopalanc, *J. Nanosci. Nanotechnol.*, 2002, **2**, 293.

10 J. Norton, K. R. Malik, J. A. Darr and I. Rehman, *Adv. Appl. Ceram.*, 2006, **105**, 113.

11 X. S. Zhao, G. Q. Lu and G. J. Millar, *Ind. Eng. Chem. Res.*, 1996, **35**, 2075.

12 P. Selvam, S. K. Bhatia and C. G. Sonwane, *Ind. Eng. Chem. Res.*, 2001, **40**, 3237.

13 A. Taguchi and F. Schüth, *Micropor. Mesopor. Mater.*, 2005, **77**, 1.

14 F. Schüth, *Angew. Chem., Int. Ed.*, 2003, **42**, 3604.

15 T. Yanagisawa, T. Shimizu, K. Kuroda and C. Kato, *Bull. Chem. Soc. Jpn.*, 1990, **63**, 988.

16 S. Inagaki, Y. Fukushima and K. Kudoda, *J. Chem. Soc., Chem. Commun.*, 1993, 680.

17 C. T. Kresge, M. E. Leonowicz, W. J. Roth, J. C. Vartuli and J. S. Beck, *Nature*, 1992, **359**, 710.

18 P. Behrens, *Angew. Chem., Int. Ed.*, 1996, **35**, 515.

19 A. Sayari and P. Liu, *Micropor. Mater.*, 1997, **12**, 149.

20 F. Schüth, *Chem. Mater.*, 2001, **13**, 3184.

21 M. Tiemann and M. Fröba, *Chem. Mater.*, 2001, **13**, 3211.

22 T. Kimura, *Micropor. Mesopor. Mater.*, 2005, 77, 97.

23 C. Yu, B. Tian and D. Zhao, *Curr. Opin. Solid State Mater. Sci.*, 2003, 7, 191.

24 G. A. Ozin, N. Varaksa, N. Coombs, J. E. Davies, D. D. Perovic and M. Ziliox, *J. Mater. Chem.*, 1997, **7**, 1601.

25 I. Soten and G. A. Ozin, *J. Mater. Chem.*, 1999, **9**, 703.

26 Z. Y. Yuan, J. Q. Liu and L. M. Peng, *Langmuir*, 2002, **18**, 2450.

27 J. Yao, W. Tjandra, Y. Z. Chen, K. C. Tam, J. Ma and B. Soh, *J. Mater. Chem.*, 2003, **13**, 3053.

28 B. Prélot and T. Zemb, *Mater. Sci. Eng. C*, 2005, **25**, 553.

29 S. Sadasivan, D. Khushalani and S. Mann, *Chem. Mater.*, 2005, **17**, 2765.

30 Y. F. Zhao and J. Ma, *Micropor. Mesopor. Mater.*, 2005, **87**, 110.

31 S. M. Schmidt, J. McDonald, E. T. Pineda, A. M. Verwilst, Y. Chen, R. Josephs and A. E. Ostefin, *Micropor. Mesopor. Mater.*, 2006, **94**, 330.

32 Y. Tokuoka, Y. Ito, K. Kitahara, Y. Niikura, A. Ochiai and N. Kawashima, *Chem. Lett.*, 2006, **35**, 1220.

33 C. Liu, X. Ji and G. Cheng, *Appl. Surf. Sci.*, 2007, **253**, 6840.

34 J. Fan, J. Lei, C. Yu, B. Tu and D. Zhao, *Mater. Chem. Phys.*, 2007, **103**, 489.

35 J. Zhang, M. Fujiwara, Q. Xu, Y. Zhu, M. Iwasa and D. Jiang, *Micropor. Mesopor. Mater.*, 2008, **111**, 411.

36 N. Ikawa, Y. Oumi, T. Kimura, T. Ikeda and T. Sano, *Chem. Lett.*, 2006, **35**, 948.

37 N. Ikawa, Y. Oumi, T. Kimura, T. Ikeda and T. Sano, T. *Stud. Surf. Sci. Catal.*, 2007, **165**, 253.

38 N. Ikawa, Y. Oumi, T. Kimura, T. Ikeda and T. Sano, T. *J. Mater. Sci.*, 2008, 43, 4198.

39 M. J. Larson, A. Thorsen and S. J. Jensen, *Calcif. Tissue. Int.*, 1985, **37**, 189.

40 L. E. Hammari, A. Laghzizil, P. Barboux, A. Saoiabi and K. Lahlil, *J. Solid State Chem.*, 2004, **177**, 134.

41 N. Ikawa, M. Iwata, Y. Oumi, T. Kimura, T. Ikeda and T. Sano, *J. Nanosci. Nanotechnol.*, in press.

42 T. Yokoi, H. Yoshitake and T. Tatsumi, *Chem. Mater.*, 2003, **15**, 4536.

43 A. E. Garcia-Bennett, O. Terasaki, S. Che and T. Tatsumi, *Chem. Mater.*, 2004, **16**, 813.

44 S. Che, A. E. Garcia-Bennett, T. Yokoi, K. Sakamoto, H. Kunieda, O. Terasaki and T. Tatsumi, *Nat. Mater.*, 2003, **2**, 801.

45 J. Sjöblom, R. Lindberg and S. E. Friberg, *Adv. Colloid Intersurface Sci.*, 1996, **65**, 125.

46 V. E. Limanov, S. A. Rapin and S. B. Ivanov, *Khim. Farm. Zh.*, 1981, **15**, 84.

47 JCPDS card Nos.: brushite; 01-072-0713, monetite; 01-070-0359, hydroxyapatite; 00-001-1008.

48 R. Lieckfeldt, J. Villalaín, J.-C. Gómez-Fernández and G. Lee, *Pharm. Res.*, 1995, **12**, 1614.

49 A. S. Posner and F. Betts, *Acc. Chem. Res.*, 1975, **8**, 273.

50 A. Ohta, S. Nakashima, H. Matsuyanagi, T. Asakawa and S. Miyagishi, *Colloid Polym. Sci.*, 2003, **282**, 162.

51 M. Takehara, H. Moriyuki, I. Yoshimura and R. Yoshida, *J. Am. Oil Chem. Soc.*, 1972, **49**, 143.

52 D. Kaneko, U. Olsson and K. Sakamoto, *Langmuir,* 2002, **18**, 4699.

53 S. Cazalbou, C. Combes, D. Eichert and C. Rey, *J. Mater. Chem.*, 2004, **14**, 2148.

54 C. B. Baddiel and E. E. Berry, *Spectrochim. Acta,* 1966, **22**, 1407.

55 S. Kim, H. Ryo, H. Shin, H. S. Jung and K. S. Hong, *Mater. Chem. Phys.*, 2005, **91**, 500.

56 P. Gendraud, M. E. de Roy and J. P. Besse, *Inorg. Chem.*, 1996, **35**, 6108.

Chapter 5

Synthesis of mesoporous calcium phosphate and its adsorption property

5.1. Introduction

Calcium phosphate with high surface area has attracted much attention for not only biomaterials [1-10] but also catalysts [11-17] and adsorbents [18-20] because of the high-potential abilities due to the presence of many active and adsorption sites. Several research groups already reported the syntheses of micro- and macro-porous calcium phosphates with high surface area by using structural and morphological control methods [21-24]. From a standpoint of nano-metersized molecule adsorption, the synthesis of mesoporous calcium phosphate is also important. Especially, low crystallized or amorphous calcium phosphates with mesopores can be expected to have the great advantage in their adsorption ability because of the presence of active and adsorption sites with protons and/or hydroxyl groups, which are placed at the defects instead of calcium and phosphate ions for the charge neutralization [17, 25].

Since synthesis of mesoporous silica with tunable pore size and large pore volume by using surfactants as a template was firstly reported [26, 27], the surfactant templating method has been applied to other inorganic components such as metal oxides and phosphates [28-33] with covalently bonded frameworks. The structure of these mesoporous materials is strongly affected by self-assembled surfactant. The surface properties are based on that of each amorphous inorganic material, because these mesoporous materials are nano-ordered materials, but atomically its frameworks are amorphous. Some research groups have tried to synthesize mesoporous silicas with crystallized frameworks to improve the surface properties [34-39], but it has not been achieved for non-silica based mesoporous materials yet.

Although the surfactant templating method is also useful for the synthesis of mesoporous calcium phosphate, it is not so easy due to the preferential crystallization of ionitically bonded frameworks. Indeed, some research groups reported the syntheses of

mesostructured and mesoporous calcium phosphates including original crystalline calcium phosphates such as DCPD ($CaHPO_4 \cdot 2H_2O$), DCPA ($CaHPO_4$) and HA ($Ca_{10}(PO_4)_6(OH)_2$) [40-51]. Syntheses of wormhole-like mesoporous calcium phosphates using *n*-hexadecyltrimethylammonium bromide ($C_{16}H_{33}N(CH_3)_3Br$) and $EO_{99}PO_{65}EO_{99}$ (F127) were reported by Y. Tokuda et al. [48] and Y. F. Zhao et al. [46], respectively. These inorganic layers include crystalline calcium phosphate phases such as DCPA or HA. Although TEM images of these mesoporous calcium phosphates showed wormhole-like mesopores, these surface areas were not described. S. M. Schmidt et al. also reported the synthesis of nano-metersized calcium phosphate rod with mesopores at the interparticles by using both $C_{12}H_{25}OPO_3H$ and $C_{16}H_{33}N(CH_3)_3Br$, and the BET surface area is 90 $m^2\ g^{-1}$ [47].

While I have already described in the previous Chapters that the synthesis of lamellar and wormhole-like mesostructured calcium phosphates without any original crystalline phases using cationic and anionic surfactants in the mixed solvent system of EtOH and H_2O (Chapter 2~4) [52-56]. The EtOH/H_2O mixed solvent system can suppress the crystallization of ionitically bonded frameworks during the formation of these mesostructures. According to the result of Chapter 4, the frameworks of the wormhole-like mesostructured calcium phosphates prepared using cationic type surfactant 4-dodecyldiethylenetriamine and anionic surfactant *N*-lauroyl-L-glutamic acid are constructed by amorphous calcium phosphate [56]. In general, it is difficult to maintain the structure of amorphous calcium phosphate at high temperature. However, it is reported that the amorphous structure can be stabilized by the presence of carbonate (CO_3^{2-}), Mg, Zn and pyrophosphate ($P_2O_7^{4-}$) ions [57, 58]. Therefore, the formation of mesoporous calcium phosphate with amorphous frameworks from the wormhole-like mesostructured calcium phosphates would be possible after the removal of surfactants because of the partial generation of calcium pyrophosphate units.

In this Chapter, I investigated the synthesis of mesoporous calcium phosphate from wormhole-like mesostructured calcium phosphates prepared using 4-dodecyldiethylenetriamine and *N*-lauroyl-L-glutamic acid. Mesoporous calcium phosphate with ortho and pyro type polymorphs can be obtained from the mesostructured calcium phosphate including 4-dodecyldiethylenetriamine after calcination for removal of the surfactant molecules. In addition, the formation

mechanism of the mesoporous calcium phosphate and the adsorption properties were also investigated by using water and cyclohexane.

5.2. Experimental

5.2.1. Materials

Phosphoric acid (85% H_3PO_4),. calcium acetate monohydrate ($Ca(OAc)_2 \cdot H_2O$), ethanol (EtOH), paraformaldehyde ($(CH_2O)_n$), and hydroxyapatite ($Ca_{10}(PO_4)_6(OH)_2$) were obtained from Wako Chemical Co. 4-Dodecyldiethylenetriamine ($C_{12}H_{25}N(C_2H_4NH_2)_2$: 80%) and tetramethylammonium hydroxide (TMAOH) pentahydrate ($(CH_3)_4NOH \cdot 5H_2O$) were obtained from ACROS. *N*-lauroyl-L-glutamic acid ($C_{11}H_{23}CONHCH(CO_2H)C_2H_4CO_2H$) was supplied by Ajinomoto Co., Inc. Calcium diisopropoxide ($Ca(O^iPr)_2$) was obtained from Kojundo Chemical Lab. Co. Diammonium hydrogenphosphate ($(NH_4)_2HPO_4$) was obtained from Nacalai Tesque Co.

5.2.2. Synthesis of mesostructured and mesoporous calcium phosphates

Mesostructured calcium phosphate was prepared by the same procedure in Chapter 4. 4-Dodecyldiethylenetriamine was used as a template in the mixed solvent system of ethanol and water. In a typical synthesis, 85% H_3PO_4 (0.58 g), pentahydrated TMAOH (0.09 g), and 80% 4-dodecyldiethylenetriamine (0.85 g) were added to EtOH (30.0 g) and then a white slurry was obtained after stirring for 2 h. A clear aqueous solution of $Ca(OAc)_2$ (0.88 g) was added to the white slurry under stirring and the stirring was kept for 30 min. The resultant mixture was filtered, washed with EtOH, and air-dried. Mesoporous calcium phosphate was obtained from the mesostructured calcium phosphate after heating at 400 °C for 1 hour in flowing N_2 and followed calcination for 5 hours in flowing O_2 at same temperature.

Mesostructured calcium phosphates were prepared using *N*-lauroyl-L-glutamic acids as anionic surfactants. In a typical synthesis using *N*-lauroyl-L-glutamic acid, $Ca(O^iPr)_2$ (1.58 g) and *N*-lauroyl-L-glutamic acid (4.87 g) were added to a mixed solvent of EtOH (5.0 g) and H_2O (14.4 g) and then a white slurry was obtained after stirring for 2 h. $(NH_4)_2HPO_4$ (0.79 g) was added to the white slurry under stirring and the stirring was kept for 2 h. The resultant mixture was filtered, washed with EtOH, and air-dried. The composition of the mixture was $Ca(O^iPr)_2$: $0.6(NH_4)_2HPO_4$:

$1.5C_{11}H_{23}CONHCH(CO_2H)C_2H_4CO_2H$ (pH = 5.5). Calcination of the mesostructured calcium phosphate prepared using *N*-lauroyl-L-glutamic acid was carried out at 400 °C for 1 hour in flowing N_2 and for 2 hours in flowing O_2 at same temperature.

5.2.3. Characterization

X-ray diffraction (XRD) patterns were obtained by using a Bruker AXS D8 ADVANCE with graphite monochromatized Cu Kα radiation (40 kV, 30 mA). Transmission electron microscopic (TEM) images were taken by a JEOL JEM-2010 microscope, operated at 200 kV. The compositions were measured by inductively coupled plasma atomic emission spectroscopy (ICP-AES, Seiko SPS 7700) and thermogravimetric (TG) analysis (Seiko TG/DTA320 thermal analyzer). ^{31}P MAS NMR spectra were obtained by using a Bruker DRX-400 spectrometer with a 7 mm zirconia rotor at a resonance frequency of 161.9 MHz with a spinning rate of 6 kHz, a 90° pulse width of 4.5 μs, and 10 s recycle delay. 85% H_3PO_4 aqueous solution was used as a reference. FT-IR spectra were recorded on JEOL JIR-7000 spectrometer with 2 cm^{-1} resolution using KBr disc method. N_2 adsorption isotherm was measured by using BELSORP-mini, specific surface area was calculated by the BET method and pore size distribution of the product was calculated by the BJH method from adsorption data. Adsorption isotherms of cyclohexane and methanol were measured by using BELSORP 18. Adsorption of formaldehyde was carried out by using paraformaldehyde. The sample was preheated at 200 °C for 10 hours under vacuum before all of the formaldehyde adsorption measurements.

5.3. Results and discussion

5.3.1. Syntheses of wormhole-like mesostructured and mesoporous calcium phosphates using 4-dodecyldiethylenetriamine

The XRD pattern of wormhole-like mesostructured calcium phosphate prepared using 4-dodecyldiethylenetriamine showed a sharp peak with the *d* spacing of 4.4 nm in the 2θ region lower than 5° without any obvious peaks in high diffraction angles (Figure 5.1(a)). The wormhole-like structure was confirmed by TEM observation (Figure 5.2 (a)). The ^{31}P MAS NMR spectrum of the mesostructured product showed a broad peak centered at 1.2 ppm due to orthophosphate species in amorphous calcium phosphate

(Figure 5.3(a)) [59, 60]. The composition of wormhole-like mesostructured calcium phosphate was calculated by the TG and ICP data as $0.16C_{12}H_{25}N(C_2H_4NH_2)_2$: $0.95CaO$: $0.5P_2O_5$, indicating the presence of pure amorphous calcium phosphate which cannot directly interact with the surfactant headgroups. In the FT-IR spectrum of the mesostructured calcium phosphate, two broad peaks at 560 and 1090 cm^{-1} assignable to the phosphate units in amorphous calcium phosphate and two peaks corresponding to neutral primary amine groups at 1580 and 1650 cm^{-1} (Figure 5.4) were observed [61, 62]. The FT-IR spectrum also showed broad peaks due to ammonium groups in the range of 2800-3300 cm^{-1}, indicating the presence of protons at the interface between calcium phosphate species and the surfactant molecules.

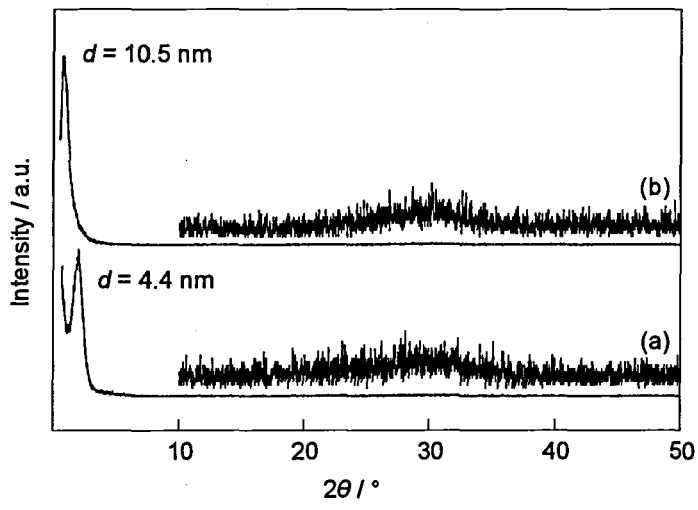

Figure 5.1. XRD patterns of wormhole-like mesostructured calcium phosphates prepared using 4-dodecyldiethylenetriamine (a) before and (b) after calcination.

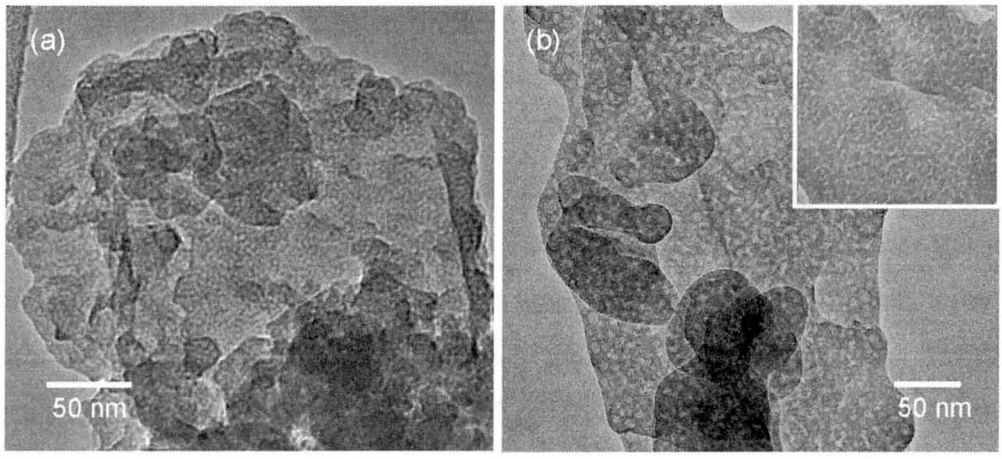

Figure 5.2. TEM images of wormhole-like mesostructured calcium phosphates prepared using 4-dodecyldiethylenetriamine (a) before and (b) after calcination.

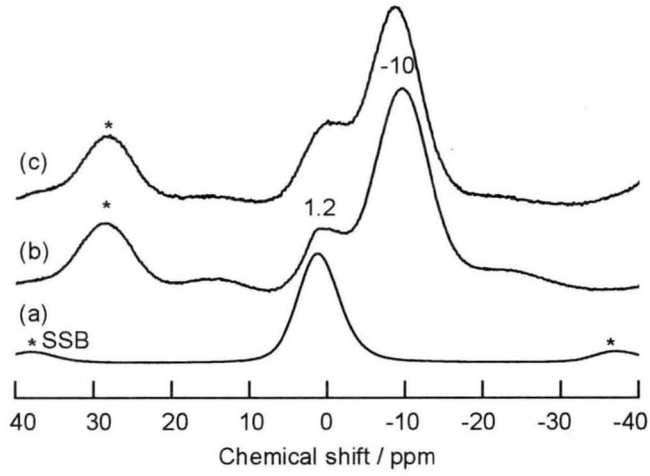

Figure 5.3. ^{31}P MAS NMR spectra of wormhole-like mesostructured calcium phosphates prepared using 4-dodecyldiethylenetriamine (a) before and (b) after calcination, and (c) mesoporous calcium phosphate after water adsorption.

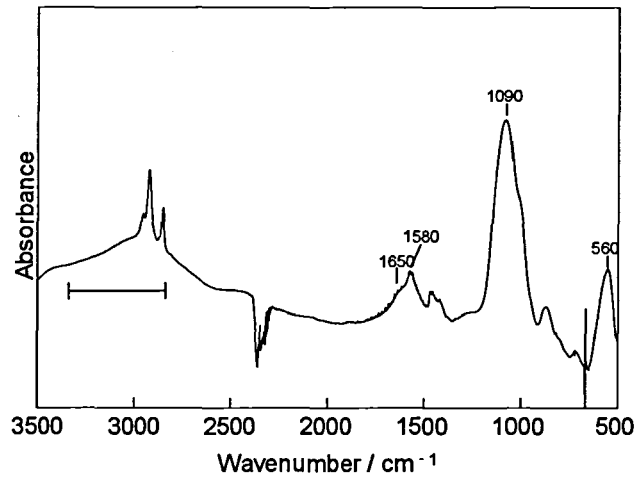

Figure 5.4. FT-IR spectrum of wormhole-like mesostructured calcium phosphate prepared using 4-dodecyldiethylenetriamine.

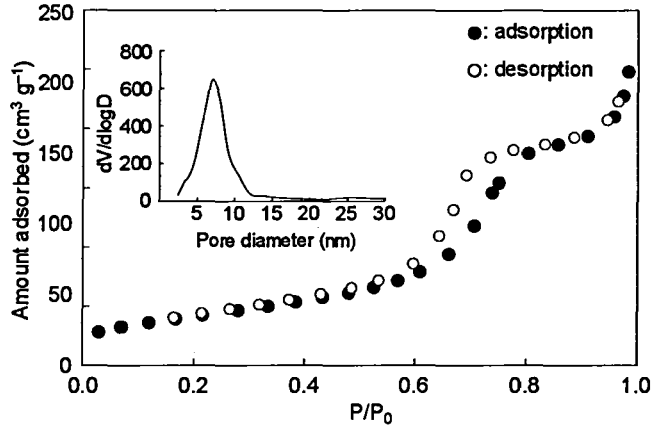

Figure 5.5. N_2 adsorption-desorption isotherm of the mesostructured product prepared using 4-dodecyldiethylenetriamine after calcination.

The XRD pattern of the product obtained from the wormhole-like mesostructured calcium phosphate after calcination also showed only one peak with the *d* spacing of 10.5 nm without any obvious peaks in high diffraction angles (Figure 5.1(b)). In the TEM images of the mesostructured product, larger mesopores than the non-calcined product were mainly observed (Figure 5.2(b)), while corded-like pores which would be formed by the collapse of the large mesopores were partially observed (Figure 5.2(b) inset). In the ^{31}P MAS NMR spectrum of the mesostructured product, two broad peaks centered at 1.2 and −10 ppm which can be assigned to orthophosphate (PO_4^{3-}) and

pyrophosphate ($P_2O_7^{4-}$) units were observed (Figure 5.3(b)) [63]. The nitrogen adsorption isotherm of the calcined product was type IV, and the BET surface area, the pore volume and the pore diameter were 140 m^2 g^{-1}, 0.47 cm^3 g^{-1} and 7.1 nm, respectively (Figure 5.5(a)).

Mesoporous calcium phosphate was obtained from mesostructured calcium phosphate prepared using 4-dodecyldiethylenetriamine as a template after calcination for the removal of the surfactants. Calcium pyrophosphate ($Ca_2P_2O_7$) units exist in the mesoporous calcium phosphate, supported by ^{31}P MAS NMR data. In general, pyrophosphate, metaphosphate (PO_3^-) and polyphosphate ($(PO_3)_n^{n-}$) were generated from protonated orthophosphates through dehydration process at high temperatures. Here, protons exists at the interface between phosphate units of inorganic species and amino groups of the surfactant molecules in wormhole-like mesostructured calcium phosphate and in pure amorphous calcium orhtophosphate species. While the pure amorphous calcium phosphate concurrently includes deprotonated orthophosphate units which can be maintained their ortho type polymorph at even high temperature (~1000 °C). Therefore, original orthophosphate and generated pyrophosphate units are co-existed in the mesoporous calcium phosphate.

5.3.2. Synthesis of wormhole-like mesostructured calcium phosphate using *N*-lauroyl-L-glutamic acid and its calcination

The XRD pattern of the wormhole-like mesostructured calcium phosphate showed only a peak with the *d* spacing of 3.8 nm in low diffraction angles, and no any peaks were observed in high diffraction angles (Figure 5.6). The wormhole-like structure of the mesostructured calcium phosphate was confirmed by TEM observation (Figure 5.7 In the ^{31}P MAS NMR spectrum, a broad peak due to orthophosphate units was observed at around 1.3 ppm (Figure 5.8(a)). After calcination of the wormhole-like mesostructured calcium phosphate for 3 hours at 400 °C, the product with black in color was obtained and the XRD peak observed in low diffraction angles before calcination disappeared (Figure was not shown here). The ^{31}P MAS NMR spectrum of the calcined product showed 1.3 ppm due to orthophosphate units as well as the mesostructured product before calcinations (Figure 5.8(b)). On the basis of the above results, the wormhole-like structure was collapse during calcination.

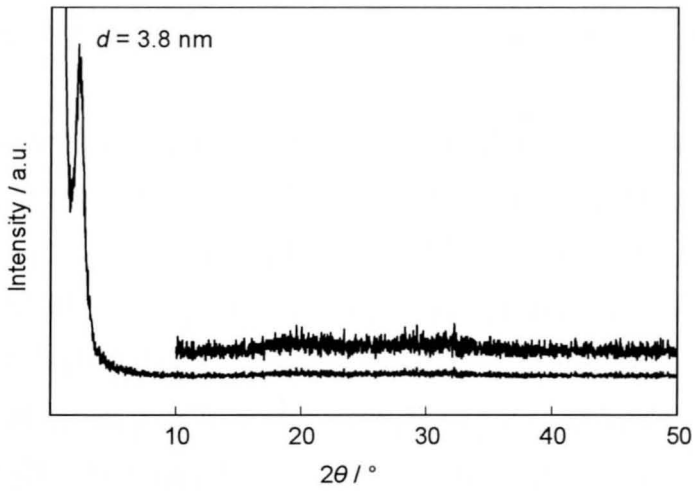

Figure 5.7. XRD pattern of wormhole-like mesostructured calcium phosphate prepared using *N*-lauroyl-L-glutamic acid..

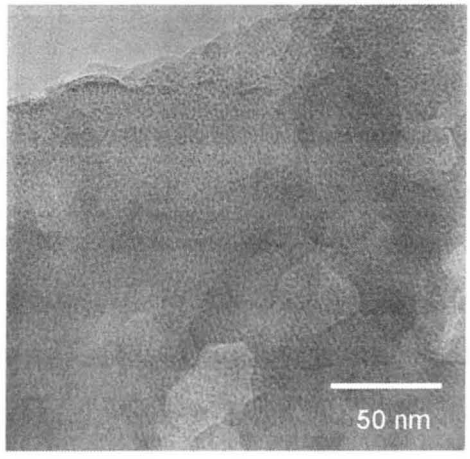

Figure 5.8. TEM image of wormhole-like mesostructured calcium phosphate prepared using *N*-lauroyl-L-glutamic acid.

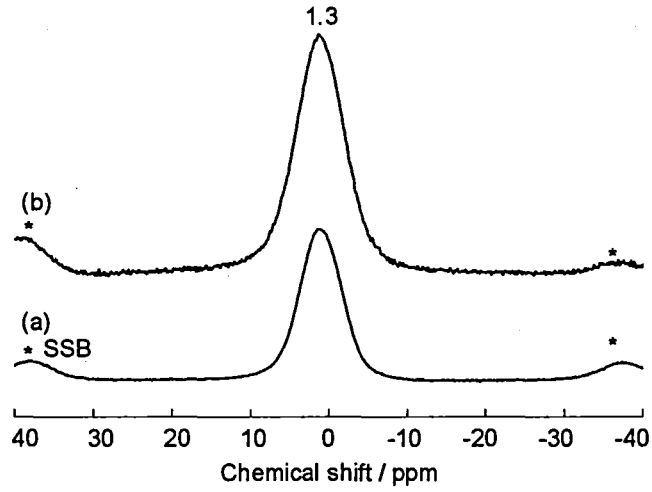

Figure 5.9. ^{31}P MAS NMR spectra of wormhole-like mesostructured calcium phosphates prepared using *N*-lauroyl-L-glutamic acid (a) before and (b) after calcination.

5.3.3. Formation of mesoporous calcium phosphate

In general, carbonate (CO_3^{2-}), Mg, Zn and pyrophosphate ($P_2O_7^{4-}$) ions can enhance formation of amorphous calcium phosphate [57, 58], suggesting that the structure of amorphous calcium phosphate including these ions with different size and valence is more stabilized at high temperature than pure amorphous structure. Therefore, mesoporous calcium phosphate with pyrophosphate units was obtained from only the wormhole-like mesostructured calcium phosphate including protons in their frameworks prepared using 4-dodecyldiethylenetriamine. On the other hand, in the wormhole-like mesostructured calcium phosphate prepared using *N*-lauroyl-L-glutamic acid, protons slightly exist both at the interface between deprotonated carboxyl groups and calcium ions and in their Ca-rich frameworks. Because Ca-rich (Ca/P = 1.5~2.0) calcium phosphate frameworks can hardly include HPO_4^{2-} and/or $H_2PO_4^-$ ions, such as HAP ($Ca_{10}(PO_4)_6(OH)_2$), TCPs ($Ca_3(PO_4)_2$) and TTCP ($Ca_4(PO_4)_2O$). Thus, the structure of the wormhole-like mesostructured calcium phosphate prepared using *N*-lauroyl-L-glutamic acid was collapse during the calcination because of the absence of any ions without calcium and phosphate ions.

The *d* value of the mesoporous calcium phosphate (10.5 nm) was larger than that of the mesostructured calcium phosphate (4.4 nm) before the calcinations for removal of the surfactant. In the case of conventional mesoporous materials, the *d* values slightly

decrease by the shrinkage of their inorganic frameworks during calcination. The increase in the *d* value of the mesostructured calcium phosphate can be considered as follows; the wormhole-like mesostructured calcium phosphate including organic molecules is constructed by inorganic walls with different thickness, and the thin walls would be merged into the surface of the thick walls during the calcination process, leading to the formation of the larger mesopores by combination of some smaller pores (Scheme 5.1). Therefore, the pore size distribution of the mesoporous calcium phosphate is wider than highly ordered mesoporous materials already reported in literatures. The large mesopores disappeared after the calcination for longer time (6 hours ~) or higher temperature (400 °C ~), checked by XRD. The corded-like pores observed in the TEM image are partially formed due to the collapse of the large mesopores by even the calcination at 400 °C for 6 hours.

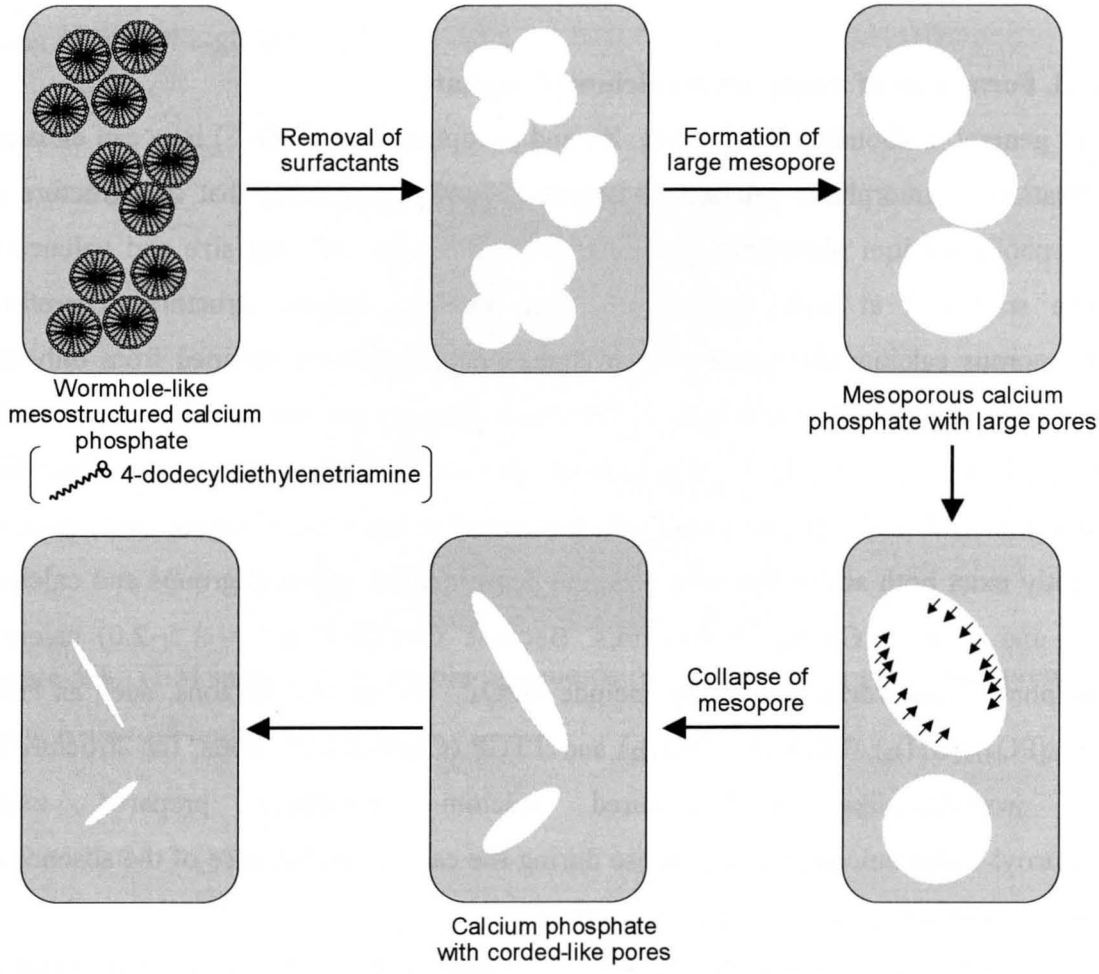

Scheme 5.1. Proposal formation mechanism of mesoporous calcium phosphate from wormhole-like mesostructured calcium phosphate.

5.3.4. Adsorption property of mesoporous calcium phosphate

The adsorption property of the mesoporous calcium phosphate was investigated using H_2O and C_6H_{12} as probe molecules. The only adsorption isotherm of H_2O on the mesoporous calcium phosphate showed type IV (Figure 5.9), and the adsorption of H_2O occurred at low pressure under the P/P_0 value of 0.1. Whereas, the adsorption of cyclohexane hardly took place at the low pressure, indicating obviously hydrophilic property of the mesoporous calcium phosphate (Figure 5.10). The hydrophilic property would be due to polar character of ionitically bonded frameworks of mesoporous calcium phosphate. Thus, hydrophobic molecules cannot be adsorbed on the mesoporous calcium phosphate. The ^{31}P MAS NMR spectrum of the mesoporous calcium phosphate after the H_2O adsorption was shown in Figure 5.3 (c). The intensity of peaks due to orthophosphate and pyrophosphate units were not changed before and after the H_2O adsorption, suggesting H_2O molecules adsorbed on not phosphate species but calcium ions. In general, alkaline earth metal cations in micro- and mesoporous materials act as Lewis acid and adsorb H_2O molecules. Thus H_2O molecules would be adsorbed on the surface of the mesoporous calcium phosphate.

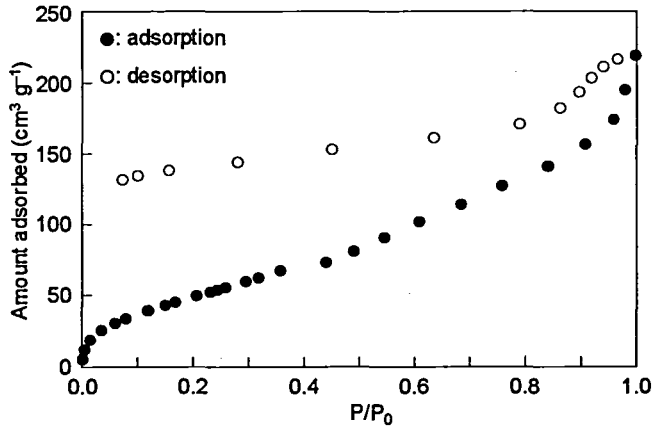

Figure 5.9. H_2O adsorption-desorption isotherm of the mesoporous calcium phosphate.

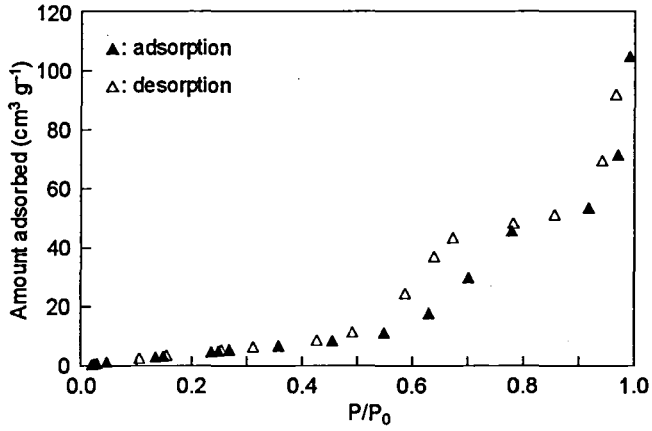

Figure 5.10. C_6H_{12} adsorption-desorption isotherm of the mesoporous calcium phosphate.

5.4. Conclusion

Amorphous calcium phosphate with mesoporous structure containing ortho- and pyro-phosphates can be obtained from wormhole-like mesostructured calcium phosphate prepared using 4-dodecyldiethylenetriamine as a template after removal of the surfactant molecules by calcination. Unlike most of mesoporous materials already reported in literature, the mesoporous calcium phosphate has larger mesopores (ca.7.1 nm) than the molecular size of the surfactant. The inorganic frameworks in the mesoporous calcium phosphate are constructed by amorphous calcium phosphate including ortho- and pyro-phosphate units which were derived from deprotonated and protonated orthophosphates, respectively. The surface of the mesoporous calcium phosphate is obviously hydrophilic, and H_2O molecules can physically be adsorbed on calcium ions of the mesoporous calcium phosphate. The synthetic method will open a new chemistry of structural control of ionitically boned inorganic materials by using organic molecule templating method.

References

1 K. J. L. Burg, S. Porter and J. F. Kellam, *Biomaterials*, 2000, **21**, 2347.

2 E. I. Dorozhkina and S. V. Dorozhkin, *Chem. Mater.*, 2002, **14**, 4267.

3 M. Vallet-Regí and J. M. González-Calbet, *Progr. Solid State Chem.*, 2004, **32**, 1.

4 L. Le Guéhennec, P Layrolle and G. Daculsi, *Eur. Cell. Mater.*, 2004, **8**, 1.

5 A. El-Ghannam, *Expert Rev. Med. Devices*, 2005, **2**, 87.

6 V. Karageorgiou and D. Kaplan, *Biomaterials*, 2005, **26**, 5474.

7 G. K. Toworfe, R. J. Composto, I. M. Shapiro and P. Ducheyne, *Biomaterials*, 2006, **27**, 631.

8 A. M. Pietak, J. W. Reid, M. J. Stott and M. Sayer, *Biomaterials*, 2007, **28**, 4023.

9 K. Ganesan, A. Kovtun, S. Neumann, R. Heumann and M. Epple, *J. Mater. Chem.*, 2008, **18**, 3655.

10 M. Gungormus, H. Fong, I. W. Kim, J. S. Evans, C. Tamerler and M. Sarikaya, *Biomacromolecules*, 2008, **9**, 966.

11 B. Liptakova, M. Hronec and Z. Cvergrosova, *Catal, Today*, 2000, **61**, 143.

12 S. Sugiyama, H. Mitsuoka, T Shono, T. Moriga and H. Hayashi, *J. Chem. Eng. Jpn.*, 2003, **36**, 210.

13 K. Mori, T. Hara, T. Mizugaki, K. Ebitani and K. Kaneda, *J. Am. Chem. Soc.*, 2003, **125**, 11460.

14 J. A. S. Bett, L. G Christner and W. K. Hall, *J. Am. Chem. Soc.*, 1967, 5135.

15 H. Monma, *J. Catal.*, 1982, **75**, 200.

16 Y. Matsumura and J. B. Moffat, *J. Chem. Soc., Faraday Trans.*, 1996, **92**, 1981

17 T. Tsuchida, S. Sakuma, T. Takeguchi and W. Ueda, *Ind. Eng. Chem. Res.*, 2006, **45**, 8634.

18 K. Kandori, A. Fudo and T Ishikawa, *Phys. Chem. Chem. Phys.*, 2000, **2**, 2015.

19 K. Kandori, S. Tsuyama, H. Tanaka and T Ishikawa, *Colloids Surf.* B, 2007, **58**, 98.

20 P. H. Chen, Y. H. Tseng, Y. Mou, Y. M. Tsai, S. J. Guo, S. J. Huang, S. S. F. Yu and C. C. Chan, *J. Am. Chem. Soc.*, 2008, **130**, 2862.

21 L. M. Rodríguez-Lorenzo and M. Vallet-Regi, *Chem. Mater.*, 2000, **12**, 2460.

22 K. Sonoda, T. Furuzono, D. Walsh, K. Sato and J. Tanaka, *Solid State Ionics*, 2002, **151**, 321.

23 S. Bose and S. K. Saha, *Chem. Mater.*, 2003, **15**, 4464.

24 M. Uota, H. Arakawa, N. Kitamura, T. Yoshimura, J. Tanaka and T. Kijima, *Langmuir*, 2005, **21**, 4724.

25 S. Cazalbou, C. Combes, D. Eichert and C. Rey, *J. Mater. Chem.*, 2004, **14**, 2148.

26 T. Yanagisawa, T. Shimizu, K. Kuroda and C. Kato, *Bull. Chem. Soc. Jpn.*, 1990, **63**, 988.

27 C. T. Kresge, M. E. Leonowicz, W. J. Roth, J. C. Vartuli and J. S. Beck, *Nature*, 1992, **359**, 710.

28 P. Behrens, *Angew. Chem., Int. Ed.*, 1996, **35**, 515.

29 A. Sayari and P. Liu, *Micropor. Mater.*, 1997, **12**, 149.

30 F. Schüth, *Chem. Mater.*, 2001, **13**, 3184.

31 M. Tiemann and M. Fröba, *Chem. Mater.*, 2001, **13**, 3211.

32 T. Kimura, *Micropor. Mesopor. Mater.*, 2005, **77**, 97.

33 C. Yu, B. Tian and D. Zhao, *Curr. Opin. Solid State Mater. Sci.*, 2003, **7**, 191.

34 M. Choi, H. S. Cho, R. Srivastava, C. Venkatesan, D. H. Choi and R. Ryoo, *Nat. Mater.*, 2006, **5**, 718.

35 S. P. B. Kremer, C. E. A. Kirschhock, A. Aerts, K. Villani, J. A. Martens, O. I. Levedev and G. V. Tendeloo, *Adv. Mater.*, 2003, **15**, 1705.

36 L. Huang, W. Guo, P. Deng, Z. Xue and Q. Li, *J. Phys. Chem. B*, 2000, **104**, 2817.

37 T. Kimura, T. Kamata, M. Fuziwara, Y. Takano, M. Kaneda, Y. Sakamoto, O. Terasaki, Y. Sugawara and K. Kuroda, *Angew. Chem. Int. Ed.*, 2000, **39**, 3855.

38 Y. Fang and H. Hu, *J. Am. Chem. Soc.*, 2006, **128**, 10636.

39 T. Kimura, H. Tamura, M. Tezuka, D. Mochizuki, T. Shigeno, T. Ohsuna and K. Kuroda, *J. Am. Chem. Soc.*, 2008, **130**, 201.

40 G. A. Ozin, N. Varaksa, N. Coombs, J. E. Davies, D. D. Perovic and M. Ziliox, *J. Mater. Chem.*, 1997, **7**, 1601.

41 I. Soten and G. A. Ozin, *J. Mater. Chem.*, 1999, **9**, 703.

42 Z. Y. Yuan, J. Q. Liu and L. M. Peng, *Langmuir*, 2002, **18**, 2450.

43 J. Yao, W. Tjandra, Y. Z. Chen, K. C. Tam, J. Ma and B. Soh, *J. Mater. Chem.*, 2003, **13**, 3053.

44 B. Prélot and T. Zemb, *Mater. Sci. Eng. C*, 2005, **25**, 553.

45 S. Sadasivan, D. Khushalani and S. Mann, *Chem. Mater.*, 2005, **17**, 2765.

46 Y. F. Zhao and J. Ma, *Micropor. Mesopor. Mater.*, 2005, **87**, 110.

47 S. M. Schmidt, J. McDonald, E. T. Pineda, A. M. Verwilst, Y. Chen, R. Josephs and A. E. Ostefin, *Micropor. Mesopor. Mater.*, 2006, **94**, 330.

48 Y. Tokuoka, Y. Ito, K. Kitahara, Y. Niikura, A. Ochiai and N. Kawashima, *Chem. Lett.*, 2006, **35**, 1220.

49 C. Liu, X. Ji and G. Cheng, *Appl. Surf. Sci.*, 2007, **253**, 6840.

50 J. Fan, J. Lei, C. Yu, B. Tu and D. Zhao, *Mater. Chem. Phys.*, 2007, **103**, 489.

51 J. Zhang, M. Fujiwara, Q. Xu, Y. Zhu, M. Iwasa and D. Jiang, *Micropor. Mesopor. Mater.*, 2008, **111**, 411.

52 N. Ikawa, Y. Oumi, T. Kimura, T. Ikeda and T. Sano, *Chem. Lett.*, 2006, **35**, 948.

53 N. Ikawa, Y. Oumi, T. Kimura, T. Ikeda and T. Sano, T. *Stud. Surf. Sci. Catal.*, 2007, **165**, 253.

54 N. Ikawa, Y. Oumi, T. Kimura, T. Ikeda and T. Sano, T. *J. Mater. Sci.*, 2008, 43, 4198.

55 N. Ikawa, M. Iwata, Y. Oumi, T. Kimura, T. Ikeda and T. Sano, *J. Nanosci. Nanotechnol.*, in press.

56 N. Ikawa, H. Hori, T. Kimura, Y. Oumi and T. Sano, *Langmuir*, 2008, **24**, 13113.

57 G. Daculsi, J. M. Bouler and R. Z. Legeros, *Int. Rev. Cytology.*, 1997, **172**, 129.

58 S. V. Dorozhkin, J. Mater. Sci., 2007, 42, 1061.

59 W. P. Aue, A. H. Rpufosse, M. J. Glimcher and R. G. Griffin, *Biochemistry*, 1984, **23**, 6110.

60 J. L. Miquel, L. Facchini, A. P. Legrand, C. Rey and J. Lemaitre, *Colloid and Surface*, 1990, **45**, 427.

61 M. Julien, I. Khairoun, R. Z. LeGeros, S. Delplace, P. Pilet, P. Weiss, G. Daculsi, J. M. Bouler and J. Guicheux, *Biomaterials*, 2007, **28**, 956.

62 P. Gendraud, M. E. de Roy and J. P. Besse, *Inorg. Chem.*, 1996, **35**, 6108.

63 A. Stamboulis, R. G. Hill and R. V. Law, *J. Non-Cryst. Solids*, 2005, **351**, 3289.

Chapter 6

Amino acid containing amorphous calcium phosphates and the rapid transformation into apatite

6.1. Introduction

Calcium phosphates are highly bioactive and then very attractive for application as precursors for artificial bones [1−10]. Crystalline calcium phosphates such as brushite ($CaHPO_4{\cdot}2H_2O$), octacalcium phosphate ($Ca_8(HPO_4)_2(PO_4)_4{\cdot}5H_2O$), and α-, β- and γ- tricalcium phosphates (TCPs, $Ca(PO_4)_3$) have often been used for artificial bones so far [11−19]. Especially, calcium phosphate cement prepared from one or more crystalline calcium phosphates is well known as bone substituents [11, 20−29]. Autogeneous bones in our body are precisely modulated by biomolecules, such as collagen and bone morphogenetic protein, and low crystalline apatite including their composite species in molecular level at the inorganic-organic interface [30]. Such biomolecule-calcium phosphate composite species play important roles in regulator of ion concentration in our body and precursor of apatite in autogeneous bones [30]. Although there have been many papers on artificial bones including the biomolecules, biomolecule-calcium phosphate composites have not been obtained artificially until now for the creation of analogical autogeneous bones.

Amorphous calcium phosphate has attracted much attention for use in precursors for artificial bones because amorphous calcium phosphate (additive) promotes the transformation of calcium phosphate cement into apatite [14, 16]. Amorphous calcium phosphate shows a tendency to dissolve faster than crystallize calcium phosphate species, and calcium phosphate cement with a lot of pores is then obtained by the addition of amorphous calcium phosphate, being suitable as a precursor for artificial bones. In general, amorphous calcium phosphates are prepared by freeze-dry [12−14] and ball milling [16]. The Ca/P molar ratio of the calcium phosphates is below 1.5 [19], being lower than that of apatite (1.67) as well as those of brushite (1.00), octacalcium phosphate (1.33) and TCPs (1.50). During the

transformation of crystalline calcium phosphates with low Ca/P molar ratios into apatite, phosphate species are released with the risk of toxicity [22]. Therefore, tetracalcium phosphate ($Ca_4O(PO_4)_2$) and calcium carbonate ($CaCO_3$) should be added for the adjustment of total Ca/P molar ratio in calcium phosphate cement to 1.67 [11]. However, those additives do not show enough solubility, and thus amorphous calcium phosphate with Ca/P molar ratio similar to and/or larger than that of apatite has strongly been in demand for the preparation of intelligent calcium phosphate cement.

Calcium phosphate composites containing organic molecules in molecular level is promissing to show unique property different from crystalline calcium phosphates, and the synthetic method will be useful for controlling Ca/P molar ratio on the basis of electrostatic interaction between inorganic and organic species. However, it is quite difficult to synthesize such inorganic-organic composites because calcium phosphate species are preferential to crystallize according to strong interactions between calcium cations and anionic phosphate species. Following the successful preparation of lamellar mesostructured calcium and magnesium phosphates using alkylamines (Chapter 2, 3) [31–33], I have already described that the use of designed surfactants with amino and carboxyl groups leads to the formation of wormhole-like mesostructured calcium phosphates (Chapter 4) [34]. The syntheses were performed in mixed solvents of ethanol and water in order to prevent calcium phosphate species from fully crystallizing to dense calcium phosphates such as brushite and monetite ($CaHPO_4$) [31, 32]. Designed amine-type and amino acid-type surfactants with large headgroups distorted the surface curvature of calcium phosphates frameworks, effectively affording amorphous calcium phosphate frameworks with wormhole-like mesostructures [34]. The Ca/P molar ratios of the wormhole-like composites are around 2.0 and 1.0, being controllable by changing functional groups in designed surfactants. The Ca- and P-rich composites can be obtained using carboxylic acid- and amine-type surfactants, respectively. A Ca-rich composite was also prepared using an amino acid-type surfactant with carboxyl groups. The insight will be available to improve facile synthetic method to control the Ca/P molar ratio of biomolecule-calcium phosphate composite because both of carboxyl and amino groups are present in biomolecules.

In this Chapter, I successfully synthesized amino acid containing amorphous calcium phosphates using L-glutamic acid (Glu), L-aspartic acid (Asp), and L-lysine (Lys) as typical amino acids. Molecular structures of the amino acids are illustrated in Scheme 6.1, which contain functional groups analogous to those in biomolecules. I investigated the transformation of the amorphous composites into apatite in simulated body fluid (SBF). Such amino acid containing composites were transformed in SBF faster than crystalline calcium phosphates such as α-TCP used for artificial bones. I confirmed further that the composites were practical additives to calcium phosphate cement for the promotion of rapid transformation into apatite, which will be useful in the research field of artificial bones.

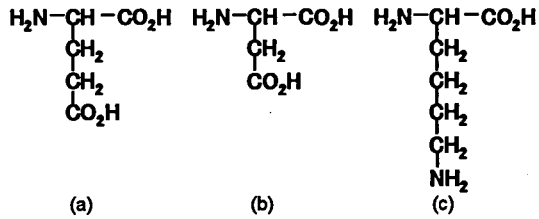

Scheme 6.1. Molecular structures of (a) L-glutamic acid (Glu), (b) L-aspartic acid (Asp), and (c) L-lysine (Lys).

6.2. Experimental

6.2.1. Materials

L-Glutamic acid (Glu), L-aspartic acid (Asp), and L-lysine (Lys) were obtained from Tokyo Kasei Kogyo Co. Calcium bis(dihydrogenphosphate) monohydrate (MCPM, $Ca(H_2PO_4)_2 \cdot H_2O$), calcium hydrogen phosphate dihydrate (brushite, $CaHPO_4 \cdot 2H_2O$), calcium carbonate ($CaCO_3$), sodium chloride, potassium chloride, disodium sulfate (Na_2SO_4) were obtained from Kanto Chemical Co. Phosphoric acid (85% H_3PO_4), disodium hydrogenphosphate (Na_2HPO_4), calcium acetate monohydrate ($Ca(OAc)_2 \cdot H_2O$), sodium hydrogencarbonate ($NaHCO_3$), hydrochloric acid, and ethonol (EtOH) were obtained from Wako Chemical Co. Tris(hydroxymethyl)-aminomethane ($NH_2C(CH_2OH)_3$), magnesium chloride, and diammonium hydrogenphosphate ($(NH_4)_2HPO_4$)) were obtained from Nacalai Tesque Co. Calcium diisopropoxide ($Ca(O^iPr)_2$) was obtained form Kojundo Chemical Laboratory Co. Dipotassium

hydrogenphosphate trihydrate ($K_2HPO_4 \cdot 3H_2O$) and calcium chloride were obtained from Merck Ltd., Japan.

6.2.2. Syntheses of amino acid containing amorphous calcium phosphates

In a typical synthesis using Glu, Glu (1.47 g) and $Ca(O^iPr)_2$ (1.58 g) were added to a mixed solvent of ethanol (EtOH, 4.61 g) and water (14.3 g) and stirred over 4 h, and then 85% H_3PO_4 (0.58 g) was added to the white slurry under vigorous stirring. The stirring was maintained for 60 min and the resultant mixture ($1.00(Ca(O^iPr)_2$: $0.50H_3PO_4$: 1.00Glu : $80H_2O$: 10EtOH, pH = 5.7) was filtered, washed with EtOH repeatedly, and air-dried. In the case using Asp (1.33 g), the synthetic procedure was almost similar, but $(NH_4)_2HPO_4$ (0.66 g) was used instead of 85% H_3PO_4. The composition of the resultant mixture was $1.00Ca(O^iPr)_2$: $0.50(NH_4)_2PO_4$: 1.00Asp : $80H_2O$: 10EtOH, pH = 9.6).

In the case using Lys, the synthetic procedure was different from those using Glu and Asp described above. Lys (1.46 g) and 85% H_3PO_4 (1.15 g) were added to a mixed solvent of EtOH (18.4 g) and water (6.8 g). A white slurry was obtained after stirring over 4 h and then $Ca(OAc)_2 \cdot H_2O$ (1.76 g) was added to the white slurry under vigorous stirring. The stirring was maintained for 60 min. The composition of the resultant mixture was $1.00Ca(OAc)_2$: $1.00H_3PO_4$: 1.00Lys : $40H_2O$: 40EtOH (pH = 5.9).

6.2.3. Assessment of in vitro bioactivity in simulated body fluid

A simulated body fluid (SBF) was prepared by mixing NaCl (7.996 g), $NaHCO_3$ (0.350 g), KCl (0.224 g), $K_2HPO_4 \cdot 3H_2O$ (0.228 g), $MgCl_2$ (0.143 g), 1M HCl (40 mL), $CaCl_2$ (0.278 g), Na_2SO_4 (0.071 g), and $NH_2C(CH_2OH)_3$ (6.057 g). The solution was heated at 37 °C and the pH was adjusted to 7.25 by the addition of 1M HCl.

Disks (20 mm in diameter and 1 mm in height) composed of amino acid containing amorphous calcium phosphates were obtained by compacting powders (0.50 g) and immersed in SBF (45 mL) at 37 °C [35]. Calcium phosphate cement was prepared from a mixture of α-TCP (63.8 mass %), $CaCO_3$ (9.0 mass %), MCPM (2.2 mass %), 3% aqueous solution of Na_2HPO_4 [11, 36, 37], and the composite. The cement was prepared at the ratio of liquid components and powders (mixed over 1 h and air-dried) of 0.36 mL g^{-1}. α-TCP was prepared by heating the mixture of monetite ($CaHPO_4$, 2.72 g) obtained

by dehydration of brushite (at 250 °C for 10 h) and $CaCO_3$ (1.00 g) at 1350 °C for 4 h [16].

6.2.4. Characterization

X-ray diffraction (XRD) patterns were obtained by using a Bruker AXS D8 ADVANCE with graphite monochromatized Cu Kα radiation. ^{31}P MAS NMR spectra were obtained by using a Bruker DRX-400 spectrometer with a 7 mm zirconia rotor at a resonance frequency of 161.9 MHz with a spinning rate of 6 kHz. The spectra were accumulated with 4.5 μs pulses and 40 s recycle delay. H_3PO_4 aqueous solution (85%) was used as a reference. ^{13}C CP/MAS NMR spectra were obtained by using the same spectrometer at a resonance frequency of 100.7 MHz with a spinning rate of 4 kHz. The spectra were accumulated with a 90° pulse width of 6.8 μs and 15 s recycle delay. Tetramethylsilane was used as a reference. FT-IR spectra were recorded on a JEOL JIR-7000 spectrometer with 2 cm^{-1} resolution by using KBr pellets. The compositions were measured by inductively coupled plasma atomic emission spectroscopy (ICP-AES, Seiko SPS 7700). Thermogravimetric (TG) analyses were conducted by using a Seiko TG/DTA320 thermal analyser.

6.3. Results and discussion

6.3.1. Synthesis of mesostructured calcium phosphates using anionic surfactants

The XRD pattern of a calcium phosphate prepared using L-glutamic acid (Glu) did not show any obvious peaks, indicating that no periodicity is present in the calcium phosphate networks (Figure 6.1(a)). In the ^{31}P MAS NMR spectrum of the amorphous calcium phosphate, a broad peak was observed, centered at 1.2 ppm (Figure 6.2(a)). Several broad peaks due to carbon atoms in Glu were observed in the ^{13}C CP/MAS NMR spectrum of the amorphous product (Figure 6.3(a)). The peaks can be assigned on the basis of the chemical shifts observed for Glu. Two peaks at around 180 ppm were due to carbon atoms in carboxyl groups (C1 and C5) of Glu. Other peaks at around 55 and 30 ppm were assignable to carbon atom in methine group bonded to amino and carboxyl groups (C2) and those in side alkyl chain (C3 and C4), respectively (Figure 6.3(a), (b)). The peak due to the C4 carbon would be shifted in the calcium phosphate matrix by a disordered conformation of the methylene group such as anti and gauche

ones. Interactions among ions in the present systems strongly affect the states of carbon atoms in side alkyl chains. The composition of the amorphous calcium phosphate composite was calculated to be 0.89Glu : 1.76CaO : 0.50P_2O_5 (ICP and TG). The FT-IR spectrum of the amorphous product showed a broad peak centered at 1600 cm^{-1} due to ionized carboxyl groups without any peaks due to unionized carboxyl group at around 1720 cm^{-1} (Figure 6.4(a)) [38]. Phosphate units in amorphous calcium phosphate were broadly observed at around 1070 cm^{-1} [12, 39]. Broad peaks in the range of 2500–3200 cm^{-1} can be assigned to ammonium group in Glu [40].

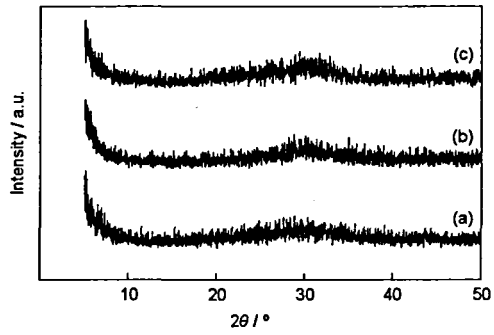

Figure 6.1. XRD patterns of calcium phosphates prepared using (a) Glu, (b) Asp, and (c) Lys.

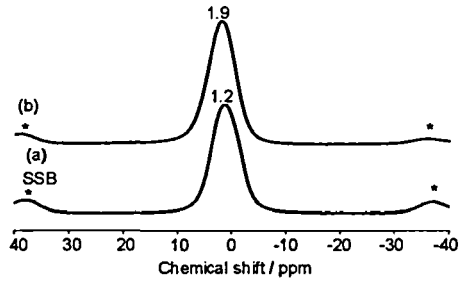

Figure 6.2. ^{31}P MAS NMR spectra of calcium phosphates prepared using (a) Glu and (b) Asp.

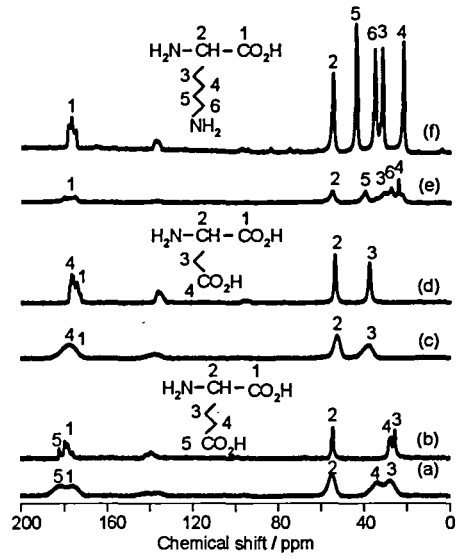

Figure 6.3. ^{13}C CP/MAS NMR spectra of calcium phosphates prepared using (a) Glu, (c) Asp, and (e) Lys, with the corresponding spectra of (b) Glu, (d) Asp, and (f) Lys.

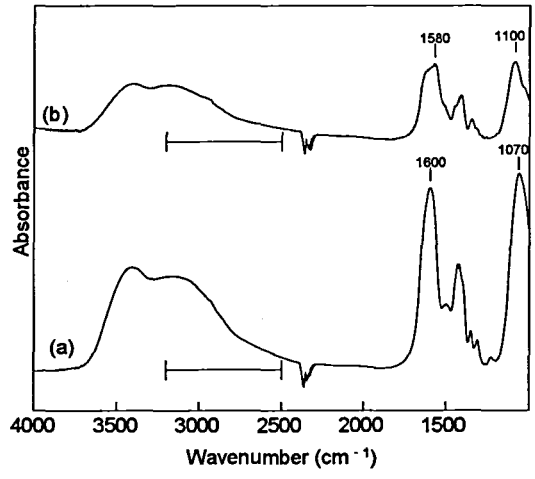

Figure 6.4. FT-IR spectra of calcium phosphates prepared using (a) Glu and (b) Asp.

Amino acid containing amorphous calcium phosphate was also prepared in the presence of L-aspartic acid (Asp). The XRD pattern of a calcium phosphate prepared using Asp is shown in Figure 6.1(b), also exhibiting a XRD profile typically observed for amorphous phases. The ^{31}P MAS NMR spectrum showed that a broad peak was

observed, centered at 1.9 ppm (Figure 6.2(b)) and the ^{13}C CP/MAS NMR spectrum suggested that all peaks are assigned to carbon atoms in Asp (Figure 6.3(c), (d)). The FT-IR spectrum demonstrated the presence of ionized carboxyl groups (at around 1580 cm^{-1}) [38], phosphate units in amorphous calcium phosphate (at around 1100 cm^{-1}) [12, 39], and primary ammonium group (in the range of 2500–3200 cm^{-1}) (Figure 6.4(b)) [40]. The chemical composition was calculated to be 1.00Asp : 1.90CaO : 0.50P_2O_5, whose Ca/P molar ratio (1.90) was larger than that of the composite prepared using Glu (1.76).

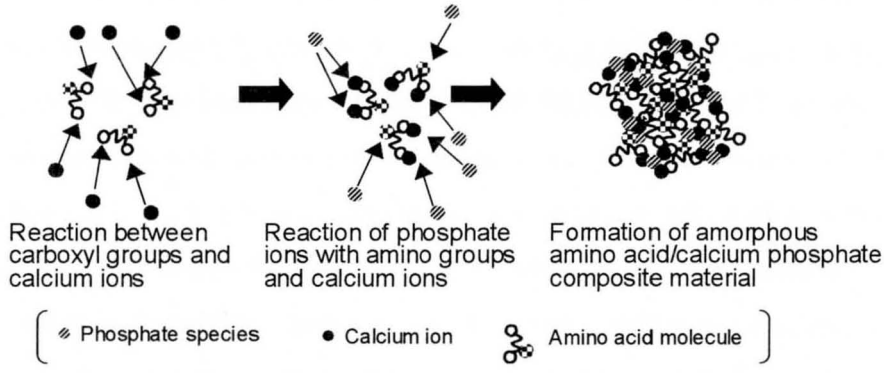

Scheme 6.2. Proposed formation mechanism of amino acid containing amorphous calcium phosphate composite.

The results suggest that Glu and Asp were interacted with calcium phosphate species and homogeneously distributed in amorphous calcium phosphate matrix. Ionized two carboxyl groups in Glu and Asp interact with calcium cations and protonated amino (ammonium) group interact with anionic phosphate species. Formation mechanism of the amorphous calcium phosphates in the presence of Glu and Asp is proposed, as shown in Scheme 6.2. Carboxyl groups are ionizied ($-COO^-$) and interacted with Ca^{2+}, and anionic phosphate species are reacted with the ammonium group ($-NH_3^+$) with the reaction with Ca^{2+}.

Amorphous calcium phosphate can be obtained by freeze-dry [12–14] and the Ca/P molar ratio is lower than apatite (1.67). I succeeded in synthesizing amorphous calcium phosphates in the presence of Glu and Asp, and the Ca/P molar ratios of the amorphous composites (1.76 and 1.90) is much larger than those of brushite (1.00),

octacalcium phosphate (1.33), and TCPs (1.50), that are famous crystalline calcium phosphates used as precursors for artificial bones, including apatite (1.67) in our body. Accordingly, the synthetic strategy is quite facile and the amorphous calcium phosphate will be applicable to an intelligent additive during the transformation into artificial bones without the release of toxic phosphate species.

L-Lysine (Lys) containing amorphous calcium phosphate can be obtained under the condition applied for the preparation of lamellar and wormhole-like mesostructured calcium phosphates using amine-type surfactants [31, 32, 34]. Any obvious peaks were not observed in the XRD pattern (Figure 6.1(c)). The ^{31}P MAS NMR spectrum showed two broad peaks at 2.2 and −0.4 ppm (Figure 6.5(a)), and the peak at −0.4 ppm was enhanced by cross-polarization (Figure 6.5(b)), revealing the presence of two kinds of phosphate anions. The ^{13}C CP/MAS NMR spectrum exhibited several broad peaks that corresponded to carbon atoms in Lys (Figure 6.3(e) and (f)). The chemical composition was calculated to be 0.40Lys : 1.00CaO : 0.50P_2O_5. A part of phosphate anions cannot interact with primary ammonium group in Lys, possibly suggesting the presence of pure amorphous calcium phosphate species, being in good agreement with the ^{31}P MAS NMR data. The Ca/P molar ratio of the Lys containing amorphous calcium phosphate synthesized using amine-type organic molecule is smaller (1.00) than those of other Ca-rich crystalline calcium phosphates [19] and amino acid containing amorphous calcium phosphates prepared using carboxylic acid-type organic molecules. In the case using Lys, two protonated amino (ammonium) groups were firstly interacted with anionic phosphate species. According to the synthetic procedure, calcium cations react with anionic phosphate species attached with the ammonium groups and ionized carboxyl groups after the addition of calcium source ($Ca(OAc)_2 \cdot H_2O$). This formation route is similar to those observed for lamellar and wormhole-like mesostructured calcium phosphates using amine-type surfactants [31, 32, 34].

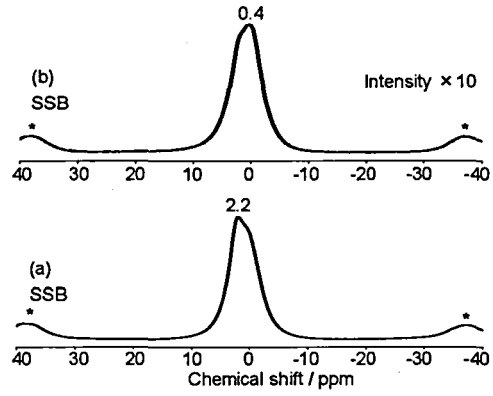

Figure 6.5. ^{31}P MAS NMR spectra of calcium phosphates prepared using Lys (a) with and (b) without cross-polarization.

6.3.2. Synthesis conditions of amino acid containing amorphous calcium phosphates

Synthesis of amorphous calcium phosphates in the presence of simple amino acids was investigated further by using Glu as a representative one. The $EtOH/H_2O$ molar ratio of the starting mixture was changed as followed; 0/90, 10/80, 40/50, and 70/20. The XRD pattern of the product obtained in water ($EtOH/H_2O$ = 0/90) showed several peaks assignable to brushite (Figure 6.6(a)). The Ca/P molar ratio of the product was 1.38 though the Ca/P molar ratio of brushite is typically 1.00, possibly indicating the presence of amorphous calcium phosphate as a mixed phase. Actually, Glu containing amorphous calcium phosphate with large Ca/P molar ratio (1.76) was obtained in a mixed solvent ($EtOH/H_2O$ = 10/80 used in Section 3.1) without any crystalline phases (Figure 6.6(b)). Several XRD peaks due to Glu were observed and was gradually increased with the increase in the $EtOH/H_2O$ molar ratio ($EtOH/H_2O$ = 40/50, 70/20, Figure 6.6(c), (d)).

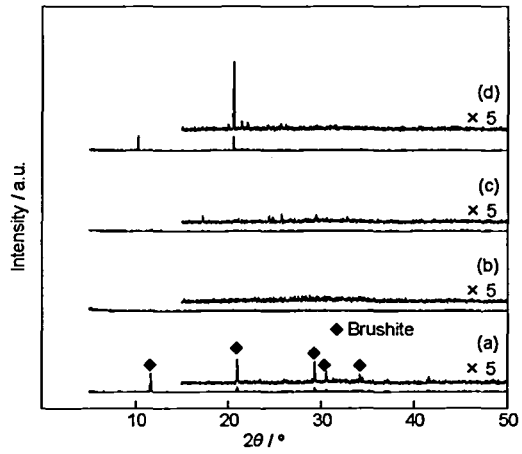

Figure 6.6. XRD patterns of the products prepared using Glu under the synthetic conditions with various EtOH/H_2O molar ratios of (a) 0/90, (b) 10/80, (c) 40/50, and (d) 70/20.

Effects of the EtOH/H_2O molar ratio in the starting mixture was also investigated in the case using Lys, because the formation mechanism is considered to be different from those observed for the composites prepared in the presence of Glu and Asp. The XRD pattern showed that brushite ($CaHPO_4 \cdot 2H_2O$) was formed in water (Figure 6.7(a)). The amount of brushite as a byproduct was gradually decreased with the increase in the EtOH/H_2O molar ratio (EtOH/H_2O = 20/60, Figure 6.7(b)), and then Lys containing amorphous calcium phosphate was obtained under the condition with EtOH/H_2O = 40/40) (Figure 6.7(c)). $Ca(OAc)_2 \cdot H_2O$ used as a calcium source was not dissolved in the EtOH-rich mixed solvent (EtOH/H_2O = 60/20, Figure 6.7(d)). The formation of brushite with two crystal water molecules was suppressed using the EtOH/H_2O mixed solvent system, as reported previously [31–34]. It has been reported that monetite ($CaHPO_4$) is formed instead of hydrated brushite in EtOH-rich mixed solvent [31, 32, 34, 41]. Soluble species such as residual and/or unreacted Glu and $Ca(OAc)_2 \cdot H_2O$ cannot be removed by filtration and then co-existed in the product prepared under the EtOH-rich condition.

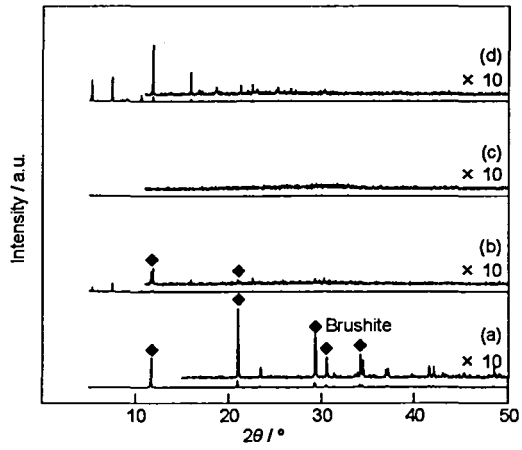

Figure 6.7. XRD patterns of the products prepared using Lys under the conditions with different EtOH/H_2O molar ratios of (a) 0/80, (b) 20/60, (c) 40/40, and (d) 60/20.

Amorphous calcium phosphates can be obtained under the conditions with different EtOH/H_2O molar ratios (10/80 and 40/40) in the presence of the amino acids (Glu and Lys, respectively). This is possibly due to not only the presence of isopropanol generated from $Ca(O^iPr)_2$ but also the Ca/P molar ratio in the starting mixture. The synthesis of calcium phosphates was strongly affected by pH value because the state of the amino acids is drastically changed according to pH value of the starting mixtures. The XRD patterns of the products prepared under acidic conditions (adjusted by acetic acid, pH = 3.9, 4.7) in the presence of Glu showed several peaks due to brushite and residual Glu (Figure 6.8(a), (b)). When the pH value of the starting mixture was in a range of 5.7–8.2, no obvious peaks were observed in the XRD patterns, being related to the formation of amorphous calcium phosphate composites (Figure 6.8(c)-(e)). Some XRD peaks due to the intermediate prepared by the reaction between Glu and $Ca(O^iPr)_2$ were observed in the product prepared at pH = 10.0 (Figure 6.8(f)). The presence of brushite in the products (pH = 3.9, 4.7) is also supported by elemental analysis that the Ca/P molar ratios of the products (1.06 and 1.18) are close to that of brushite (1.00). Glu containing amorphous calcium phosphate can be obtained at pH values ranging from 5.7 to 8.2, and the Ca/P molar ratios are changed from 1.76 to 1.90, respectively, indicating that a part of phosphate species cannot react with the intermediate. A product with the Ca/P molar ratio of 2.10 was recovered from the starting mixture at pH = 10.0 and it

contained the intermediate in addition to Glu containing amorphous calcium phosphate.

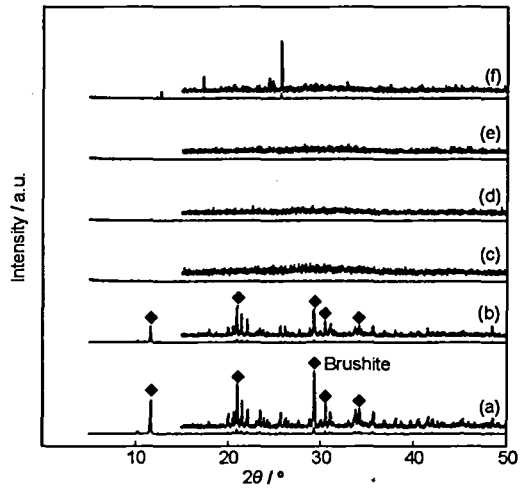

Figure 6.8. XRD patterns of the products prepared using Glu under the conditions with different pH values of (a) 3.9, (b) 4.7, (c) 5.7, (d) 7.0, (e) 8.2, and (f) 10.0.

6.3.3. Transformation of amino acid containing amorphous calcium phosphates into apatite in simulated body fluid (SBF)

Transformation of amorphous calcium phosphates prepared using Asp, Glu, and Lys into apatite in simulated body fluid (SBF) was investigated. The XRD pattern of the product obtained after immersion of Asp containing calcium phosphate in SBF for 1 day showed two broad peaks assignable to apatite (Figure 6.9(b)), and the Ca/P molar ratio (1.90) was changed to 1.64. In the case of Glu containing calcium phosphates prepared under the synthetic condition with higher pH value, only XRD peaks due to apatite were observed after immersing in SBF for 1 day, and the Ca/P molar ratios (1.87 and 1.90) were changed to 1.52 and 1.59, respectively. Peaks due to apatite and brushite were observed in the XRD pattern of the product obtained after immersion of Glu containing calcium phosphate (Ca/P = 1.76) in SBF for 1 day (Figure 6.9(d)). The peaks due to brushite disappeared completely after immersion for 3 days (Figure 6.9(e)), and the final Ca/P molar ratio of the product was 1.46. The result indicates that the Ca/P molar ratio strongly affects the transformation into apatite in SBF.

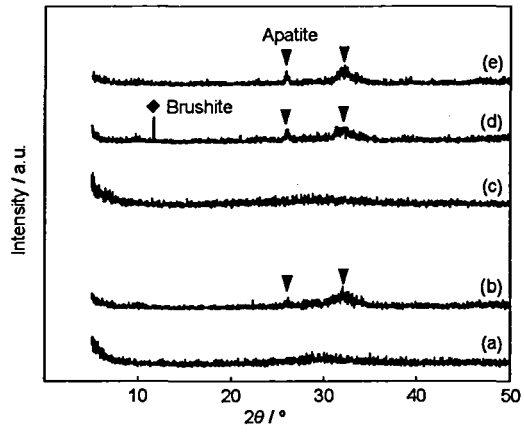

Figure 6.9. XRD patterns of the products obtained from Asp containing calcium phosphate (a) before and (b) after immersing in SBF for 1 day, and those from Glu containing calcium phosphate (c) before and after the SBF treatment for (d) 1 and (e) 3 days.

The XRD pattern of the product obtained after immersion of Lys containing calcium phosphate (Ca/P = 1.00) in SBF for 1 day showed some peaks due to brushite and apatite, indicating that the Lys containing calcium phosphate was partially transformed into apatite (Figure 6.10A(b)). The peaks due to brushite was gradually decreased with the increase in the immersing time (Figure 6.10A(b)-(d)). Only peaks assignable to apatite were observed after 14 days (Figure 6.10A(e)), and the final Ca/P molar ratio was changed to 1.41.

Transformation of α-TCP, which has often been used as a precursor for artificial bones, into apatite in SBF was also investigated for comparison. The XRD peaks due to α-TCP disappeared gradually (Figure 6.10B(a)-(e)), and peaks due to apatite appeared after immersion for 3 days (Figure 6.10B(c)). All of α-TCP was converted to apatite after immersion for 14 days (Figure 6.10B(e)). In general, nucleation of apatite occurs in highly concentrated solution of Ca^{2+} and phosphate species which are dissolved at the surfaces of crystalline calcium phosphates [16, 42–46]. Although nucleation of apatite is promoted by the presence of carboxyl and amino groups in biomolecules, Lys containing calcium phosphate was slowly transformed into apatite as well as α-TCP (Ca/P = 1.50) because the Ca/P molar ratio (1.00) was not close to that of apatite (1.67). Accordingly, rapid transformation into apatite was observed

for Glu and Asp with carboxyl and amino groups containing calcium phosphates (Ca/P = 1.76 and 1.90).

Amino acid molecules partly remained in the final products with various Ca/P molar ratios even after immersion in SBF, checked by TG and ICP. The formation of low crystalline apatite would be allowed by the presence of amino acid molecules. It is difficult to obtain ideal apatite with the Ca/P molar ratio of 1.67 in SBF which is different from the real biological system, proposing apatite nucleation mechanism in SBF as shown in Scheme 6.3. Ca^{2+} and phosphate species, which are dissolved at the surfaces of amorphous calcium phosphates, react with ionic species interacted with amino acid molecules. Such reactions occur continuously and then apatite species are nucleated in SBF. A small amount of amino acid molecules are still interacted with Ca^{2+} and anionic phosphate species in the apatite species with the retention of total charge matching, leading the nucleation of apatite through rapid transformation of amorphous calcium phosphates.

Even when the Ca/P molar ratio of Asp containing amorphous calcium phospahte are similar to that of Glu containing amorphous product, the Ca/P molar ratios are different in the final resultant apatite. This is related to difference in solubilities in SBF between Asp and Glu. For instance, N-lauroyl-L-glutamic acid containing amorphous calcium phosphate (Ca/P = 1.90) with wormhole-like mesostructure [34] is not transformed into apatite in SBF within 3 days, supporting that the solubility of organic molecules is important for rapid transformation of organic molecule-calcium phosphate composites into apatite.

6.3.4. Effect of the presence of amino acid containing amorphous calcium phosphate on the transformation of calcium phosphate cement into apatite in SBF

Transformation of calcium phosphate cement prepared in our lab. into apatite in SBF was investigated with amino acid containing amorphous calcium phosphate (25 mass %). The XRD patterns of the calcium phosphate cement mixed with Glu containing calcium phosphate (Ca/P = 1.76) showed several sharp peaks due to corresponding crystalline phases such as α-TCP, $CaCO_3$, and calcium bis(dihydrogenphos-phate) monohydrate (Figure 6.11(A)(a)). Two broad peaks due to apatite appeared at around 2θ = 26 and 32° after immersion of the cement for 1 day

(Figure 6.11(A)(b)). The peaks due to the parent crystalline phases in the cement were decreased after immersing in SBF for 3 days, (Figure 6.11(A)(c)), and only peaks due to apatite were observed after immersing for 7 days (Figure 6.11(A)(d), (e)). The Ca/P molar ratio of the final product after immersing for 14 days was changed to 1.63, indicating that the final product was not ideal apatite. Similar results were obtained in the case of calcium phosphate cements mixed with Glu and Asp containing calcium phosphates (Ca/P = 1.90), and the final Ca/P molar ratios were 1.59 and 1.51, respectively. In the case of the calcium phosphate cement without the composites, the sharp peaks due to the original crystalline phases did not disappear completely after immersing in SBF for 14 days (Figure 6.11(B)(e)). Peaks due to apatite were observed after immersing for 3 days (Figure 6.11(B)(c)), and the final Ca/P molar ratio was 1.68, being close to that of apatite (1.67). In the case of the cement mixed with Lys containing calcium phosphate, peaks due to octacalcium phosphate and apatite were observed after immersing for 14 days, and the Ca/P molar ratio was 1.45.

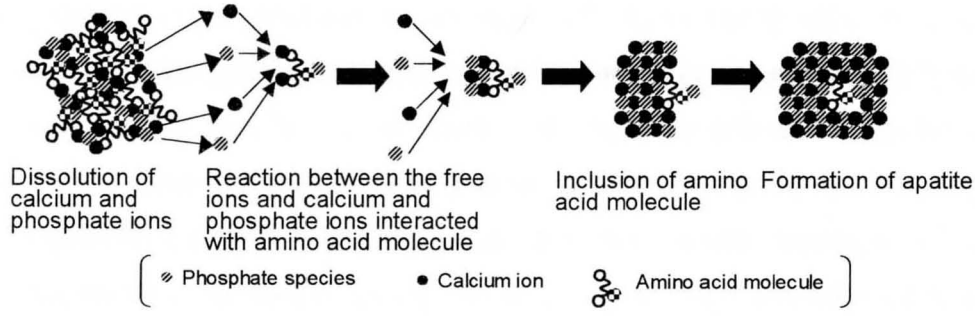

Scheme 6.3. Proposed mechanism of apatite nucleation from amino acid containing amorphous calcium phosphate composite.

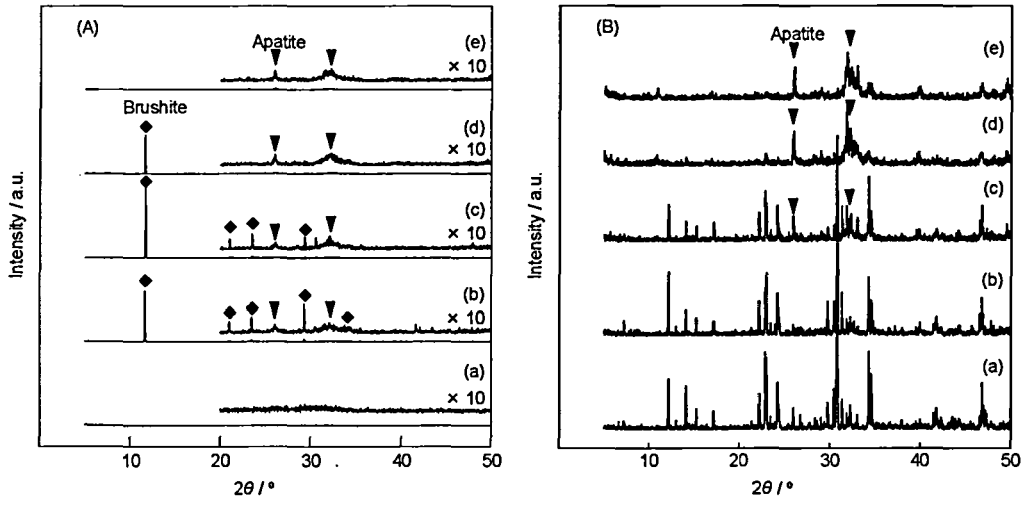

Figure 6.10. XRD patterns of (A) Lys containing calcium phosphate and (B) α-TCP (a) before and after the SBF treatment for (b) 1, (c) 3, (d) 7, and (e) 14 days.

Calcium phosphate cements mixed with the amino acid containing amorphous calcium phosphates were transformed into apatite faster than the additive-free cement. There have been some reports on calcium phosphate cements mixed with amorphous calcium phosphates (without organic molecules) [12–14, 16]. Such calcium phosphate cements were also transformed fast because of resultant high porosity by the preferential dissolution of amorphous calcium phosphates. In this study, the presence of amino acid molecules also promotes the nucleation of apatite in addition to the high porosity of calcium phosphate cements, leading to rapid transformation of the cements into apatite. A part of calcium phosphate cement mixed with Lys containing calcium phosphate transformed into octacalcium phosphate, indicating that nucleation of octacalcium phosphate occurred in highly concentrated solution of Ca^{2+} and phosphate species with low Ca/P molar ratio than that of apatite. Calcium phosphate cements with different compositions have been reported so far [21]. When mixtures of Glu containing calcium phosphate and crystalline calcium phosphates (α-, β-TCPs and brushite) were immersed in SBF, only the mixture with α-TCP was transformed into apatite, probably suggesting that the addition of amino acid containing calcium phosphates is useful for rapid transformation of α-TCP in calcium phosphate cements into apatite [11, 36, 37, 47, 48].

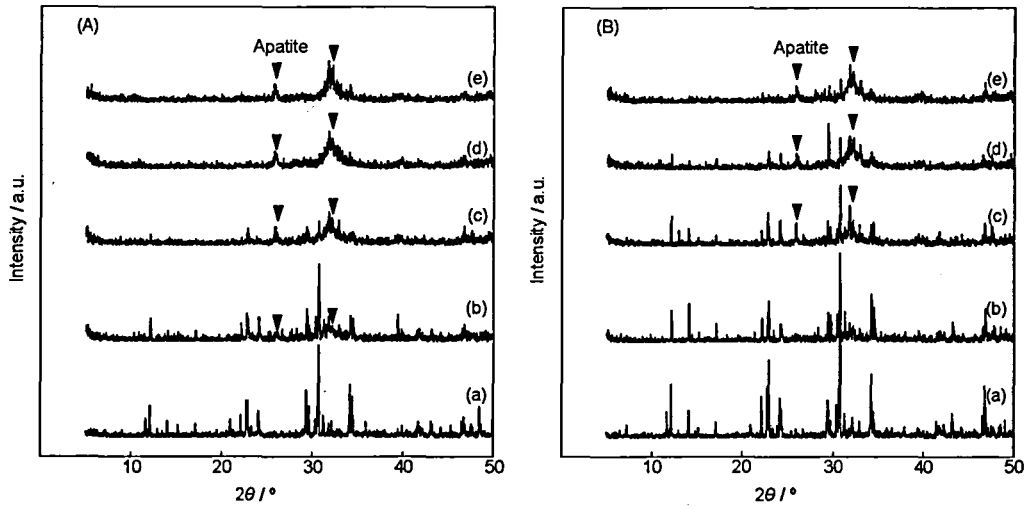

Figure 6.11. XRD patterns of calcium phosphate cements (A) with and (B) without the addition of Glu containing calcium phosphate (a) before and after the SBF treatment for (b) 1, (c) 3, (d) 7, and (e) 14 days.

6.4. Conclusions

Amorphous calcium phosphates can be obtained using simple amino acids having similar functional groups to those in collagen. Controlled interaction among calcium cations, anionic phosphate species, ionized amino acid molecules in mixed solvents of ethanol and water leads to the formation of amorphous inorganic-organic composites with designed Ca/P molar ratios. Designed frameworks with high Ca/P molar ratios are actually applicable for rapid transformation into apatite in simulated body fluid. Calcium phosphate cement is also transformed into apatite fast by the addition of amino acid containing amorphous calcium phosphates, being valuable for application of amorphous calcium phosphate to analogical autogeneous bones.

References

1 K. J. L. Burg, S. Porter and J. F. Kellam, *Biomaterials*, 2000, **21**, 2347.

2 E. I. Dorozhkina and S. V. Dorozhkin, *Chem. Mater.*, 2002, **14**, 4267.

3 M. Vallet-Regí and J. M. González-Calbet, *Progr. Solid State Chem.*, 2004, **32**, 1.

4 L. Le Guéhennec, P Layrolle and G. Daculsi, *Eur. Cell. Mater.*, 2004, **8**, 1.

5 A. El-Ghannam, *Expert Rev. Med. Devices*, 2005, **2**, 87.

6 V. Karageorgiou and D. Kaplan, *Biomaterials*, 2005, **26**, 5474.

7 G. K. Toworfe, R. J. Composto, I. M. Shapiro and P. Ducheyne, *Biomaterials*, 2006, **27**, 631.

8 A. M. Pietak, J. W. Reid, M. J. Stott and M. Sayer, *Biomaterials*, 2007, **28**, 4023.

9 K. Ganesan, A. Kovtun, S. Neumann, R. Heumann and M. Epple, *J. Mater. Chem.*, 2008, **18**, 3655.

10 M. Gungormus, H. Fong, I. W. Kim, J. S. Evans, C. Tamerler and M. Sarikaya, *Biomacromolecules*, 2008, **9**, 966.

11 M. Bohner, U. Gbureck and J. E. Barralet, *Biomaterials*, 2005, **26**, 6423.

12 A. L. Boskey and A. S. Posner, *J. Phys. Chem.*, 1973, **77**, 2313.

13 A. S. Posner and F. Betts, *Acc. Chem. Res.*, 1975, **8**, 273.

14 M. Julien, I. Khairoun, R. Z. LeGeros, S. Delplace, P. Pilet, P. Weiss, G. Daculsi, J. M. Bouler and J. Guicheux, *Biomaterials*, 2007, **28**, 956.

15 P. B-Y. Ofir, R. Govrin-Lippman, N. Garti and H. Füredi-Milhofer, *Cryst. Growth Des.*, 2004, **4**, 177.

16 C. L. Camiré, U. Gbureck, W. Hirsiger and M. Bohner, *Biomaterials*, 2005, **26**, 2787.

17 J. Tao, H. Pan, Y. Zeng, X. Xu and R. Tang, *J. Phys. Chem.* B, 2007, **111**, 13410.

18 M. Kazanci, P. Fratzl, K. Klaushofer and E. P. Paschalis, *Calcif. Tissue Int.*, 2006, **79**, 354.

19 S. V. Dorozhkin, *J. Mater. Sci.*, 2007, **42**, 1061.

20 W. E. Brown and L. C. Chow, *J. Dent. Res.*, 1983, **62**, 672.

21 E. Ferńndez, F. J. Gil, M. P. Ginebra, F. C. M. Driessens, J. A. Planell and S. M. Best, *J. Mater. Sci. Mater. Med.*, 1999, **10**, 169.

22 M. Bohner, *Injury*, 2000, **31**, S-D37.

23 R. W. Bucholz, *Clin. Orthop.*, 2002, **395**, 44.

24 E. Ferńndez, F. J. Gil, M. P. Ginebra, F. C. M. Driessens, J. A. Planell and S. M. Best, *J. Mater. Sci. Mater. Med.*, 1999, **10**, 177.

25 J. P. Schmitz, J. O. Hollinger and S. B. Milam, *J. Oral Maxillofac. Surg.*, 1999, **57**, 1122.

26 M. P. Ginebra, T. Traykova and J. A. Planell, *J. Control. Release*, 2006, **113**, 102.

27 A. J. Ambard and L. Mueninghoff, *J. Prosthodontics*, 2006, **15**, 321.

28 E. F. Burguera, F. Guitian and L. C. Chow, *J. Biomed. Mater. Res.* A, 2007, **85A**, 674.

29 M. Bohner, *J. Mater, Chem.*, 2007, **17**, 3980.

30 S. Cazalbou, C. Combes, D. Eichert and C. Rey, *J. Mater. Chem.*, 2004, **14**, 2148.

31 N. Ikawa, Y. Oumi, T. Kimura, T. Ikeda and T. Sano, *Chem. Lett.*, 2006, **35**, 948.

32 N. Ikawa, Y. Oumi, T. Kimura, T. Ikeda and T. Sano, *J. Mater. Sci.*, 2008, **43**, 4198.

33 N. Ikawa, M. Iwata, Y. Oumi, T. Kimura and T. Sano, *J. Nanosci. Nanotechnol.*, in press.

34 N. Ikawa, H. Hori, T. Kimura, Y. Oumi and T. Sano, *Langumir*, 2008, **24**, 13113.

35 T. Kokubo, *Biomaterials*, 1991, **12**, 155.

36 B. R. Constantz, I. C. Ison, M. T. Fulmer, R. D. Poser, S. T. Smith, M. VanWagoner, J. Ross, S. A. Goldstein, J. B. Jupiter and D. I. Rosenthal, *Science*, 1995, **267**, 1796.

37 E. Fernandez and J. A. Planell, *J. Mater. Sci. Mater. Med.*, 1998, **8**, 789.

38 R. Lieckfeldt, J. Villalaín, J.-C. Gómez-Fernández and G. Lee, *Pharm. Res.*, 1995, **12**, 1614.

39 A. L. Boskey and A. S. Posner, *Mater. Res. Bull.*, 1974, **9**, 907.

40 P. Gendraud, M. E. de Roy and J. P. Besse, *Inorg. Chem.*, 1996, **35**, 6108.

41 M. J. Larsen, A. Thorsen and S. J. Jensen, *Calcif. Tissue Int.*, 1985, **37**, 189.

42 E. Fernández, M. P. Ginebra, M. G. Boltong, F. C. M. Driessens, J. Ginebra, E. A. P. DeMaeyer, R. H. M. Verbeeck and J. A. Planell, *J. Biomed. Mater. Res.*, 1996, **32**, 367.

43 K. S. TenHuisen and P. W. Brown, *Biomaterials*, 1998, **19**, 2209.

44 C. Durucan and P. W. Brown, *J. Am. Cream. Soc.*, 2002, **85**, 2013.

45 C. Durucan and P. W. Brown, *J. Mater. Sci. Mater. Med.*, 2000, **11**, 365.

46 M. P. Ginebra, E. Fernández, F. C. M. Driessens and J. A. Planell, *J. Am. Cream. Soc.*, 1999, **82**, 2008.

47 K. Kurashina, H. Kurita, M. Hirano, A. Kotani, C. P. A. T. Klein and K. de Groot, *Biomaterials*, 1997, **18**, 539.

48 S. Tanaka, T. Kishi, R. Shimogoryo, S. Matsuya and K. Ishikawa, *Dental. Mater. J.*, 2003, **22**, 301.

Chapter 7

Summary

Synthesis of calcium phosphate and organic molecule composites was investigated based on the concept of suppressing the identical crystallization of calcium phosphates, such as brushite ($CaHPO_4 \cdot 2H_2O$), octacalcium phosphate ($Ca_8(HPO_4)_2(PO_4)_4 \cdot 5H_2O$) and hydroxyapatite ($Ca_{10}(PO_4)_6(OH)_2$). The composites without any identical crystalline calcium phosphate phases can successfully be obtained by using several kinds of organic molecules with carboxyl and/or amino groups in the mixed solvent systems of alcohol and water. The interaction of calcium phosphate with these organic moelcules in these composites was understood. In this synthetic method, the most important point is how to keep the interactions between deprotonated carboxyl groups and calcium ions and/or protonated amine groups and phosphate ions by the avoiding the identical calcium phosphate crystallizations. This synthetic method has enabled the structual and solubility controls of calcium phosphate with ionitically bonded frameworks by using organic molecules.

Most features of the composites are based on the organic moiety. The composition (mainly Ca/P molar ratio) of the composites can be controlled by the kind and number of functional groups. Ca-rich (~2.0) and P-rich (~1.0) composites were obtained using carboxylic acid- and amine-type organic molecules, respectively. The structure of the composites strongly depends on these of organic molecules. Lamellar mesostructured calcium phosphates were obtained amphiphic surfactant molecules with small head group regardless of the kind of functional groups. Wormhole-like mesostructured calcium phosphates were also obtained using diamine- and dicarboxylic acid-type surfactants with larger head groups. Amorphous composites were formed under the presence of amino acid molecules without self-assembling ability. The solubility of the composites is affected by that of organic moiety. Indeed, the amorphous composite with amino acid molecules were transformed into crystalline phases fastly (brushite and/or hydroxyapaite) in simulated body fluid (SBF) due to its high solubility. Especially, amorphous calcium phosphate/glutamic acid and /aspartic acid composites have high

potential for a Ca-rich and high soluble material instead of poorly soluble TTCP ($Ca_4(PO_4)_2O$) and calcium carbonate ($CaCO_3$). The addition of the Ca-rich composites to calcium phosphate cement (mixture of α-TCP ($Ca_3(PO_4)_2$), MCPM ($Ca(H_2PO_4)_2 \cdot H_2O$) and $CaCO_3$) can promote the transformation into apatite in SBF. On the other hand, the wormhole-like mesostructured calcium phosphates with atomically amorphous frameworks which was prepared using poorly-soluble surfactants are slightly soluble in short time.

Mesoporous calcium phosphate can be synthesized from wormhole-like mesostructured calcium phosphate prepared using 4-dodecyldiethylenetriamine after removal of the surfactants. Surface property of the mesoporous calcium phosphate is hydrophilic due to its ionitically bonded frameworks. The formation of mesoporous calcium phosphate demonstrated that amorphous inorganic frameworks with even ionic bond can maintain their nano-ordered structure stabilized by the presence of calcium pyrophosphate units.

The synthetic technology developed in this research will open new synthetic route of composites composed of calcium phosphates and organic molecules such as collagen, surfactants and polymers for new applications which cannot be expected by the classical crystalline materials.